2016-01-01

Identification and Characterization of Small Molecules Targeting FKBP52 as a Novel Treatment for Prostate Cancer

Naihsuan C. Guy
University of Texas at El Paso, nguy08@gmail.com

IDENTIFICATION AND CHARACTERIZATION OF SMALL MOLECULES TARGETING FKBP52 AS A NOVEL TREATMENT FOR PROSTATE CANCER

NAIHSUAN C. GUY

Doctoral Program in Biological Sciences

APPROVED:

Marc B. Cox, MSPH, Ph.D., Chair

Siddhartha Das, Ph.D.

Igor C. Almeida, Ph.D.

Arshad Khan, Ph.D.

Delfina C. Dominguez, Ph.D.

Kyle L. Johnson, Ph.D.

Charles Ambler, Ph.D.
Dean of the Graduate School

DEDICATION

This dissertation is dedicated to my family. All of my accomplishments would not have been achieved without their never-ending love, support, and encouragement.

IDENTIFICATION AND CHARACTERIZATION OF SMALL MOLECULES TARGETING FKBP52 AS A NOVEL TREATMENT FOR PROSTATE CANCER

by

NAIHSUAN C. GUY, B.S. M.S.

DISSERTATION

Presented to the Faculty of the Graduate School of

The University of Texas at El Paso

in Partial Fulfillment

of the Requirements

for the Degree of

DOCTOR OF PHILOSOPHY

Department of Biological Sciences

THE UNIVERSITY OF TEXAS AT EL PASO

May 2016

ACKNOWLEDGEMENTS

First and foremost, I would like to thank my parents and sisters for their love and encouragement throughout my life. I cannot express how grateful I am for the strength and support they have shown me in the pursuit of my goals and dreams. There are no words in the world that can describe my gratitude and how fortunate I feel to be their daughter and baby sister.

I would like to sincerely thank my dissertation advisor, Dr. Marc B. Cox, for his guidance and support throughout this project. He has challenged and helped me to grow and mature as a scientist. He has also provided me with opportunities and encouragement to experience different aspects in science, which I believe have prepared me to be a well-versed scientist. I thank the members of my dissertation committee: Dr. Siddhartha Das, Dr. Igor C. Almeida, Dr. Arshad Khan, Dr. Delfina C. Dominguez, and Dr. Kristin Gosselink. The knowledge and guidance they provided me have been invaluable during my doctoral study. I would also like to thank our collaborators: Dr. Artem Cherkasov's laboratory from the Prostate Centre at Vancouver General Hospital, Dr. Robert J. Matusik's laboratory from Vanderbilt University Medical Center, Dr. Jaideep Chaudhary from Clark Atlanta University, Dr. Huan Xie's laboratory from Texas Southern University, and Dr. Felix Hausch's laboratory from Max Planck Institute for Psychiatry.

I thank all the past and present members of the Cox laboratory. I would like to give special thanks to Jeffrey C. Sivils, Yenni A. Garcia, Angie Lopez, Zack Martinez, and Gloria Polanco. They have been there for me through the highs and lows of my doctoral career. I would also like to give a special recognition to Heather Balsiger. She has not only been my graduate student mentor who was there to show me the ropes when I began my research career, but has also become my friend who is like an older sister to me and provided me with guidance and comfort. Special thanks to Paola Ramos, the undergraduate student who helped me tremendously with my dissertation work and a sheer joy to mentor. I couldn't have asked for a

better mentee. Her laughs and optimisms helped us overcome the frustrations we experienced during the project and she has become like a younger sister I never had.

I truly appreciate all my close friends' love, support, and friendship. I know I can and have always depended on them through thick and thin. I am thankful and grateful for having the Shearer family in my life and for opening their home to me, and loving and caring for me like their own. Lastly, I would like to give huge thanks to Stephen Shearer for being there for me, believing in me, providing me with endless emotional support and love. He has been my therapist and cheerleader who kept me going through difficult and challenging times.

This graduate study was supported by the UTEP Department of Biological Sciences Teaching Assistantships (NCG), the Dr. Keelung Hong Graduate Research Fellowship (NCG), and the UTEP Graduate School Dodson Research Grant (NCG). The dissertation project was funded by the National Institutes of Health (NIH) Support of Competitive Research (SCORE) Grant 1SC1GM084863 (MBC) and an American Recovery and Reinvestment Act (ARRA) supplement through grant number SC1GM084863 (MBC) from the National Institute of General Medical Sciences, NIH. This work was also supported by the UTEP grant number 5G12RR008124 of the Border Biomedical Research Center (BBRC)/University of Texas at El Paso from the National Center for Research Resources (NCRR), a component of the NIH (MBC), the National Institute on Minority Health and Health Disparities (NIMHD), a component of NIH under grant number 2G12MD007592 (MBC), and Cancer Prevention and Research Institute of Texas (CPRIT) under grant number RP110444-P2 (MBC).

ABSTRACT

Prostate cancer (PCa) is one of the most commonly diagnosed diseases and the second leading cause of cancer deaths among men worldwide. Its growth is dependent upon androgen receptor (AR) signaling and the mainstay for treatment is hormone-ablation therapy using antiandrogens and/or androgen-deprivation therapies (ADT). Treatment of PCa with antiandrogens and/or ADT are initially effective; they act to repress the AR by directly competing with androgens for the ligand binding domain (LBD) and prevent activation of the receptor resulting in tumor regression. Unfortunately, the resistance to these treatments invariably emerges and results in a much more aggressive form of tumor that is androgen-independent termed castration-resistant prostate cancer (CRPC). Given the AR signaling axis is still active in CRPC and the heat shock protein (Hsp) 90-associated co-chaperone 52-kDa FK506-binding protein (FKBP52) plays important positive regulatory roles in AR, glucocorticoid receptor (GR), and progesterone receptor (PR) functions, FKBP52 represents a promising therapeutic candidate for treating PCa. Structure-based *in silico* drug screens of a virtual compound library representing lead-like molecules identified a list of 40 molecules that are predicted to bind to FKBP52. Functional screens of these hit compounds identified a lead molecule, termed GMC1, that inhibits FKBP52-enahnced AR, GR, and PR function, and impairs AR-mediated activation of PSA promoter activity. Additionally, our data show that GMC1 reduces endogenous androgen-dependent AR-regulated gene expression and PSA secretion. Finally, GMC1 impedes androgen-stimulated prostate cancer cell proliferation through destabilization of AR resulting in disruption of the hormone-binding ability of the receptor-HsP90-FKBP52 complex. Preclinical evaluations of GMC1 were performed by administering co-solvent GMC1 formulation via intratumoral injection into human xenograft mouse model. The data demonstrate promising potential in treating CRPC; tumor volumes are significant reduced compare to vehicle-treated controls. This proof-of-principle data in whole animal model further establishes FKBP52 PPIase-targeting drugs as effective therapies for PCa and warrant

further preclinical development. Together, these findings demonstrate that FKBP52 is a viable target for PCa treatment and will lead to the development of more potent and effective drugs for the treatment of CRPC. Given GMC1's unique mechanism of action, GMC1 is likely to circumvent AR-based therapy-induced resistance mechanisms, thereby filling a major unmet need in prostate cancer therapy.

TABLE OF CONTENTS

ACKNOWLEDGEMENTS v

ABSTRACT vii

TABLE OF CONTENTS ix

LIST OF TABLES xiii

LIST OF FIGURES xiv

CHAPTER 1: INTRODUCTION 1

1.1 Chaperone-Mediated Steroid Hormone Receptor Maturation 2

1.1.1 Early Complex 3

1.1.2 Protein Quality Control: Ubiquitin/Proteasomal System 6

1.1.3 Intermediate Complex 7

1.1.4 Mature Complex 10

1.2 The FKBP52 Co-Chaperone 11

1.2.1 C-Terminal Tail 15

1.2.2 TPR Domain 15

1.2.3 FK2 Domain 16

1.2.4 FK Linker 17

1.2.5 FK1 Domain 18

1.3 FKBP52 in Steroid Hormone-Regulated Physiology an d Disease 19

1.3.1 Phenotypes in *fkbp52*-Deficient Mice 22

1.3.2 FKBP52 in Hsp90-Independent Physiology and Disease 23

1.4 FKBP52 AS A NOVEL TARGET FOR PROSTATE CANCER TREATMENT 27

1.4.1 AR BF3 Surface 29

1.4.2 Cross-talk between the AR and Wnt/β-Catenin Signaling Pathways in CRPC 30

1.4.3 FKBP52 and β-Catenin Act in Concert to Promote Hormone-Independent AR Function 32

1.4.4 FKBP52 Proline-Rich Loop 32

1.4.5 Targeting FKBP52 Proline-Rich Loop Interactions 33

1.5 Dissertation Project Rationale and Hypothesis 38

1.6 Dissertation Goals 38

CHAPTER 2: IDENTIFICATION OF SMALL MOLECULE INHIBITORS SELECTIVELY TARGETING FKBP52 PROLINE-RICH LOOP INTERACTIONS USING STRUCTURE-BASED METHODOLOGY 40
2.1 Rationale 41
2.2 Materials and methods 42
2.2.1 Protein and Ligand Preparation 42
2.2.2 Molecular Docking-Based *In Silico* Screening of Potential FKBP52 PPIase Pocket Inhibitors 42
2.2.3 Cell Culture 43
2.2.4 Mammalian Cell-Based Luciferase Reporter Assays 43
2.2.5 Statistical Analysis 45
2.3 Results 45
2.3.1 Identification of Key Interaction Sites on the FKBP52 PPIase Pocket 45
2.3.2 *In Silico* Identification of Hit Compounds Targeting the FKBP52 PPIase Catalytic Pocket 48
2.3.3 *In Vitro* Evaluation and Identification of a Small Molecule Inhibitor that Targets FKBP52-Specific Regulation of AR Function 48
2.4 Discussion 52
CHAPTER 3: *IN VITRO* EVALUTION AND CHARACTERIZATION OF GMC1 IN PROSTATE CANCER CELLULAR MODELS 53
3.1 Rationale 54
3.2 Materials and Methods 56
3.2.1 Cell Culture 56
3.2.2 Transient Transfections and Luciferase Reporter Assays 57
3.2.3 Western Immunoblot Analysis 58
3.2.4 Prostate-Specific Antigen (PSA) ELISA Assay 60
3.2.5 Cell Proliferation Assay 61
3.2.6 Statistical Analysis 61
3.3 Results 62
3.3.1 GMC1 Demonstrates FKBP52-Specific Inhibition of GR and PR-Mediated Functions 62
3.3.2 GMC1 Impairs PSA Expression in Prostate Cancer Cellular Models 66
3.3.3 GMC1 Reduces Transactivation of PSA Promoter in LNCaP Cells 69
3.3.4 GMC1 Decreases Endogenous AR Protein Expression in Prostate Cancer Cells 71

3.3.5 GMC1 Reduces Endogenous AR-Dependent Gene Expression in Prostate Cancer Cells 73
3.3.6 GMC1 Inhibits AR-Dependent Proliferation in Prostate Cancer Cellular Models 76
3.4 Discussion 79
CHAPTER 4: VERIFICATION OF GMC1 TARGET SITE AND PRELIMINARY ANIMAL EVALUATIONS 82
4.1 Rationale 83
4.2 Materials and methods 84
4.2.1 Cell Culture 84
4.2.2 Transient Transfection and Luciferase Reporter Assay 84
4.2.3 GMC1 Formulation 84
4.2.3.1 Solubility 84
4.2.3.2 Lipophilicity 85
4.2.3.3 Plasma Protein Binding 85
4.2.3.4 Co-Solvency 85
4.2.4 Xenograft Mouse Model 86
4.2.4.1 Preparation of Tumor Cells 86
4.2.4.2 Tumor inoculation 86
4.2.5 Preclinical Efficacy 87
4.2.6 Statistical Analysis 87
4.3 Results 87
4.3.1 Characterization of GMC1 Binding to PPIase Catalytic Pocket with Competitive Fluorescence Polarization Assay 87
4.3.2 Identification of GMC1 Target Site on PPIase Catalytic Pocket Using Functional Mutagenesis Studies 88
4.3.3 Optimal Formulation of GMC1 93
4.3.4 Preclinial GMC1 Efficacy 97
4.4 Discussion 100
CHAPTER 5: CONCLUSIONS 102
5.1 Structure-Based *In Silico* Screen is a Viable Methodology for Identification of GMC1 Targeting FKBP52 PPIase Pocket 105
5.2 Small Molecule FKBP52 Inhibitor GMC1 as a Potential Treatment for Advanced PCa 106

5.3 Confirmation of GMC1 Binding to the Proposed Site on the FKBP52 PPIase Catalytic Pocket 109
5.4 Solution Formulation Development and Efficacy of GMC1 in Preclinical CRPC Animal Model 110
5.5 Proposed Mechanism 110
5.6 Concluding Remarks 114
5.7 Future Directions 115
REFERENCES 116
GLOSSARY 131
CURRICULUM VITA 136

LIST OF TABLES

Table 1.1 Alternative FKBP52 Interacting Proteins 25
Table 4.1 Solubility of GMC1 in Various Solvents 95
Table 4.2 GMC1 Co-Solvent Systems 96

LIST OF FIGURES

Figure 1.1: Chaperone-Mediated Steroid Hormone Receptor Folding 4
Figure 1.2: Structure of FKBP52 and the Putative FKBP52 Regulatory Surfaces on AR .. 13
Figure 1.3: FKBP52-Regulated Hsp90-Dependent and Independent Physiology and Disease 20
Figure 1.4: FKBP52-Receptor Interactions and Therapeutic Targeting Strategies..... 36
Figure 2.1: Structure-Based Design of Direct FKBP52 Targeting Small Molecule Inhibitors 47
Figure 2.2: GMC1 Inhibits FKBP52-Specific AR-Mediated Activity..... 50
Figure 3.1: GMC1 Inhibits FKBP52-Specific GR and PR-Mediated Activity..... 64
Figure 3.2: GMC1 Reduces AR-Dependent PSA Secretion in Prostate Cancer Cells 67
Figure 3.3: GMC1 Suppresses Androgen-Dependent PSA Promoter Activation at Concentrations Comparable to MJC13 and Classic AR Antagonists in LNCaP 70
Figure 3.4: GMC1 Decreases Endogenous Androgen-Dependent AR Expression in Prostate Cancer Cellular Models..... 72
Figure 3.5: GMC1 Reduces Endogenous AR-Dependent Gene Expression in Prostate Cellular Models 75
Figure 3.6: GMC1 Down-Regulated Hormone-Dependent AR-Specific Proliferation in Prostate Cancer Cellular Models 77
Fig. 4.1: FKBP52 PPIase Domain Mutants and Receptor Function..... 90
Figure 4.2: FKBP52-D68A PPIase Domain Mutants Disrupted GMC1 Binding and Affected Its Inhibitory Effect on Receptor Function..... 92
Figure 4.3: Treatment of LNCaP-Id4$^{-/-}$ Generated Prostate Tumor with GMC1 Significantly Decreased Tumor Size and Induced Tumor Regression 98
Figure 5.1: Proposed Mechanism of Action of FKBP52-Specific Small Molecule Inhibitors 112

CHAPTER 1: INTRODUCTION

The proper folding and activity of steroid hormone receptors (SHRs) requires no less than twelve proteins and at least three distinct chaperone/receptor complexes. Many of these chaperones and co-chaperones are attractive targets for the treatment of a variety of diseases. The heat shock protein (Hsp) 90-associated 52-kDa FK506-binding protein (FKBP52) is of particular interest as FKBP52 is a known positive regulator of androgen (AR), progesterone (PR), and glucocorticoid receptor (GR) activity, and serves as an attractive therapeutic target for any disease that depends on a functional AR, PR, and/or GR signaling pathway. Much progress has been made in understanding the mechanisms by which FKBP52 regulates receptor signaling and the resulting roles it plays, not only in hormone-dependent processes, but also in endocrine-independent functions, including cell architecture, neurodifferentiation, and metal transport, etc. This chapter summarizes the current understanding of chaperone-dependent SHR folding, FKBP52 interactions within the receptor-chaperone complex, FKBP52 contributions to health and disease, and FKBP52's potential as a therapeutic candidate for hormone-dependent and hormone-independent diseases. Furthermore, based on the progress that has been made in understanding residues and/or domains critical for function, we discuss the most promising strategies for the therapeutic targeting of FKBP52.

1.1 Chaperone-Mediated Steroid Hormone Receptor Maturation

Steroid hormones are small lipophilic molecules whose functions are mediated by intracellular receptor proteins termed steroid hormone receptors including AR, PR, GR, mineralocorticoid (MR), and estrogen receptors (ER). These receptors are ligand-regulated transcription factors that are required to be in continuous interactions with molecular chaperones and co-chaperones to establish and maintain their functionally mature conformations necessary for hormone binding and the subsequent control of a diverse array of physiological processes and/or promotion of disease states. The activation and maturation of the SHRs depend on interactions within the Hsp90-mediated chaperoning pathway, which is an ordered, dynamic, and cooperative series of events that involves multiple chaperone and co-chaperone components.

The heat shock proteins Hsp40, Hsp70, and Hsp90 in addition to the co-chaperones Hsp70/Hsp90 organizing protein (HOP) and p23 are minimally required for efficient SHR folding and maintenance of receptor hormone binding ability *in vitro*. Furthermore, SHRs must chronologically cycle through three distinct complexes, each with different chaperone and co-chaperone compositions, to reach their final active conformations (Fig. 1.1) [1-12]. While this chapter focuses on FKBP52 as a therapeutic target, it is important to point out that the chaperone-dependent folding, activation, and regulation of SHRs presents a variety of opportunities for therapeutic intervention. Thus, we also discuss the chaperone-dependent folding and activation pathway, and other potential targets for the disruption of SHR folding in detail below.

1.1.1 Early Complex

Little is known about the SHR folding process prior to nascent chain folding as the receptors emerge from the ribosome. However, *in vitro* receptor-chaperone complex assembly studies suggest Hsp40 and Hsp70 binding as the first step in the recognition of PR and GR, respectively, in the Hsp90-dependent chaperoning pathway through binding to a single site in the receptor ligand binding domain (LBD), yet the exact binding site has not been identified [4, 13]. Regardless of the exact details, an early primary role for Hsp70 in receptor maturation is clear. The nascent SHRs are bound by Hsp70 in an adenosine triphosphate (ATP)-dependent manner. The J-domain of Hsp40 stimulates Hsp70 ATPase activity leading to a conformational change resulting in a tight association of Hsp70 with the substrate [4, 14]. Thus, the early complex of the chaperoning pathway consists of Hsp70 and Hsp40 components that prime the receptor for a second ATP-dependent interaction with Hsp90 to form the intermediate complex [4, 15]. A surveillance system in eukaryotic cells also functions at this stage in the folding cycle to modulate “protein triage” decisions that regulate the balance between protein folding and degradation for chaperone substrates [16].

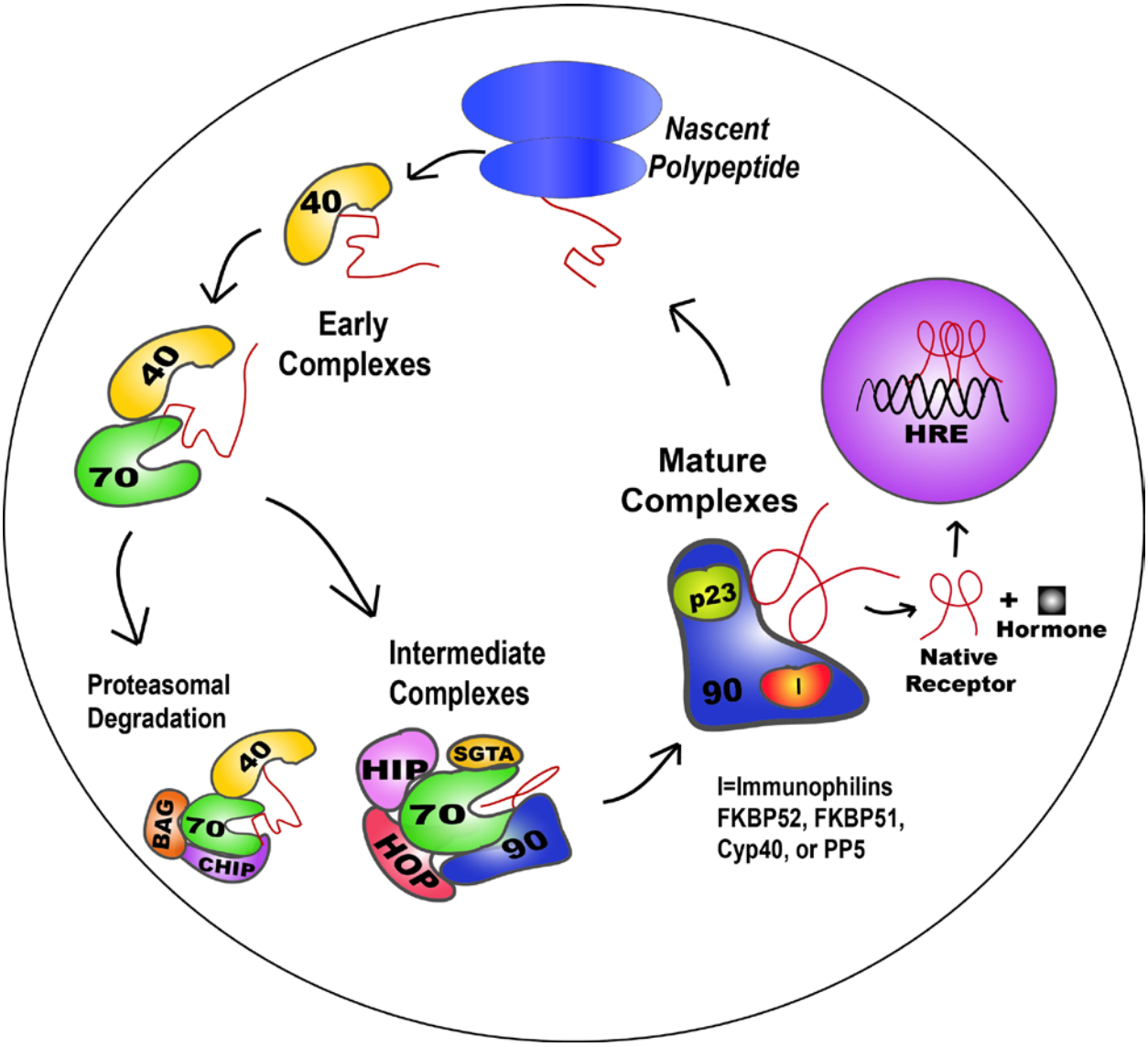

Figure 1.1: Chaperone-Mediated Steroid Hormone Receptor Folding

Fig. 1.1: Chapterone-Mediated Steroid Hormone Receptor Folding. Receptors associate with chaperones and co-chaperones as they cycle through early, intermediate, and mature complexes offering a variety of opportunities for therapeutic intervention. Early complex assembly is initiated upon Hsp40 binding to the nascent receptor polypeptide residing in the cytosol. Hsp40 recruits Hsp70 where the fate of the nascent polypeptide is determined to proceed with the intermediate complexes or towards proteasomal degradation. The carboxyl terminus of CHIP is an E3 ubiquitin ligase that, along with BAG proteins, directs misfolded receptors towards the ubiquitin and proteasomal degradation pathways. In the intermediate complex SGTA binds to Hsp70. Hsp70 then recruits HIP and HOP forming a bridge for Hsp90's binding into the complex. As the nascent polypeptide travels through the intermediate complex the immunophilins (I) bind in a competitive fashion to Hsp90 allowing for a conformational change. Further, the mature complex forms as HIP, HOP, and SGTA dissociate and p23 binds to stabilize the receptor-Hsp90 complex in the mature conformation to which hormone can bind with high affinity. The receptor is then able to translocate to the nucleus, dimerize and bind to hormone response elements to initiate gene transcription.

1.1.2 Protein Quality Control: Ubiquitin/Proteasomal System

Carboxyl terminus of Hsp70-interacting protein (CHIP) is a tetratricopeptide repeat (TPR)-containing co-chaperone that functions as a U-box dependent E3 ubiquitin ligase [17, 18]. It binds to both Hsp70 and Hsp90 through its TPR domain and inhibits the folding activity of the chaperones by confining the chaperone in an ATP-bound conformational state [16, 18]. CHIP plays a pivotal role in the conversion of the chaperone complex from a protein-folding apparatus to a protein-degradation machine by promoting the ubiquitination of chaperone substrates and stimulates their degradation by targeting them to the ubiquitin/proteasome pathway [16, 19]. In addition, biochemical studies have demonstrated that CHIP participates in triage decisions based on stochastic sampling of chaperone-bound substrate complexes [20]. CHIP randomly samples the chaperone-bound substrates and the ones that cannot be folded efficiently and/or correctly would consequently stay in the chaperoning cycle longer and eventually be ubiquitinated and targeted for degradation [20]. In addition to CHIP, the co-chaperone Bcl-2-associated athanogene 1 (BAG-1) has also been reported to act as a coupling factor between the Hsp70 chaperone system and the protein degradation machinery [21, 22]. BAG-1 binds to Hsp70 via its C-terminal BAG domain while its N-terminal ubiquitin-like domain associates with the ATPase domain of the chaperones leading to the release of the ubiquintylated substrate and, at the same time, serves as a physical link between the Hsp70 and the 26S proteasome [21, 23-25]. Thus, BAG-1 plays a dual role, both as a scaffolding factor at the proteasome and as a substrate release factor of Hsp70. It is worth noting that CHIP cooperates with BAG-1 in targeting Hsp70 substrates to the ubiquitin/proteasome system [26]. CHIP associates with Hsp70 via its TPR domain and mediates ubiquitin attachment to the aberrantly folded substrate bound to the chaperone by recruiting and binding of the E2 ubiquitin-conjugating enzyme to its C-terminal U-box. At the same time, BAG-1 binds the Hsp70 via its BAG domain and utilizes its ubiquitin-like domain for releasing of the ubiquitylated substrate from the chaperone and targets it to the 26S proteasome where their de-ubiquitylation, unfolding, and degradation occur [26]. Interestingly, recent biochemical assays indicated that S100 proteins bind to TPR domains and

interfere with CHIP/Hsp70 interactions leading to suppression of CHIP-dependent ubiquitination and degradation [27]. Therefore, the association of the S100 proteins with CHIP provides a calcium (Ca^{2+})-dependent regulatory mechanism for the ubiquitination and degradation of intracellular proteins by the CHIP-proteasome pathway.

1.1.3 Intermediate Complex

Those substrates deemed suitable for continued folding, as described above, are shuttled to intermediate complexes. Hsp70-interacting protein (Hip) facilitates intermediate complex formation by interacting with Hsp70 through its N-terminal TPR domain, which prevents dissociation of ADP from Hsp70. Since ADP-bound Hsp70 binds substrate with higher affinity, the binding of Hip with Hsp70 enhances the interaction of SHR with Hsp90 and Hop [1, 28-32]. Hop is another member of the TPR-containing co-chaperone family, which contains a specialized and conserved TPR-clamp domain consisting of TPR1, TPR2A, and TPR2B. Hop functions as a scaffold protein between the Hsp90 dimer and Hsp70 by their binding to its TPR2A and TPR1/TPR2B motifs, respectively, enabling the client transfer between the chaperones [1, 6, 33, 34]. Recent studies have shown one Hop bound to Hsp90 dimer is sufficient to stabilize the dimer in an open conformation. In this intermediate complex, Hop binding to the TPR-acceptor site introduces a steric hindrance that prevents the other C-terminal TPR-acceptor site on the Hsp90 dimer to be bound.

Apart from the C-terminal TPR-acceptor motif, a novel site for TPR co-chaperone interaction near the N-terminal ATP binding domain of Hsp90 has recently been discovered [35]. This TPR-acceptor motif on the Hsp90 dimer is preferentially occupied by TPR-containing co-chaperones containing a PPIase domain and the interaction leads to the formation of an asymmetric Hsp90 intermediate complex [36-38]. GCUNC-45 is such an example of a PPIase that binds to Hsp90 via its TPR domain forming an asymmetric intermediate complex during PR chaperoning. Yeast two-hybrid analyses have revealed that GCUNC-45 directly interacts with a novel TPR-acceptor site near the N-terminus of Hsp90 [35]. The primary function of N-terminal

domain (NTD) of Hsp90 is to bind ATP, which then induces an interaction between the NTDs of the Hsp90 dimer. This dimerization is further facilitated by the binding of activator of Hsp90 ATPase homologue 1 (Aha1) to the middle domain (MD) of the chaperone leading to the repositioning of a catalytic loop of this domain that interacts with the γ phosphate of ATP bound in the NTD [39, 40]. Mutational analyses have revealed that the GCUNC-45 binding motif on Hsp90 was generated by a spatial positioning of noncontiguous residues in the ATP binding domain [41]. Thus, it is suggested that binding of GCUNC-45 to the novel TPR-acceptor site near the N-terminus of Hsp90 may result in a spatial re-orientation between the NTD and MD leading to inhibition of ATPase activity of the chaperone by blocking the binding of Aha1 to MD, even though the two proteins do not share a common binding site [35, 41]. Thus, GCUNC-45 enters the chaperoning pathway at the intermediate stage forming an asymmetric intermediate complex with Hsp90/Hop intermediate complex and blocks progression of the PR complex to the next step with the purpose of allowing time for additional needed chaperoning events to occur. This confined regulation event by GCUNC-45 can be reversed in the presence of another PPIase TPR-containing co-chaperone, such as FKBP52, whose structure and function will be discussed in further detail below. PR assembly studies have demonstrated that GCUNC-45 functions upstream of FKPB52 during the chaperoning [35]. In addition, FKBP52 can reverse the confined inhibition by GCUNC-45 and promotes the progression of the PR chaperoning cycle toward the hormone binding competent mature state by competitively binding with GCUNC-45 for the novel TPR binding site near the N-terminus of Hsp90 [35, 41]. What induces the displacement of GCUNC-45 is unknown; it could be a response to specific signals and/or imbalance in intracellular homeostasis during the receptor chaperoning. It has recently been reported that S100 proteins, which are a subfamily of the EF-hand type Ca^{2+}-sensing proteins, compete with Hsp90 for the TPR domain of FKBP52 and cyclophilin 40 (Cyp40), which is another TPR-containing PPIase protein that is able bind to the N-terminal TPR acceptor site, in a Ca^{2+}-dependent manner [41, 42]. Given that GCUNC-45, FKBP52, and Cyp40, but not Hop, bind to S100 suggests that only a selective subgroup of TPR co-chaperones is able to bind to the

N-terminal TPR-acceptor site. S100 proteins regulate this subgroup of co-chaperones by binding to the TPR domain to competitively inhibit the FKBP52-Hsp90 and Cyp40-Hsp90 interactions. Interestingly, studies have shown that S100 proteins can also regulate the Hsp70/Hop/Hsp90 intermediate complex in a Ca^{2+}-dependent manner by binding to the TPR domains of Hop, hence disrupting the Hop-Hsp70 and Hop-Hsp90 interactions [43]. No matter what the details, it is undeniable that the presence of two Hsp90 sites for TPR protein interaction provides additional flexibility and control in modulating the Hsp90 co-chaperones and its clients during the chaperoning process.

Small glutamine-rich tetratricopeptide repeat-containing protein alpha (SGTA) is a co-chaperone that interacts directly with Hsp70, but weakly with Hsp90, via its C-terminal TPR domain and predominantly precipitates with Hsp70 from cell lysates [44, 45]. Interestingly, SGTA lacks a PPIase domain, which is a common feature among the related TPR proteins. Studies have shown that interaction with SGTA enhances Hsp70's and/or Hsp90's substrate binding affinity and the ATPase activity of the chaperones by favoring their ADP-dependent association with client molecules [44, 46, 47]. Studies by Buchanan *et al.* demonstrated that the binding of dihydrotestosterone (DHT) induces the dissociation of SGTA from the hinge region of AR, and conversely, its overexpression decreases the capacity of the hormone to mediate receptor transport to the nucleus [48]. In agreement with their experiments, our lab has reported that SGTA associates not just with AR, but also with GR and PR to regulate receptor activity. Furthermore, knockdown/deletion of SGTA enhances receptor activity, whereas the overexpression of the co-chaperone suppresses receptor activity [45]. Taken together, the data suggest that SGTA participates in the Hsp70/Hsp90-mediated intermediate complex and plays a quality control role in the chaperone-dependent receptor maturation. It suggests that SGTA enters the chaperoning pathway at the intermediate stage forming an intermediate complex and/or asymmetrical intermediate complex with Hsp70, Hsp90, Hop, and receptor substrate by interacting with the hinge region of the receptor and binding to Hsp70 via its TPR domain. However, the binding of SGTA to the hinge region affects receptor nuclear transport since the

receptor nuclear targeting sequence overlaps with the SGTA binding site [49]. Thus, this putative model provides an explanation for the fact that SGTA is a negative regulator of the receptors and its overexpression suppresses receptor activity, abrogates the regulation of receptor function by FKBP52, and decreases ligand-mediated receptor transport to nucleus.

1.1.4 Mature Complex

Biophysical studies using fluorescence resonance energy transfer (FRET) have shown that, once the temporary inhibition of Hsp90 ATPase activity imposed during the asymmetrical intermediate complex has been removed, ATPs quickly bind and secure the nucleotides by closing the ATP lids resulting in conformational changes in Hsp90 leading to the closing of the NTDs [50, 51]. This structural modification reduces the affinity of Hop for the assembly resulting in the exiting of the adaptor protein and its associated Hsp70. At the same time, Aha1 binds the MD to facilitate the domain repositioning and interaction with NTDs [39]. The dimerized N-terminal conformation recruits the p23 co-chaperone and one of several TPR-containing PPIases (*e.g.* FKBP52) [52]. p23 is a small acidic protein containing an unstructured C-terminal tail, which is essential for its intrinsic chaperone activity [53, 54]. Additionally, it is a conformation-specific co-chaperone that binds exclusively to the closed conformation of Hsp90 [55, 56]. Furthermore, p23 facilitates the maturation of client proteins (*e.g.* SHRs) by stabilizing the closed conformation of Hsp90 [7, 52, 53]. In fact, studies have shown that the presence of p23 can partially inhibit Hsp90 ATP hydrolysis, which is indispensable for the release of the client protein, such as SHRs [10, 57-61]. It is worth noting that it is in this active Hsp90/p23/TPR-containing PPIase mature complex that the SHR is capable of high affinity hormone binding. Upon ligand binding, the receptor dimerizes and translocates to the nucleus, which then binds to the hormone response element (HRE), and in turn, recruits other co-regulators resulting in regulation of various physiological functions such as development, differentiation, metabolic homeostasis, and reproduction. Ligand binding to the receptor has long been thought to be the trigger that stimulates release of the receptor from the chaperone

complex allowing receptor translocation to the nucleus. However, studies have shown that ligand-bound GR is able to undergo dynamic cycling with the chaperone machinery, which is essential for receptor trafficking to, and within, the nucleus [62, 63]. In the absence of ligand binding, the mature complex stays active until the hydrolysis of ATP followed by the dissociation of the NTDs of Hsp90 leading to the release of p23, the TPR-containing PPIase, and the folded client protein from the chaperone [37, 64]. Finally, the free hormone receptors re-enter the chaperoning cycle by binding to Hsp40 and Hsp70 for refolding.

1.2 THE FKBP52 CO-CHAPERONE

FKBP52 has been identified as one of the TPR-containing PPIase co-chaperones that are involved, together with Hsp90 and p23, in the mature SHR/chaperone complex. It is in this form of the complex that the SHRs are capable of high affinity hormone binding and consequently translocate to the nucleus to modulate transcriptional activity. While FKBP52 is not an absolute requirement for SHR hormone binding and signaling *in vitro* [9, 65, 66], it is required for efficient AR, GR, and PR hormone binding and activity at low concentrations of hormone [67, 68]. Thus, it is assumed that receptor activity *in vivo* is dependent on FKBP52 at physiological hormone concentrations. FKBP52 belongs to a family of immunophilins that is characterized by a conserved PPIase domain, which has peptidyl-prolyl cis/trans isomerase activity and also serves as a binding site for the immunosuppressive drug, FK506 [69]. Sequence data, hydrophobic cluster analysis, and crystallographic structures of overlapping FKBP52 fragments suggested the protein is composed of four distinct domains (Fig. 1.2a) [70-73]. The first two consecutive FKBP domains, FK1 and FK2, are structurally similar to the PPIase domain of 12-kDa FK506-binding protein 12 (FKBP12); which includes a functional site for PPIase activity (FK1) and a PPIase-like domain that lacks PPIase activity (FK2) [74]. Three TPR motifs occupy the third structural domain [75] while the fourth C-terminal domain (C-Terminal Tail) contains a motif important for binding Hsp90 and putative calmodulin (CaM) binding sites [71]. In the following sections, we will discuss the current understanding of FKBP52 structural features and

how those features contribute to FKBP52 interactions and functions within the SHR/chaperone complex.

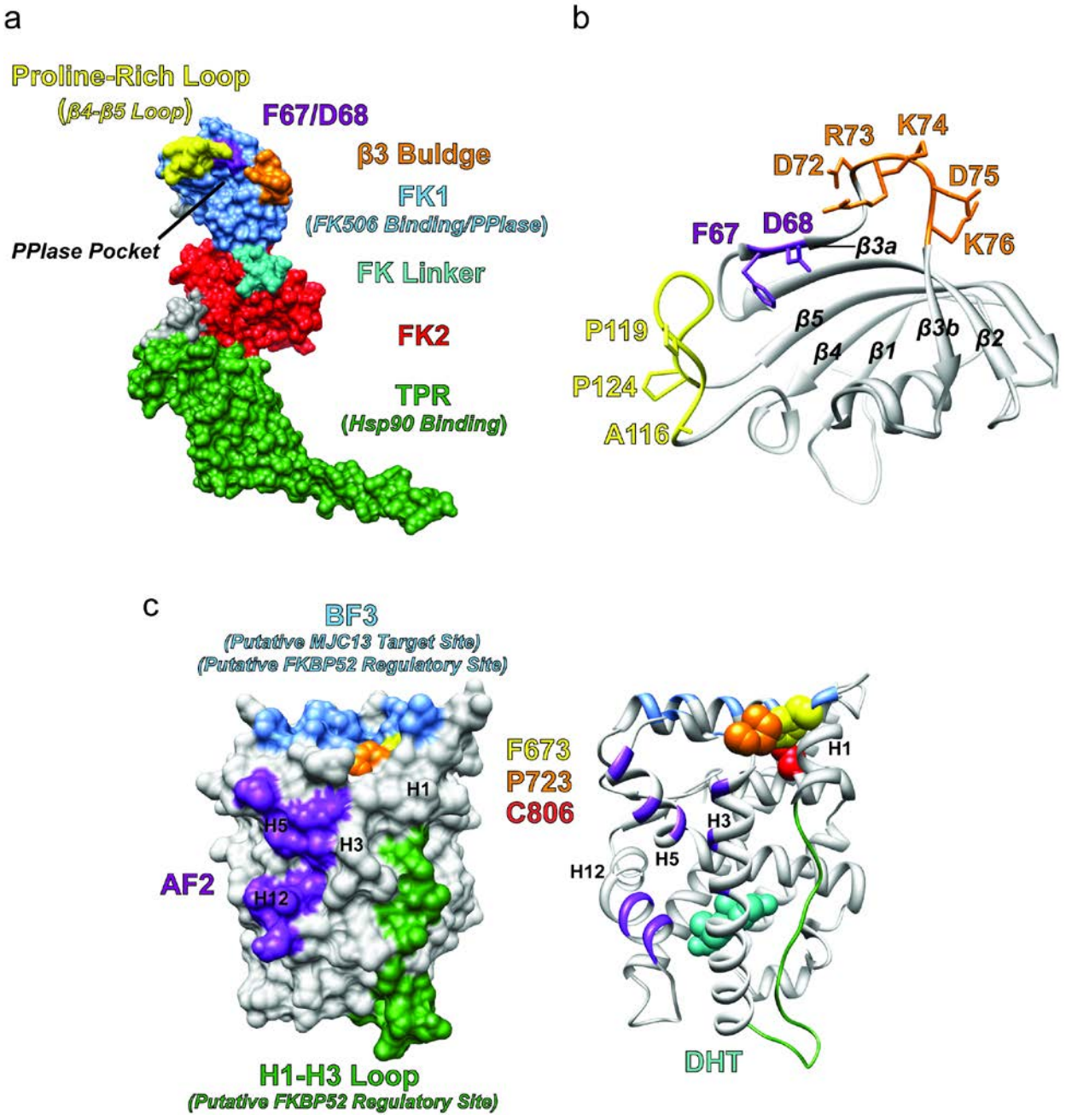

Figure 1.2: Structure of FKBP52 and the Putative FKBP52 Regulatory Surfaces on AR

Fig. 1.2: Structure of FKBP52 and the Putative FKBP52 Regulatory Surfaces on AR. (a) A composite of two partial structures for human FKBP52 (protein databank number 1Q1C and 1P5Q) showing the locations of the functional domains of FKBP52. The individual domains as well as regions of functional importance are individually colored. The TPR domain (green) mediates binding to Hsp90 via the MEEVD motif at the extreme C-terminus of Hsp90. The FK2 domain (red) is structurally similar to FK1, but lacks PPIase activity and the ability to bind to the immunosuppressive ligand FK506. The FK linker (teal), which connects the FK1 (blue) and FK2 (red) domains, contains a casein kinase II (CKII) phosphorylation sequence that, when phosphorylated, abrogates FKBP52 function due to the re-orientation of FK1 domain conformation. The FK1 domain (blue) is the primary regulatory domain for SHRs that displays FK506 binding and PPIase activity. FK1 is also important for FKBP52-mediated receptor potentiation. In particular, the proline-rich loop (yellow), also known as the β4-β5 loop, overhanging the PPIase pocket of the FK1 domain is crucial for receptor regulation and has been proposed to serve as a functionally important interaction surface. **(b)** A ribbon model of the FKBP52 FK1 domain is shown. The β4-β5 loop (yellow) and the β3 bulge (orange), and their respective residues (same colors), are structurally the most divergent regions at the periphery of the PPIase pocket between FKBP52 and its paralog, FKBP51. Mutational changes in the residues in and/or around the loop and bulge, such as residues F67/D68 (purple), can induce conformational changes in the pocket resulting in the obstruction of FKBP52-mediated receptor activity. **(c)** The left panel is a surface rendering of the AR ligand binding domain showing the relative locations of the putative FKBP52 regulation sites including BF3 (blue), the H1-H3 loop (green), and AF2 (purple). The right panel is a ribbon representation of the AR ligand binding domain, with dihydrotestosterone (teal) bound, showing the location of the mutated residues in relation to the BF3 surface. F673 (yellow) and P723 (orange) are within the BF3 surface and C806 (red) is buried directly below the surface. Mutations of these residues within the BF3 surface result in increased dependence on FKBP52 for function. This is also the site to which the recently characterized inhibitor of FKBP52-regulated AR activity, MJC13, is predicted to bind.

1.2.1 C-Terminal Tail

The C-terminal 60 amino acids, more specifically a 20-amino acid consensus sequence motif within this region, play an important role for Hsp90 binding. Within this consensus sequence motif is an 11-amino acid conserved region (charge-Y motif), which can be found in other human TPR-containing Hsp90 co-chaperones. The charge-Y motif is defined by the sequence -+-+XΦYXXMF, where - represents Glu or Asp, + represents Lys or Arg, Φ represents a hydrophobic amino acid, and X represents any amino acid [76]. In addition to the charged-Y motif, the extreme C-terminal amino acids also have a significant impact on Hsp90 binding [76]. Thus, the C-terminal regions outside the core TPR regions are important for optimum FKBP52 binding to Hsp90. The extreme C-terminus of FKBP52 (amino acid 400-458) also contains two predicted CaM binding sites, which enables the protein to bind to CaM-Sepharose in a Ca^{2+}-dependent manner [71]. Amino acid sequence analysis revealed the presence of PEST sequences within the predicted sites, which are generally present in CaM-binding proteins [71, 77]. However, the biological function of these CaM binding sites is still unknown.

1.2.2 TPR Domain

The core TPR domain (amino acids 264-400) is composed of three tandem repeats of a degenerate 34-amino acid motif. Crystallographic data have shown that each TPR motif adopts a helix-loop-helix conformation and adjacent units stack in parallel to form a saddle-shaped domain with a concave binding pocket that mediates protein-protein interactions [78-80]. It is in this conformation that the TPR domain interacts with the MEEVD sequence in the extreme C-terminus of Hsp90. Mutagenesis studies have shown that peptide bonding is mediated through electrostatic interactions by which the basic residues of the TPR domain interact with the terminal aspartate of the pentapeptide [81]. The importance of the interaction is evident by the fact that a single mutation (K354A) within the TPR can significantly reduce FKBP52 binding to Hsp90 and abolished FKBP52-mediated potentiation of receptor function. In addition, FKBP52 domain truncation mutants demonstrated the TPR domain interaction with Hsp90 alone is

necessary but not sufficient for FKBP52 regulation of SHR function [82]. Thus, the core TPR domain is required for binding to Hsp90, but is inadequate for functional interaction with SHR/Hsp90 complexes [83]. In fact, additional contacts involving charged and hydrophobic residues upstream of the Hsp90 MEEVD sequence are required for enhancement of the affinity and specificity of the interaction [47, 81]. The MEEVD pentapeptide is located at the extreme C-terminus of Hsp90 is not the only interaction site for TPR domain-containing proteins. As discussed above, recent studies have identified a novel region for TPR co-chaperone interaction at the N-terminal ATP binding domain of Hsp90 [35, 41]. Mutational analyses demonstrated that an acidic motif can be generated by a spatial positioning of noncontiguous residues (E42, N46, D49, D52, L51, and D88) within and/or near the ATP binding pocket of Hsp90, which are necessary for the binding of TPR domain-containing proteins [41]. As aforementioned, recent biochemical studies have demonstrated S100 proteins compete with Hsp90 for FKBP52 TPR domain in a Ca^{2+}-dependent manner, hence regulating the immunophilin-Hsp90 complex formation [42].

1.2.3 FK2 Domain

A direct functional role for the FK2 domain (amino acids 167 to 253) has not been identified. It is a required domain to maintain the overall size and structure of the large FKBPs. Despite the fact that it is structurally similar to FKBP12, it only has 26% sequence identity (44% similarity) and marginal to no PPIase and drug-binding activities [74, 84]. Evolutionarily, FK2 appears to result from a duplication event of the FK domain. Mutagenesis and 51-kDa FK506-binding protein (FKBP51)/FKBP52 chimeric protein studies demonstrated that there is a unique interaction between the FK2 and TPR domains that is important for full SHR potentiating ability [85]. Furthermore, deletion of three residues (D195, H196, and D197) within the FK2 domain of FKBP51, a closely related protein that often antagonizes FKBP52-mediated functions, resulted in abnormal integration of FKBP51 into PR complexes [84]. Thus, specific residues and/or regions likely exist within FK2 that contribute directly to receptor regulation and possibly

influence interactions with the components of the receptor-chaperone complex or the receptor itself. Further studies are needed to define those critical residues and/or regions within FK2 that are required for regulation of receptor activity. Interestingly, FK2 contains a consensus ATP/guanosine triphosphate (GTP)-binding sequence located between amino acids 199 and 222, which can be phosphorylated *in vitro* in the presence of CaM in an ATP-dependent manner [86, 87], although the ability of FKBP52 to bind and hydrolyze nucleotide has not been demonstrated. In fact, sequence and structural comparison data have demonstrated that FK2 displays structural similarity to the TPR-containing homolog FKBP38, which is PPIase-inactive under basal conditions but can be allosterically activated by CaM [88-91]. The fact that FKBP52 contains a putative CaM-binding motif at the extreme C-terminus suggests that a similar allosteric activation mechanism for the FK2 domain of FKBP52 exists.

1.2.4 FK Linker

The crystal structures of FKBP52 revealed a 9-amino acid long (amino acids 138-167) flexible and solvent-accessible hinge region that connects the FK1 and the FK2 domains termed the FK linker [92]. Within this linker region there is a consensus casein kinase II (CKII) phosphorylation site (TEEED). FKBP52 is phosphorylated by CKII at T143, which is a major phosphorylation site both *in vivo* and *in vitro* [93]. *In silico* modeling and structural analyses revealed that T143 phosphorylation destabilizes the FK linker region and induces the allosteric rearrangement of the FK1 domain [92-94]. FK1, as will be discussed in more detailed in the following section, particularly the integrity of proline-rich loop that overhangs the PPIase pocket, is a functionally important interaction surface that is required for FKBP52-mediated potentiation of SHR response to hormone. Phosphorylation of T143 destabilizes the conformation of the linker resulting in a widening of the architecture and introduces a steric hindrance by disrupting the hydrogen-bonding network within the region causing a re-orientation within the linker [94]. Subsequently, weakening the FK1-FK2 contacts introduces a remodeling of the FK1 catalytic domain by twisting a short α-helix that forms one side of the PPIase active site [94].

Interestingly, tyrosine phosphorylation of FKBP52 influences adeno-associated virus type 2 (AAV) second-strand DNA synthesis by binding to single-stranded D-sequence-binding protein within the virus' terminal repeats limiting high-efficiency transgene expression, which may have important implications for the optimal use of AAV vectors in human gene therapy [95, 96]. In addition to the T143 phosphorylation site, a conserved negatively charged motif that was predicted to be a complementary nuclear localization signal (NLS) recognition sequence also localizes within the FK linker region [67]. FKBP52 is primarily localized in the nucleus with a minority co-localizing with microtubules in the cytoplasm. Biochemical studies have shown that antibodies raised against the NLS impede the hormone-mediated translocation of glucocorticoid receptor (GR) in the nucleus [67]. This suggests that the sequence is required for anterograde movement of FKBP52 to the cytoplasm where is associated with the Hsp90 heterocomplex to facilitate the passage of the untransformed receptor through the nuclear pore.

1.2.5 FK1 Domain

The FK1 domain is located within the first 138 amino acids in the N-terminus of FKBP52. Unlike the FK2 domain, FK1 contains a functional PPIase catalytic pocket located between amino acids 4-137 that has enzymatic activity comparable to that of FKPB12 [70, 74]. *In vitro* studies demonstrated that FKBP52 selectively potentiates hormone-dependent gene activation and hormone-binding affinity of AR, PR, and GR through interaction with the receptor LBD [82, 97, 98]. Interestingly, it is not the enzymatic activity of the FK1 that is required for receptor potentiation but the integrity of the PPIase pocket. Furthermore, gain-of-function mutagenesis studies identified a proline-rich loop that overhangs the catalytic pocket that is critically involved in receptor interactions and enhanced hormone-mediated receptor activity [85]. Structural comparison of the corresponding loop of FKBP52 and FKBP51 revealed the most divergent regions in the domains between the two proteins are the β3 bulge and β4-β5 loop (Fig. 1.2b). The β3 bulge occurs when there is a discontinuity in β-strand 3. In FKBP51, P76 (K76 in FKBP52) enforces a shift of the β3 bulge toward the β2-β3 loop, which forces E75

closer to the PPIase active site compared to D75 in FKBP52, thus, compromising FK1 architecture (Fig. 1.2b) [92, 99]. The same principle applies to the FD67DV double mutation, which abolishes FKBP52–dependent potentiation of GR and AR (Fig. 1.2b). Substantial structural differences between FKBP51 and FKBP52 are also found at the tip of the β4-β5 loop; FKBP52 has a proline at amino acid position 119 while FKBP51 has a leucine (Fig. 1.2b). P119 of FKBP52 projects outward to form a hydrophobic notch alone, while with the *trans* configuration adopted by the P119-P120 peptide bond in the β4-β5 loop forms an important functional interface that contributes to the enhancing effects of FKBP52 (Fig. 1.2b) [85, 92]. On the contrary, L119 in FKBP51 projects inward and the *cis* conformation formed by the L119-P120 bond impairs the potentiation of steroid receptor activity (Fig. 1.2b) [85, 92]. Gain-of-function mutagenesis studies corroborate this structural data; the FKBP51 mutation L119P conferred significant receptor potentiating ability, whereas the converse P119L mutation in FKBP52 decreased receptor potentiation. Interestingly, when a second residue, A116, in the β4-β5 loop was also mutated, the FKBP51-A116V/L119P double mutant potentiated hormone signaling similar to that of wild type FKBP52 [85]. These results all emphasize the importance of architectural integrity of the proline-rich loop in acting as a critical interface for regulating receptor interactions and activity.

1.3 FKBP52 IN STEROID HORMONE-REGULATED PHYSIOLOGY AN D DISEASE

Biochemical and cellular studies demonstrated that FKBP52 associates with the SHR chaperone complex to specifically potentiate the activities of AR, GR, and PR. The physiological significance of these findings has been corroborated in *fkbp52*-deficient (52KO) mouse models as phenotypes related only to androgen, glucocorticoid, and progesterone insensitivity have been characterized to date (Fig. 1.3) [97, 100]. These studies firmly established FKBP52 as a relevant factor in AR, GR, and PR-related physiology and disease.

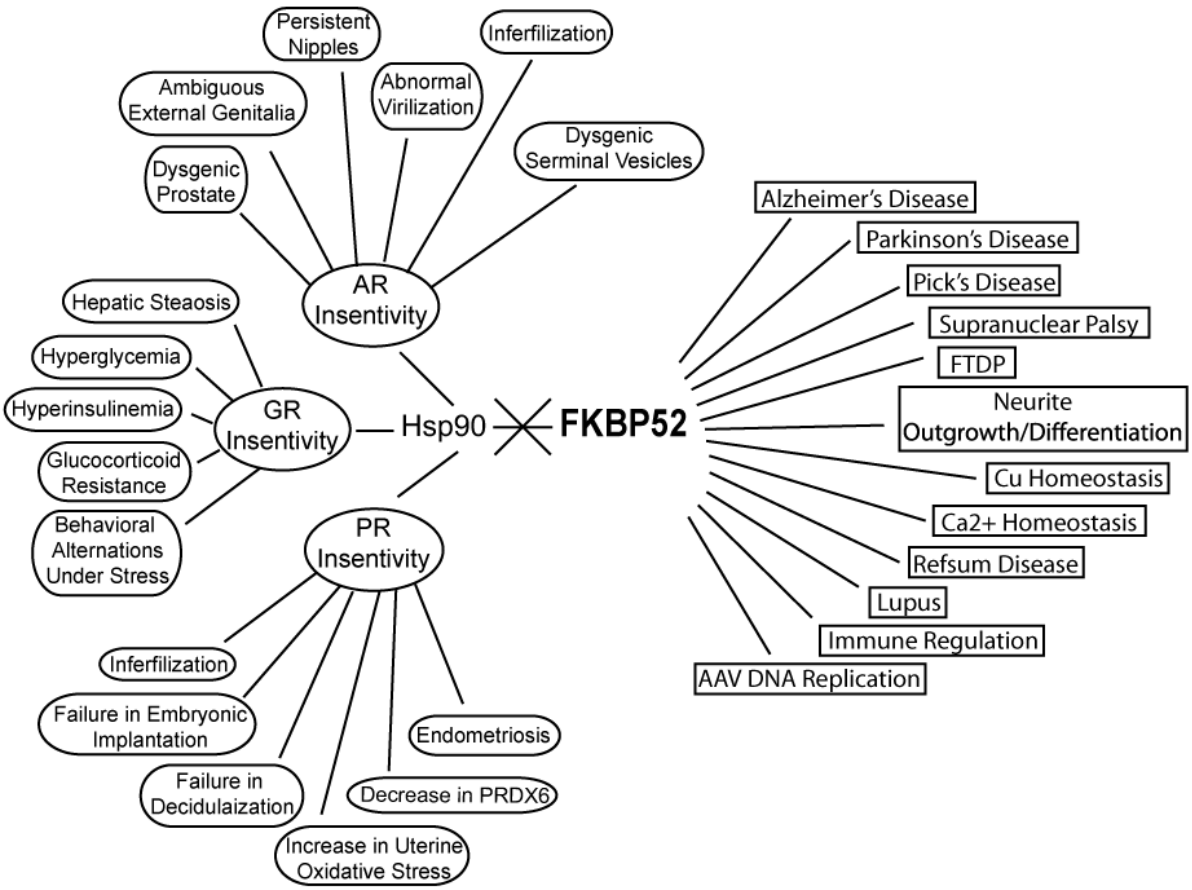

Figure 1.3: FKBP52-Regulated Hsp90-Dependent and Independent Physiology and Disease

Fig. 1.3: FKBP52-Regulated Hsp90-Dependent and Independent Physiology and Disease. The Hsp90-dependent roles for FKBP52 are largely mediated through FKBP52-Hsp90 complex regulation of AR, GR, and PR signaling, which is independent of FKBP52 PPIase activity. FKBP52 is an essential player in SHR/Hsp90-regulated physiological development and reproductive success. The left side of the diagram depicts receptor-specific phenotypes that are due to defective AR, GR, and PR signaling in the absence of FKBP52. Given the positive role of FKBP52 in these receptor signaling pathways, FKBP52 may also serve as an attractive therapeutic target for any disease that is dependent upon functional AR, GR, and PR mechanisms (*e.g.* prostate cancer). Apart from the established roles of FKBP52 in SHR functions, the co-chaperone is also involved in various Hsp90-independent biological functions, several of which have been shown to require FKBP52 PPIase activity. The right side of the illustration shows that the absence of FKBP52 could contribute to neurodegenerative tauopathies (Alzheimer's Disease, Pick's Disease, fronto-temporal dementia and Parkinsonism linked to chromosome 17 (FTDP), progressive supranuclear palsy), disruptions in Cu and Ca^{2+} homeostasis and immune system, and inhibition of AAV DNA synthesis resulting in inefficient transgene expression from recombinant AAV vectors used in gene therapy.

1.3.1 Phenotypes in *fkbp52*-Deficient Mice

The observed reproductive phenotypes observed in the 52KO mice are attributed to the loss of SHR activities. Male 52KO mice are infertile and display abnormal virilization with persistent nipples, ambiguous external genitalia, and dysgenic seminal vesicles and prostate [97, 100], which are consistent with androgen insensitivity in these tissues. Despite the androgen insensitivity, the testicular morphology, descent, histology, and spermatogenesis develop normally with unimpaired androgen production and release from the testes [97], which might suggest that testosterone levels produced locally within the testis is high enough to compensate for significantly reduced AR activity. Alternatively, it is possible that a factor present within the testis can complement for the loss of FKBP52. Despite no observable defect in spermatogenesis, sperm isolated from the organ displayed abnormal tail morphology and reduced motility, which is not androgen-dependent [101]. These findings may reflect FKBP52's ability to bind to dynein motor proteins [67].

In contrast to what is observed in 52KO male mice, 52KO females have no gross morphological abnormalities and display normal ovulation and fertilization, yet they are completely infertile [102]. The infertility is the result of failure in embryonic implantation and decidualization [98, 102-104]. The ER and PR are critical factors mediating embryonic implantation. Interestingly, the absence of FKBP52 leads to a selective failure of receptor function resulting in female mice sterility. In fact, FKBP52 does not alter ER function in cellular studies and 52KO mice show no signs of estrogen insensitivity. Rather, the implantation and decidualization failures result from an inability of the uterus to mount a decidualization response to progesterone due to progesterone insensitivity and uterine defects [102]. This implantation failure is also a result of an increased uterine oxidative stress and a reduced level of the antioxidant peroxiredoxin-6 (PRDX6) [104, 105]. Furthermore, the loss of FKBP52 promotes the growth of endometriotic lesions due to increased cell proliferation, inflammation, and angiogenesis [106]. These events are largely dependent upon progesterone actions, and, along with the corroborative data from both molecular and cellular studies, this confirms that FKBP52

is required for full PR activity *in vitro* and *in vivo*. Taken together, these data firmly establish a critical role for FKBP52 in reproductive development and success in both male and female mice and these roles can be traced to support of AR and PR functions.

Due to the partial embryonic lethality in null 52KO mice [107], heterozygous *fkbp52*-deficient (52+/-) mice were generated to determine the *in vivo* roles for the co-chaperone in GR-mediated physiology. 52+/- mice manifested phenotypes associated with defective GR signaling including increased susceptibility to high-fight diet induced hepatic steatosis, hyperglycemia, and hyperinsulinemia. They also displayed glucocorticoid resistance and behavioral alterations under basal and chronic stress conditions [108, 109].

As previously discussed, FKBP52 does not alter ER function in cellular studies and 52KO mice do not manifest signs of estrogen insensitivity. However, studies have reported that FKBP52 expression levels are associated with ERα, which implicates FKBP52 as a potential factor in breast cancer [110]. Treatment of breast cancer cells with estradiol resulted in an increased half-life of FKBP52 mRNA, and both FKBP52 gene and protein expressions have been reported to be significantly up-regulated and in ERα-positive cell lines as compared with ERα-negative cell lines [110, 111]. Furthermore, the FKBP52 gene is epigenetically silenced by methylation in ER-negative, but not in ER-positive, breast cancer cells [112]. Taken together, these studies have identified FKBP52 as a relevant factor in ERα-positive breast cancer. In addition, recent studies suggest an increased reliance on AR signaling in triple negative breast cancer [113]. Given the known roles for FKBP52 in AR signaling, these studies implicate FKBP52 as a potential target in triple negative breast cancer.

1.3.2 FKBP52 in Hsp90-Independent Physiology and Disease

Apart from the well-established roles of FKBP52 in SHR function, FKBP52 has been identified in complex with a variety of other client-Hsp90 heterocomplexes, such as those containing kinases, aryl hydrocarbon receptor, and heat shock transcription factor to name a few. However, many of these associations are passive and transient, and have no functional impact on

client activity. It is likely that Hsp90 continuously samples the available pool of TPR-containing PPIase co-chaperones and the co-chaperone that ultimately functionally interacts is dependent on the client protein present within the complex. In addition to the Hsp90-dependent client proteins, FKBP52 is also involved in various endocrine-independent processes (Table 1.1 and Fig. 1.3). As previously discussed, FKBP52 belongs to a family of immunophilins, which can be targeted by immunosuppressive molecules. This drug-immunophilin complex then docks and inhibits the activity of calcineurin leading to immunosuppression, although FK506 binding to FKBP52 does not inhibit calcineurin [114, 115]. Over the past decade, there has been a growing interest to understand the role of immunophilins, including FKBP52, in the nervous system. FKBP52 is ubiquitously expressed and especially abundant in the central nervous system. Thus, it is not surprising that FKBP52 is involved in neurodegenerative tauopathies including Alzheimer's Disease (AD), Pick's Disease, fronto-temporal dementia and Parkinsonism linked to chromosome 17 (FTDP), and progressive supranuclear palsy [116, 117]. Tauopathies is defined by the neuropathological characteristic of aberrant aggregation of insoluble hyperphosphorylated microtubule-associated protein (MAP) tau within the neurons termed neurofibrillary tangles (NFTs), which are also referred to as paired helical filaments (PHF) [118]. Recent studies have reported that FKBP52 interacts directly with the hyperphosphorylated form of tau, which has antagonistic effects on tubulin polymerization and microtubule assembly [119, 120]. It is worth noting that FKBP52 regulation of microtubule assembly is likely dependent on PPIase activity, which is in contrast to that observed with FKBP52 regulation of SHR activity. The α-Synuclein (α-Syn) protein is a key player in the pathogenesis of Parkinson's disease. Knockdown of FKBP52 reduced the number of α-Syn aggregates and protected against cell death, whereas overexpression of FKBP52 accelerated both aggregation of α-Syn and cell death [121]. Finally, FKBP52 expression is enhanced in regenerating neurons, which stimulates neurite outgrowth and promotes neuronal differentiation suggesting a protective or regenerative role following injury [122, 123].

Table 1.1 Alternative FKBP52 Interacting Proteins

Interactors	Experimental Approach	Physiological Implications	References
Dynein	Co-IP	Intracellular trafficking of steroid receptor complexes	[68, 137]
p53	Co-IP	Cancer	[186]
HSF-1	Co-IP	Cellular stress	[187]
TRPCs	Co-IP	B- and T-cell activation; neuronal survival and growth	[136]
FAP48	Yeast two-hybrid	T-cell activation	[140, 141, 188]
PHAX	Yeast two-hybrid	Refsum disease, lupus	[189]
IRF-4	Yeast two-hybrid	Immune regulation	[138]
AAV DNA	EMSA	Gene therapy	[95]
Atox1	Yeast two-hybrid	Copper transport	[131]
Tau	Co-IP	Tauopathy	[120]
PRDX6	Co-IP	Embryonic implantation	[105]
AAP	Co-IP	Alzheimer's disease	[130]
RET51	Yeast two-hybrid	Parkinson's disease	[139]
Tubulin	Co-IP	Neuronal differentiation	[119]
S100A1 & A2	Co-IP	Ca^{2+}-dependent signaling	[42]

Copper (Cu) is an essential nutrient, and, as a result, cells have developed elaborated systems for Cu storage and transport. In humans, disruption of the tightly regulated cellular Cu homeostasis affects normal tissue development and leads to anemia, neutropenia, cancer, and several neurodegenerative diseases including AD [124, 125]. The amyloid precursor protein (APP) plays a central role in the development of AD through the generation of peptides called beta-amyloid (Aβ) by proteolysis of the precursor protein. Cu contributes to the neuropathology of AD by interacting with copper binding domain (CuBD) of APPs and Aβ peptides causing the formation of amyloid plaques and disrupting metal ion homeostasis [126-128]. There are several lines of evidence that have linked the protective effects of FKBP52 with intracellular Cu homeostasis. First, FKBP52, more specifically its FK1 domain, interacts directly with APP and Cu metallochaperone Atox1, which is a protein that delivers copper to the copper transporting ATPases [129, 130]. Second, mutations of FKBP52 modulate the toxic effects and level of Aβ peptides in *Drosophila* [130]. Third, mutations in the copper transport genes *Ctr1A* and *Atox1*, which directly regulate intracellular copper levels, modify Aβ-induced phenotypes in *Drosophila* [130]. Fourth, dietary fluctuation in the Cu levels influences the protective effects of FKBP52 on Aβ [130]. Finally, cells isolated from 52KO mice show increased levels of Cu compared to wild type cells and overexpression of FBP52 causes efflux of copper [131].

S100A1 and S100A2 belong to the S100 family of Ca^{2+}-binding proteins that are linked to regulation of various intracellular processes and are often expressed in a cell- and tissue-specific fashion [132, 133]. Cellular data has linked S100A1 to neuronal cell dysfunction/death that occurs in AD by altering APP expression, destabilizing the intracellular Ca^{2+} homeostasis, and increasing sensitivity to Aβ toxicity [134]. Based on the biochemical evidence, FKBP52 is a novel target for S100A1 and S100A2. Both proteins interact with the FKBP52 TPR domain leading to dissociation of the immunophilin/Hsp90 complex in a Ca^{2+}-dependent manner [42]. S100A1 and S100A2 proteins are not the only proteins that associate with and/or regulate FKBP52 functions in a Ca^{2+}-dependent manner. Ca^{2+} homeostasis has been suggested to regulate intracellular FKBP52 functions leading to affects on the phosphorylation of tau and

pathology in AD. Interestingly, a *Drosophila* orthologue of FKBP52, termed dFKBP59, was found to interact with the Ca^{2+} channel transient receptor potential-like (TRPL) protein in photoreceptor cells and to influence Ca^{2+} influx [135]. Subsequent studies revealed that FKBP52 similarly interacts with a subset of rat transient receptor potential channel (TRPC) proteins that form Ca^{2+} channels in the mammalian brain [136]. Although the functional importance of the CaM-binding motifs in the C-terminal tail of FKBP52 is not known [137], these roles for FKBP52 in multiple Ca^{2+}-dependent functions suggest that the interaction of FKBP52 with CaM may be yet another Ca^{2+}-dependent mechanism by which FKBP52 could functionally affect a wide variety of CaM-dependent physiological processes including inflammation, metabolism, intracellular movement, smooth muscle contraction, and the immune response.

FKBP52 has also been found to interact directly with the interferon regulatory factor 4 (IRF-4) [138], which regulates gene expression in B and T lymphocytes; controls proto-oncogene *RET* by forming a complex with tyrosine kinase receptor RET51, which is involved in the development and maintenance of the nervous system [139]; and FKBP-associated protein 48 [140], which influences proliferation of Jurkat T cells [141]. Each of these interactions was found to be disrupted by FK506 and to target the FKBP52 PPIase domain to specific proline sites in each partner protein. Phenotypes potentially related to these interactions have not yet been assessed in 52KO mice. Not only does FKBP52 interact with proteins, but also directly binds AAV DNA and regulates replication of the viral genome [95, 142]. The relevant DNA binding site in FKBP52 has not been identified.

1.4 FKBP52 AS A NOVEL TARGET FOR PROSTATE CANCER TREATMENT

The importance of FKBP52 as a regulator for not just hormone-dependent, but also hormone-independent diseases is becoming increasingly clear. FKBP52 is often overexpressed in malignant hepatoma, T cell leukemia, ERα-positive breast cancer cell lines, pre-invasive and breast cancer tissues, and hormone-dependent cancers [141, 143-147]. Furthermore, the prostate dysgenesis observed in 52KO mice along with enhanced FKBP52 expression in several prostate

cancer cell lines and prostate biopsy samples establish the protein as a critical regulator of AR-mediated prostate development [97, 100, 148, 149]. Androgens play an important regulatory role in the development and progression of prostate cancer (PCa) by binding to the hormone binding pocket in the C-terminal LBD core of AR [150, 151]. The AR LBD consists predominantly of 12 α-helices. Upon ligand binding, helix 12 is reorganized to an agonist conformation termed activation function 2 (AF2) for co-regulator binding [152, 153] (Fig. 2c). The primary treatment for locally advanced and metastatic PCa is androgen deprivation therapy (ADT), in which the antiandrogens including Bicalutamide, Enzalutamide, and ARN-509 bind to the LBD of AR [154]. These antiandrogens inhibit AR action by competing for androgen binding and displacing helix 12 to prevent formation of a productive AF2 pocket [155]. Most tumors respond to the treatment initially. However, as the cancers progress they become resistant to the therapy, in which the condition is termed castration-resistant prostate cancer (CRPC) [156-158]. Preclinical and clinical studies suggest that acquired resistance to conventional ADT is caused by restoration of the AR pathway by AR overexpression and mutations, cross-talks between AR and other signaling pathways, and/or bypassing AR blockade through up-regulation of GR [159-164]. As a result, researchers have focused their efforts on the development of a new class of AR inhibitors termed nuclear receptor alternative-site modulators (NRAMs) targeting alternative sites on AR and receptor regulatory proteins including receptor-associated chaperones, co-chaperones (*e.g.* FKBP52), co-activators (*e.g.* β-Catenin), and AR inhibitors for which the binding sites are currently unknown [165]. In line with this idea, our lab has recently identified a small molecule termed MJC13 that specifically inhibits FKBP52 regulation of AR by blocking the hormone-dependent dissociation of the AR-Hsp90-FKBP52 heterocomplex resulting in a loss of AR nuclear translocation and an inhibition of androgen-dependent gene expression and proliferation in prostate cancer cells [166].

FKBP52 interacts with Hsp90, and, although the specific Hsp90 contact site on the surface of the receptor LBD has not been determined, a seven-amino acid segment located just upstream of the receptor LBD was found to be required for stable interaction with the Hsp90 MD

[62]. Furthermore, the fact that FKBP52 regulation has been localized to the receptor LBD and its regulation is receptor-specific suggests that FKBP52 directly interacts with the receptor LBD within the Hsp90 heterocomplex. Thus, we propose a model in which Hsp90 brings the FKBP52 FK1 domain, more specifically the proline-rich loop, in close proximity to the receptor LBD, which leads to a direct interaction and regulation of receptor hormone binding and subcellular localization. Importantly, recent studies have identified a surface region on the AR LBD that, when mutated, displays increased functional dependence on FKBP52 and this surface overlaps with the binding function 3 (BF3) surface (Fig. 1.2c) [166, 167].

1.4.1 AR BF3 Surface

BF3 is a recently characterized hydrophobic binding pocket on the AR LBD that is located near, but distinct from, the AF2, which acts as a major docking site for short hydrophobic peptide motifs featured in AR co-activators and mediates AR functional amino/carboxy (N/C)-terminal interactions (Fig. 1.2c) [167-172]. The role of BF3 *in vivo* is currently unknown, however, mutational and functional analyses of the surface have confirmed its role in AR activity [173]. Small molecule docking to the BF3 surface resulted in an allosteric modification that prevents the interactions of AF2 with co-activators [167]. In fact, *in vitro* studies along with computational molecular dynamic simulations revealed a structural connection between BF3 and AF2. A series of residues within BF3, the boundary of BF3/AF2, and AF2 are structurally interconnected and allosterically coupled [173]. Importantly, the experiments demonstrated that BF3 mutations function as allosteric elicitors of conformational changes in the AR LBD by altering AF2 propensity to reorganize into hydrophobic sub-pockets that accommodate the N-terminal domain and co-activator peptides, and inhibit co-regulator binding [173]. This induced conformation consequently may either potentiate or silence AR function. In fact, residues in the BF3 pocket have been identified as mutational target sites for PCa and/or androgen insensitivity syndrome (AIS) patients (McGill Androgen Receptor Gene Mutations Database: http://androgendb.mcgill.ca/). The importance of BF3 as a regulatory surface for AR activity

was further highlighted in recent studies by Jehle *et al*. [174] in which a novel hexapeptide repeat sequence, GARRPR, was identified in the N-terminus of the co-chaperone Bag-1L that is involved in the modulation of AR activity by binding to the BF3 pocket. Thus, the AR BF3 surface may serve as a promiscuous regulatory surface for a number of co-regulators, including FKBP52.

1.4.2 Cross-talk between the AR and Wnt/β-Catenin Signaling Pathways in CRPC

β-catenin is a multifunctional protein that plays an important role in embryonic development and tumorigenesis through its effect on E-cadherin-based cell adhesion and Wnt-dependent signal transduction [164]. It also functions as a co-activator of the AR that interacts with the receptor in response to androgen to increase the transcriptional activity of the AR [175]. β-catenin has a central domain consists of 12 armadillo repeats and intrinsically unstructured N- and C-terminal transactivation domains [176-178]. The crystal structure of the armadillo domain of β-catenin revealed that each of the repeat composed of three α-helices and together, adopts a unique superhelix structure that provides a long positively charged groove for protein-protein interaction [176-178]. It is the N-terminus combined with the first six armadillo repeats, especially armadillos 5 and 6 that are primarily responsible for the interaction with AR LBD [179]. It is through this specific interaction that allows β-catenin augmenting the AR activity in a ligand-dependent manner in prostate cancer cells. Unlike other steroid receptor co-regulators, β-catenin only selectively binds to AR, but not to other SHRs [179]. While the crystal structure of the armadillo domain of β-catenin revealed it contains LXXLL pentapeptide that is localized in the second helix of the armadillo repeats 1, 7, 10, and 12 [176]. However, the Leu residues in these motifs are buried in the hydrophobic core of the armadillo repeats consequently they are inaccessible to contribute to the interaction with AR via canonical co-regulator binding site, AF-2 [176]. In addition, mutational disruption of each of five LXXLL peptide motifs in the β-catenin armadillo repeats did not disrupt neither its binding to AR nor inhibit transcriptional co-activation of transcriptional mediators/intermediary factor 2 (TIF2) [180]. These findings

suggest β-catenin interacts with a region on AR LBD other than AF-2. In supporting with this idea, studies have shown β-catenin synergizes with nuclear receptor co-activator glutamate receptor-interacting protein 1 (GRIP1) via a new interaction surface differs from AF-2 on AR LBD [181]. Interestingly, recent co-crystal structural studies of liver receptor homolog-1 (LRH-1)/β-catenin revealed that the receptor utilizes a region of the LBD surface, distinct from AF-2 that was not previously implicated in protein-protein interactions with the armadillo region of β-catenin [182]. Given the high degree of structural similarity in the LBD among members of the nuclear receptor superfamily and the fact that mutations that disrupting LRH-1/β-catenin binding also disrupt AR/β-catenin binding [182], suggests that LRH-1 and AR share a similar β-catenin interaction surface.

There are emergent evidence indicating the cross-talk between AR and Wnt/β-catenin signaling pathways. As aforementioned, β-catenin binds AR directly to stimulate AR-mediated gene transcription, and importantly, the AR gene itself is transcriptional target of β-catenin [179, 180, 183-185]. Wnt-stimulated deactivation of glycogen synthetase kinase 3β (GSK3β) and stabilizing mutations of β-catenin cause an increased levels of nuclear β-catenin and promote AR transcriptional activities under the conditions of androgen ablation [186, 187]. The AR signaling has shown to repress β-catenin/T-cell factor (TCF) mediated-transcription induced by androgen in prostate cancer cells [180, 184, 188]. The enhanced communication between AR and β-catenin has been observed *in vivo* models of CRPC [189]. Finally, Wnt/β-catenin signaling has shown to be highly activated in cancer stem cells (CSCs), which are tumor-initiating cells, and these prostate stem cells are resistant to ADT and responsible for the cancer recurrence [190]. Taken together, these data suggest a role for β-catenin interaction with the AR in the development and progression of PCa from the hormone-dependent to the terminal castrate-resistant stage.

1.4.3 FKBP52 and β-Catenin Act in Concert to Promote Hormone-Independent AR Function

Given that BF-3 is the putative binding and/or regulatory site for FKBP52 with its residues being highly conserved on the surface across the SHRs and both FKBP52 and β-catenin are known positive regulators of AR, it is reasonable to predict that β-catenin interacts with an AR surface that overlaps with the BF-3 (Fig. 1.3). In fact, studies have shown β-catenin binds to a region on LRH-1 that is equivalent to the BF-3 surface on AR LBD [166, 182, 191]. Based on this fact, our lab suggests that both FKBP52 and β-catenin might work in concert at BF-3 surface. Recently, our lab has demonstrated that they do work concomitantly; however, β-catenin requires the presence of FKBP52 to promote its interaction with AR leading to a synergistic upregulation of the receptor activity [192]. Furthermore, the aforementioned MJC13, which has recently been characterized by our lab of its ability to inhibit FKBP52-enhanced AR activity via BF-3 surface in cellular models of prostate cancer, also blocks β-catenin interaction with AR (Fig. 1.3) [192]. Taken together, FKBP52 interacts with β-catenin to promote interaction and regulation of AR activity through BF-3 surface (Fig. 1.3). Thus, development of inhibitors that block protein-protein interactions between the FKBP52/β-catenin/AR may be lead to viable therapies for CRPC.

1.4.4 FKBP52 Proline-Rich Loop

The proline-rich loop that overhangs the FKBP52 PPIase catalytic pocket in the FK1 domain is required for receptor regulation and is hypothesized to serve as an interaction surface with the receptor LBD. Our lab has recently identified several residues (F673, P723, and C806) on the AR LBD that display increased dependence on FKBP52 (also termed FKBP52 hypersensitivity) for function when mutated. This region directly corresponds to the AR BF3 regulatory surface (Fig. 1.2c) [97, 166]. The small molecule FKBP52-specific inhibitor MJC13 binds the AR LBD, but does not compete with hormone and steroid receptor co-activator 2 (SRC-2) binding. In addition, mutations within the BF3 surface differentially affect MJC13 activity. Thus, several lines of evidence suggest that MJC13 targets the AR BF3 surface to

inhibit regulation of AR by FKBP52. This interaction prevents hormone-induced AR/Hsp90/FKBP52 heterocomplex dissociation and nuclear translocation, thus effectively blocking AR-dependent gene expression and androgen-stimulated proliferation in various human prostate cancer cell lines [166]. Taken together, our recent findings suggest that the AR BF3 surface is a putative FKBP52 regulatory and/or interaction surface and the targeting of this surface for the treatment of PCa is an attractive option with fewer side effects. In fact, early preclinical studies for MJC13 suggest an excellent drug safety profile with no toxicity observed at maximum soluble concentrations, and impressive effects on tumor growth in a 22Rv1 prostate cancer xenograft model [193, 194]. Given the unique mechanism of action, MJC13 and other co-chaperone targeting drugs may be able to escape the acquired resistance that is seen with conventional ADT in subsets of patients, depending on the mechanism of resistance. MJC13 and the N-terminal Hsp90 inhibitors lack the ability to inhibit the constitutive activity of AR splice variants found to be up-regulated in CRPC [195]. This is not surprising given the fact that the splice variants lack the Hsp90-binding site in the hormone binding domain. However, MJC13 does not target FKBP52 directly, but targets the putative FKBP52 regulatory site in the AR hormone binding domain.

1.4.5 Targeting FKBP52 Proline-Rich Loop Interactions

Figure 1.4 illustrates known and predicted FKBP52 interactions and possible therapeutic targeting strategies to disrupt FKBP52 regulation of AR. While the targeting of the FKBP52 regulatory surface on AR BF3 is a promising therapeutic strategy that allows for AR-specific targeting, the direct targeting of FKBP52 offers numerous advantages over MJC13 that would lead to a more potent and effective drug. First, the AR BF3 surface represents a less than ideal drug binding site, and, as a result, the effective MJC13 concentrations in cellular assays are in the low micromolar concentration range [166]. In contrast, the FKBP52 PPIase pocket not only represents an ideal hydrophobic drug binding pocket, but is a known ‘druggable target’ as the immunosuppressive drug Tacrolimus (FK506) is already FDA-approved for use in the clinic.

Also, given the conservation within the FKBP PPIase pocket, drugs targeting the FKBP52 PPIase pocket would likely target FKBP52 and the closely related FKBP51 protein simultaneously. While FKBP52, but not FKBP51, is largely considered the relevant steroid hormone receptor regulator, more recent evidence suggests that both FKBP51 and FKBP52 are positive regulators of AR in prostate cancer cells [196]. In addition, FKBP52 is a known positive regulator of AR, GR, and PR, and the direct targeting of FKBP52 would target the activity of all three receptors simultaneously. Increasing evidence suggests that many factors (*e.g.* growth factors, cytokines, and angiogenic factors) implicated in PCa progression are targets of the GR signaling pathway [197, 198]. In addition, recent evidence suggests that GR signaling confers resistance to current antiandrogen treatments [159]. Furthermore, recent studies by Cluning *et al.* showed that H1-H3 loop of GR LBD is not a direct interaction site for FKBP52, however, mutations within the loop can affect FKBP52-mediated receptor activities [199]. Thus, mechanistically, the H1-H3 loop acts as a regulatory surface that promotes conformational changes in BF-3, which is in close proximity and allosterically affects FKBP52-mediated receptor activities (Fig. 1.2c). While very little work has been done to characterize a role for PR in PCa, data suggests that PR expression is elevated in metastatic diseases and that PR antagonists are potential treatments for PCa [200, 201]. Finally, FKBP52 directly regulates NFκB transcriptional activity [202] and inhibition of NFκB was recently demonstrated to restore CRPC responsiveness to ADT [203]. Thus, the direct targeting of the FKBP52 proline-rich loop with small molecules will lead to a more potent drug with the potential to simultaneously hit a variety of targets known to have, or suspected of having, a role in PCa progression. Previous studies demonstrated the functional importance of the FKBP52 proline-rich loop, which establishes this site as the most attractive target site for disrupting FKBP52 interactions with the SHRs. While this surface does not represent an ideal hydrophobic drug binding pocket, the PPIase catalytic pocket does. In addition, the available co-crystal structure of FKBP12, a related family member, bound to FK506 suggests that molecules docked within the PPIase pocket could

re-orient proline-rich loop conformation leading to the disruption of interactions at this surface (unpublished observations).

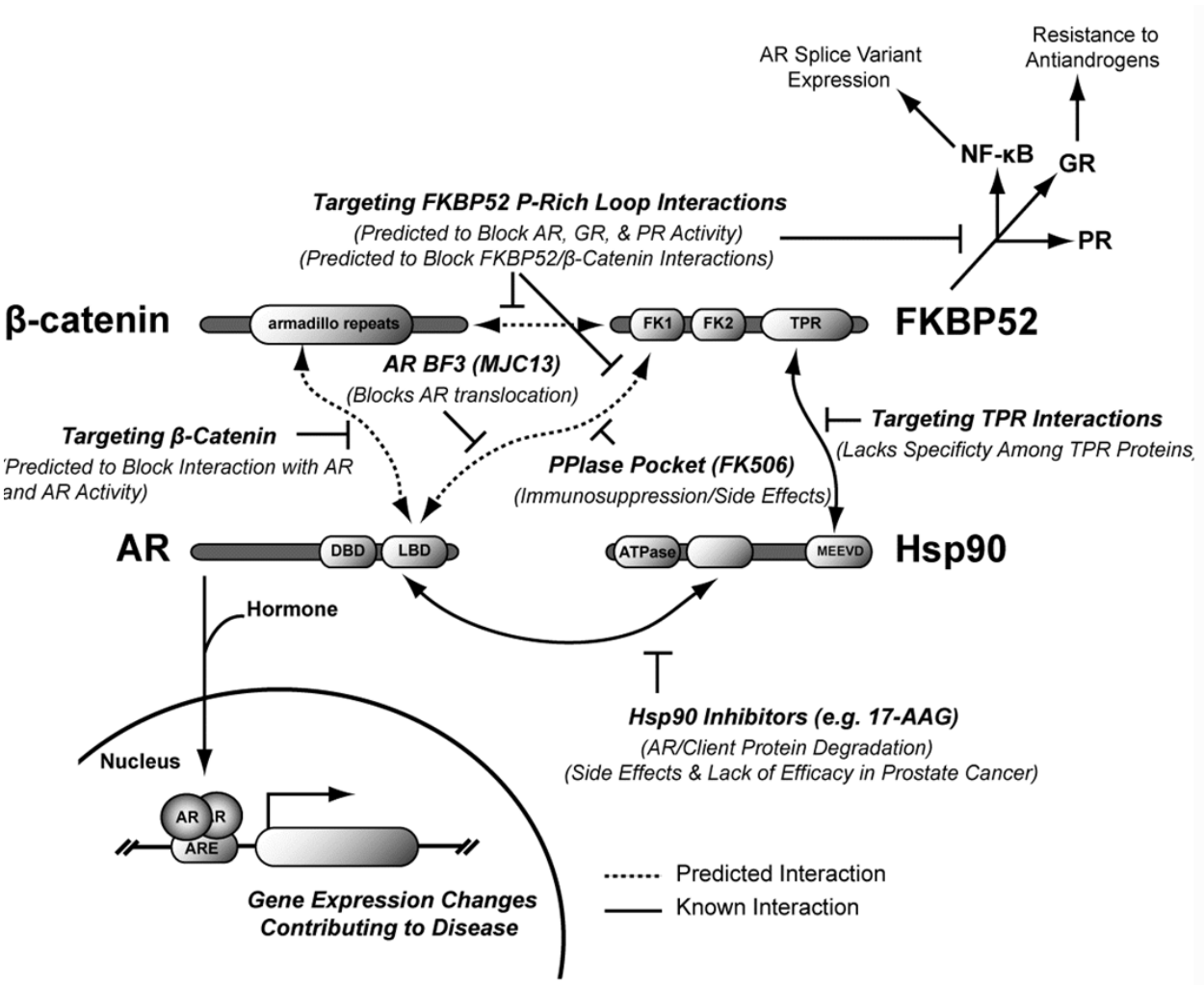

Figure 1.4: FKBP52-Receptor Interactions and Therapeutic Targeting Strategies

Fig. 1.4: FKPB52-Receptor Interaction and Therapeutic Targeting Strategies. Both known (solid arrow) and predicted (dashed arrow) FKBP52-Hsp90-receptor interactions are illustrated in addition to possible strategies for therapeutically disrupting chaperone/co-chaperone regulation of AR-mediated transcription for the treatment of prostate cancer. FKBP52 is a known positive regulator of AR function that associates with the EEVD motif in the C-terminus of Hsp90 by way of a TPR domain. In addition, the FKBP52 FK1 domain, the PPIase pocket, and the proline-rich loop in particular, comprise a functionally important interaction surface that is predicted to interact with the AR hormone binding domain. The prevailing hypothesis is that Hsp90 brings FKBP52 in close proximity to the receptor allowing the FKBP52 FK1 domain to directly contact the receptor hormone binding domain. Our recent data suggest that this contact site is the AR BF3 surface. As detailed, several drug classes already exist for the inhibition of Hsp90 (geldanamycin and derivatives) and FKBP52 (FK506 also called Tacrolimus). Geldanamycin is currently in phase III clinical trials for the treatment of various cancers, but has proven ineffective in prostate cancer. Tacrolimus is currently used clinically to suppress the immune system during organ transplantation, and the immunosuppressive effects would be undesirable in a prostate cancer drug. However, the success of Tacrolimus in the clinic indicates that FKBP52 is a "druggable" protein. Targeting of the FKBP52 TPR domain, which would theoretically disrupt FKBP52 interactions with Hsp90, is a possible approach. However, the TPR motif is highly conserved and any molecule that targets the FKBP52 TPR would also likely target a large number of other TPR proteins. The targeting of the proposed FKBP52/β-catenin binding site on the AR hormone binding domain is also an attractive option. This approach is represented by the compound termed MJC13 and derivatives that were recently developed by our laboratory. Directly targeting the FKBP52 proline-rich loop represents the most promising approach as FKBP52 is a "druggable" protein and the proline-rich loop has been found to be critical for FKBP52 regulation of AR activity.

1.5 Dissertation Project Rationale and Hypothesis

The Hsp90-associated FKBP52 co-chaperone has become increasingly associated with aberrant SHR signaling in diseases. FKBP52 is a TPR-containing co-chaperone that plays a critical role in the chaperone-dependent folding of SHRs to their functionally mature conformations that are competent for hormone binding. Given the functional roles of FKBP52 in receptor-specific phenotypes, and its direct participation in the aberrant AR hyperactivity observed in PCa, FKBP52 has emerged as a novel therapeutic target with the potential to treat CRPC; thereby filling a major unmet need in PCa treatment. We hypothesized that specific small molecules targeting the FKBP52 PPIase pocket will disrupt FKBP52 proline-rich loop interactions leading to the effective inhibition of AR, GR, and PR signaling, prostate cancer cell proliferation, and attenuate the expression and/or secretion of prostate cancer biomarkers. In addition to PCa, the therapeutic targeting of FKBP52 proline-rich loop interactions represents an attractive treatment option for a number of diseases associated with the AR, GR, and PR signaling pathways including benign prostatic hyperplasia, obesity/metabolic syndrome, stress and depression, and Cushing's syndrome. Furthermore, drugs targeting FKBP52 regulation of SHR activity may have utility as male and/or female contraceptives.

1.6 Dissertation Goals

The overall goal of the project was to develop first-in-class drugs targeting the FKBP52 PPIase pocket for the disruption of proline-rich loop interactions with AR for the treatment of PCa. The objective was addressed by the following studies:

1. Identification of novel FKBP52-specific molecules that inhibit FKBP52-enhanced receptor function using structure-based virtual screening.
2. Molecular and cellular evaluations of the lead compound in various prostate cancer cellular models.
3. Verification of the lead compound drug target site.

4. Solution formulation development of GMC1 and perform preclinical evaluations of the lead compound in murine prostate cancer model.

The data ultimately gleaned from these studies will establish “indirect AR targeting” through the inhibition of FKBP52 as a promising strategy in combating PCa with limited off-target effects. Furthermore, it may provide insights into novel roles for the FKBPs in PCa and other hormone-dependent diseases, and provide a better understanding of how the co-chaperone regulates receptors from a structural and mechanistic point of view.

CHAPTER 2: IDENTIFICATION OF SMALL MOLECULE INHIBITORS SELECTIVELY TARGETING FKBP52 PROLINE-RICH LOOP INTERACTIONS USING STRUCTURE-BASED METHODOLOGY

2.1 RATIONALE

As aforementioned, FKBP52 is an Hsp90-associated co-chaperone and acts as a positive regulator of a small subset of Hsp90 client proteins including AR, GR, and PR. The co-chaperone potentiates these receptor signaling pathways via interactions between the proline-rich loop overhanging the PPIase catalytic pocket located in the FK1 domain and the AR BF3 surface on the LBD. It is important to note that the structural integrity of the loop, not the PPIase enzymatic activity, is functionally crucial for the regulation of receptor activity. There are several lines of evidence that demonstrate direct targeting of FKBP52 for the disruption of proline-rich loop interactions with LBD can serve as a highly specific therapeutic strategy to inhibit FKBP52-mediated Hsp90-dependent and independent diseases including PCa. First, *fkbp52*-deficient mice display phenotypes related to defective AR, GR, and PR signaling. Second, prostate cancer cells have been shown to bypass AR-dependence through the GR signaling pathway [159, 204-207]. Third, studies have demonstrated PR expression is often elevated during the progression of metastatic and recurrent prostatic adenocarcinoma and PR antagonists have potential in treating PCa [200, 201]. Lastly, FKBP52 has been proven to be a "druggable" target, which means it can be targeted without significant off-target effects and circumvent undesirable side effects and resistance mechanisms associated with current ADT. In our attempts to discover new small molecules inhibitors that could specifically target the proline-rich loop, we performed a structure-based *in silico* screen of a library of commercially available molecules. Unfortunately, the proline-rich loop interaction surface does not represent an ideal hydrophobic drug binding site, but the highly conserved PPIase catalytic pocket does, which provides a foundation for structure-based drug design. In addition, the co-crystal structure of FKBP12, a related family member, bound to the FK506 ligand suggests that molecules docked within the PPIase pocket could re-orient proline-rich loop conformation leading to the disruption of the FKBP52/receptor interaction surface. Therefore, in this study, we targeted the FKBP52 PPIase catalytic pocket with small molecules to disrupt the proline-rich loop interactions leading to effective inhibition of FKBP52-regulated AR activities.

2.2 MATERIALS AND METHODS

2.2.1 Protein and Ligand Preparation

The crystal structures were prepared using the Protein Preparation Wizard implemented in Maestro 9.3 (Schrödinger, LLC) [208]. The hydrogens were added, bond orders were assigned, and missing side chains for some residues were added using Optimized Potential for Liquid Simulations (OPLS)-2005 force field, and the receptor grid was defined using a 20 Å box centered on the crystallographic ligand. A library of 3 million commercially available molecules from the ZINC database [209] was imported into Molecular Operating Environment (MOE) 2011. All the molecules were protonated/deprotonated by a washing process, added partial charges and minimized with the Merck Molecular Force Field (MMFF) 94x force field to a gradient of 0.0001 kcal/mol Å. Duplicate compounds in the database were removed using the db _unique.svl module from the MOE.

2.2.2 Molecular Docking-Based *In Silico* Screening of Potential FKBP52 PPIase Pocket Inhibitors

Two docking programs, Glide and eHiTs, were used for virtual high-throughput screening implemented on a Sun Grid Engine Cluster [210, 211]. The Glide SP mode was initially used for filtering out compounds with low docking scores (SP < -5.5). The active binding site was defined from the coordination of crystallographic ligand (PDB code: 4LAX) [92] using the default settings. To avoid any bias in docking programs, compounds with favorable Glide scores were subsequently docked by eHiTs, and compounds with eHiTs score higher than cutoff value (-1) were removed. The root-mean-square deviation (RMSD) of the docked poses generated by Glide and eHiTs were then calculated to keep compounds with consistent docked poses. Compounds with high RMSD values (> 2.5) were removed. Subsequently, the glide poses was re-scored by multiple scoring functions (glide SP, XP, Xscore, Pki, and LonDonDG). Depending upon the scores, each molecule received a vote value of “1” for every top 10% appearance by ranking of each score, which then generated a consensus voting for the selection. Following the ranking of the consensus voting value, top virtual hits were

visualized and compounds with favorable interactions were selected. All tested compounds were then purchased from commercial vendors for empirical testing.

2.2.3 Cell Culture

MDA-kb2 cells were purchased from the American Type Culture Collection (ATCC® CRL-2713™) and express firefly luciferase under control of the MMTV promoter that contains response elements for both AR and GR. They were maintained in Hyclone™ Leibovitz's L-15 Medium (Thermo Scientific) supplemented with 10% fetal bovine serum (FBS, Atlas) at 37°C without supplemental CO_2. Mouse embryonic fibroblast cells from homozygous FKBP52 knockout embryos (52KO MEF) were generated as previously described [98]. They were maintained in Hyclone™ Minimal Essential Media/Earle's Balanced Salt Solution (MEM/EBSS) containing 2 mM L-glutamine (Thermo Scientific) supplemented with 10% FBS at 37°C with supplemental 5% CO_2.

2.2.4 Mammalian Cell-Based Luciferase Reporter Assays

MDA-kb2 cells were used for the Bright-Glo™ luciferase assay system (Promega) to screen the hit compounds. The cells were plated at 4 x 10^4 cells per well in 96-well luminometer plates in 100 µl of Hyclone™ Leibovitz's L-15 Medium with 10% FBS and allow to attach at 37°C without supplemental CO_2. When cells were attached, they were washed three times and replaced with 100 µl of medium containing 10% charcoal-stripped FBS (CS-FBS; Corning) at 37°C without supplemental CO_2. The next day, the medium was replaced with 100 µl of fresh medium containing 10% CS-FBS per well dosing with ethanol (EtOH) only (agonist vehicle control), dimethyl sulfoxide (DMSO) only (hit compound vehicle control), DMSO + EtOH (negative control), DMSO plus the agonist (dihydrotestosterone, DHT, at 200 pM, which is an EC_{50} for the hormone in this cell line; positive control), or the agonist plus a hit compound at a concentration range of 10 nM, 100 nM, 1 µM, 10 µM, and 100 µM, incubated for 16-20 h at 37°C without supplemental CO_2. The final EtOH concentration in each well did not exceed 1% nor did the DMSO. Then the AR luciferase reporter assay was performed and activity measured

according to manufacturer's instructions. Relative light units (RLU) per well were determined using a microplate luminometer (Luminoskan Ascent, Thermo Labsystems). Individual compound at each concentration was assayed independently at least 3 times with duplicate wells per each replicate assay.

52KO MEFs were used to assess FKBP52-regulated AR-mediated luciferase activity. The cells were seeded at 2 x 10^5 cells per well in 6-well tissue culture-treated plates at approximately 80% confluency in 1.5 mL of Hyclone™ MEM/EBSS containing 2 mM L-glutamine with 10% FBS and allowed to attach at 37°C with supplemental 5% CO_2. Once the cells were attached, medium was removed and replaced with 1 mL of Hyclone™ MEM/EBSS containing 2 mM L-glutamine without 10% FBS plus 500 µL of transfection mixture after washed 3 times with the medium and allowed to incubate at 37°C with supplemental 5% CO_2 for 4-6 h. The plasmids were transfected using Lipofectamine® 2000 Reagent (Invitrogen™, Thermo Scientific) according to the manufacture protocol with a DNA to Lipofectamine® ratio of 1:3 in Hyclone™ MEM/EBSS containing 2 mM L-glutamine without 10% FBS. The plasmids used for the experiments were as follows: a constitutive β-galactosidase expression plasmid (50 ng per well; transfection control), a hormone-responsive firefly luciferase reporter (400 ng per well), a mammalian expression vector (pCI-Neo; Promega) expressing AR (800 ng per well), an empty pCI-Neo (800 ng per well; negative control), and a pCI-Neo expressing FKBP52 (800 ng per well). After the transfection incubation, the medium was removed and replaced with 1.5 mL of Hyclone™ MEM/EBSS containing 2 mM L-glutamine supplemented with 10% CS-FBS. 24 h after the transfection, cells were treated with indicated inhibitor concentrations for 30 min followed by the treatment with DHT in fresh 1.5 mL of Hyclone™ MEM/EBSS containing 2 mM L-glutamine supplemented with 10% CS-FBS. Stock inhibitors and DHT concentrations were prepared in DMSO and EtOH, respectively. The DHT concentrations used in the experiment corresponded to the pre-determined EC_{50} at each experimental condition; the mammalian expression vector control group at 1 nM and mammalian expression vector expressing FKBP52 group at 10 pM. In no case did the EtOH and DMSO concentrations exceeded 0.1% and 1%,

respectively. After 16-18 h of the treatment, the cells were washed with Hyclone™ phosphate buffered saline (PBS; Thermo Scientific) at room temperature, and then 150 µL lysis buffer (10 mL of M-PER™ Mammalian Protein Extraction Reagent plus 100 µL of Halt™ Protease Inhibitor Cocktail, ethylenediaminetetraacetic acid (EDTA)-free; Thermo Scientific) were added per well incubated for 10 min at room temperature on a plate shaker. The cell lysates were collected by centrifugation at 15,000 rpm at 4°C for 20 min. Luciferase expression was quantified using Luciferase Assay System (Promega) with 40 µL of cell lysate with 100 µL of the reagent per well in an opaque 96-well plate and RLU per well were determined immediately using Synergy 2 Multi-Mode Microplate Reader (BioTek). β-galactosidase expression was quantified using the Tropix® Gal-Screen™ assay system (Applied Biosystems) with 10 µL of cell lysate with 100 µL of the reagent per well in an opaque 96-well plate according to the manufacturer protocol, incubated for 2 h in the dark at room temperature, then RLU were measured using Synergy 2. Ar-dependent reporter expressions were normalized against transfection efficiencies by dividing luciferase RLU by the β-galactosidase RLU.

2.2.5 Statistical Analysis

All data are presented as mean ± standard deviation and is the average of triplicate biological samples in a single experiment. Each experiment was repeated at least three independent times. The graphs presented represent the average from all experiments. GraphPad PRISM software (GradphPad Inc.) was used for generate the graphs.

2.3 RESULTS

2.3.1 Identification of Key Interaction Sites on the FKBP52 PPIase Pocket

As aforementioned, the FKBP52 proline-rich loop is not a druggable hydrophobic binding site, but the PPIase catalytic pocket underneath the loop is. Thus, we hypothesized that specifc small molecule interactions within the PPIase pocket would reorient proline-rich loop conformation leading to the disruption of the receptor interaction surface. The PPIase catalytic pocket in the FK1 domain of FKBP52 is a very hydrophobic surface with only few polar

residues. The co-crystal structure of FKBP52 FK1 domain with FK506 bound in the PPIase pocket was not solved at the beginning of this study. Thus, FKBP12 in complex with FK506 was used as a reference. FK506 binding to FKBP12 shows three key hydrogen bond interactions between the ligand and Asp37, Ile56, and Tyr 82, which correspond to Asp68, Ile87, and Tyr113 in FKBP52 (Fig. 2.1). These polar residues were predicted to be critical in anchoring possible binding of small molecules.

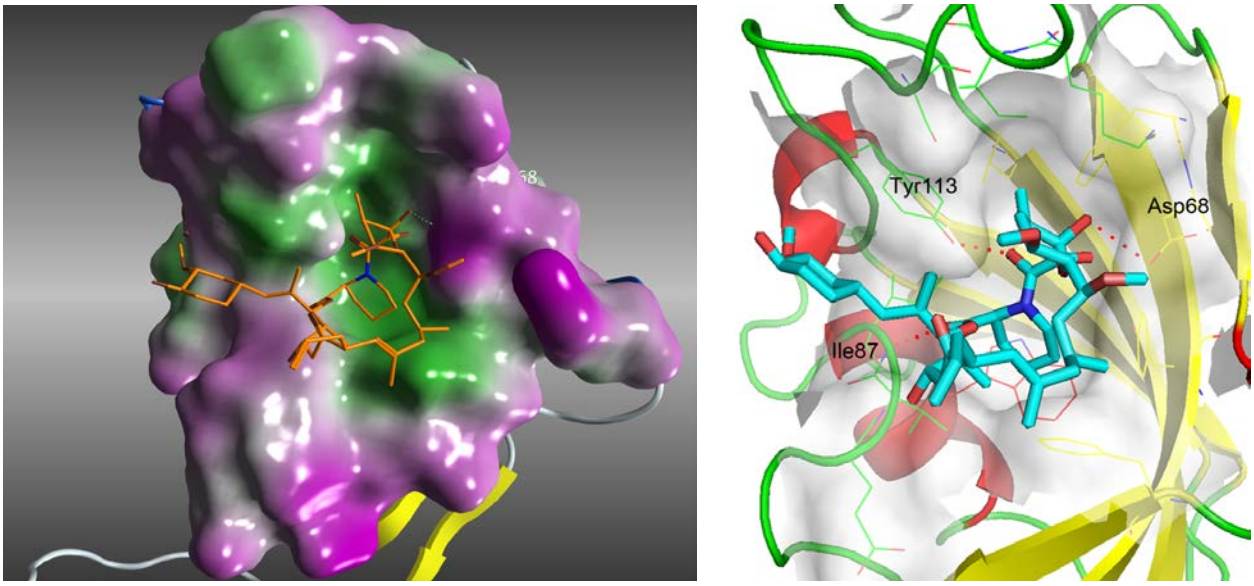

Figure 2.1: Structure-Based Design of Direct FKBP52 Targeting Small Molecule Inhibitors

Left panel depicts the 3D image of co-crystal structure of FKBP52 with FK506 in the PPIase site in FK1 domain (PDB code: 4LAX). Right panel illustrates the polar residues Asp68, Ile87, and Tyr113 form key interactions between the ligand and FKBP52 PPIase pocket. The FK1 domain and FK506 are in cartoon and stick representation, respectively. The red dashed lines indicate hydrogen bonding.

2.3.2 *In Silico* Identification of Hit Compounds Targeting the FKBP52 PPIase Catalytic Pocket

The ZINC molecular database containing approximately 3 million lead-like compounds was processed against the identified binding site on the PPIase catalytic pocket through a virtual screening pipeline. They were subjected to two docking programs, Glide and eHiTs, using SP < -5.5 and eHiTs score < -1 as cutoffs resulting 508,213 molecules left. Subsequently, RMSD values were calculated between the docked poses from these programs, and only molecules (8,072 molecules) with consistent pose were retained ($0 < RMSD < 2.5$). Finally, based on the consensus voting values, top virtual hits were visualized and those did not retain the key interactions were eliminated resulting in 40 selected hit compounds, which all maintain the hydrogen bond interactions with Asp68, Ile87, and Tyr113, for functional screening.

2.3.3 *In Vitro* Evaluation and Identification of a Small Molecule Inhibitor that Targets FKBP52-Specific Regulation of AR Function

The MDA-kb2 cell line is a breast cancer cell line that contains stable AR and GR-responsive luciferase reporter genes which means any compounds that act through either AR or GR-mediated signaling can be detected [212]. Additionally, this cell line was derived from a single stable clone, which does not require transfection of the receptors, and is relatively easy to culture and maintain. Thus, it serves as an inexpensive tool for screening drug molecules with minimal inter and intra-assay variability. The 40 hit molecules out of initial 3 million lead-like compounds from the ZINC library were commercially purchased and assessed for their ability to inhibit AR-mediated luciferase reporter expression in MDA-kb2 cells with a range of concentrations. Any molecules that displayed an increased potency with a full inhibitory curve in the assay were further assessed for inhibitory effects on FKBP52-specific regulation of AR activity in 52KO MEFs. This cell line was used because they are the only existing cells that could provide a true FKBP52-negative background for evaluating FKBP-specific effects of the drug candidates.

The selected molecules that displayed inhibitory effects on AR-mediated luciferase expression in MDA-kb2 cells were initially subjected to testing for the ability to specifically inhibit FKBP52-regulated receptor activity at a single high dose of 100 μM. Any molecules that demonstrated FKBP52-specific inhibitory effects on AR function at a single high dose were subsequently assessed at a range of concentrations to determine the IC_{50} values. It is important to note that the hormone-induced receptor activity requires a very high hormone concentration in the absence of FKBP52, therefore the receptor activity in the presence and absence of the co-chaperone was assessed at a low and high hormone concentrations at 10 pM and 1 nM, respectively. The AR activity in the absence of FKBP52 served both as controls for FKBP52-specificity and general cellular toxicity.

GMC1 was our resulting lead molecule that displayed the most potent FKBP52-specific inhibition of AR activity (Fig. 2.2). It showed an increased potency with maximal inhibition of AR activity at 100 μM and an IC_{50} value of 8.83 μM (Fig. 2.2a). GMC1 also demonstrated a significant reduction of FKBP52-regulated AR-mediated luciferase expression at 100 μM (data now shown) and displayed a full inhibitory curve with an IC_{50} value at 0.6576 μM (Fig. 2.2b). Fig 2.2c depicts the molecular docking of GMC1 into the FKBP52 PPIase site with key polar residues Asp68, Ile87, and Tyr113.

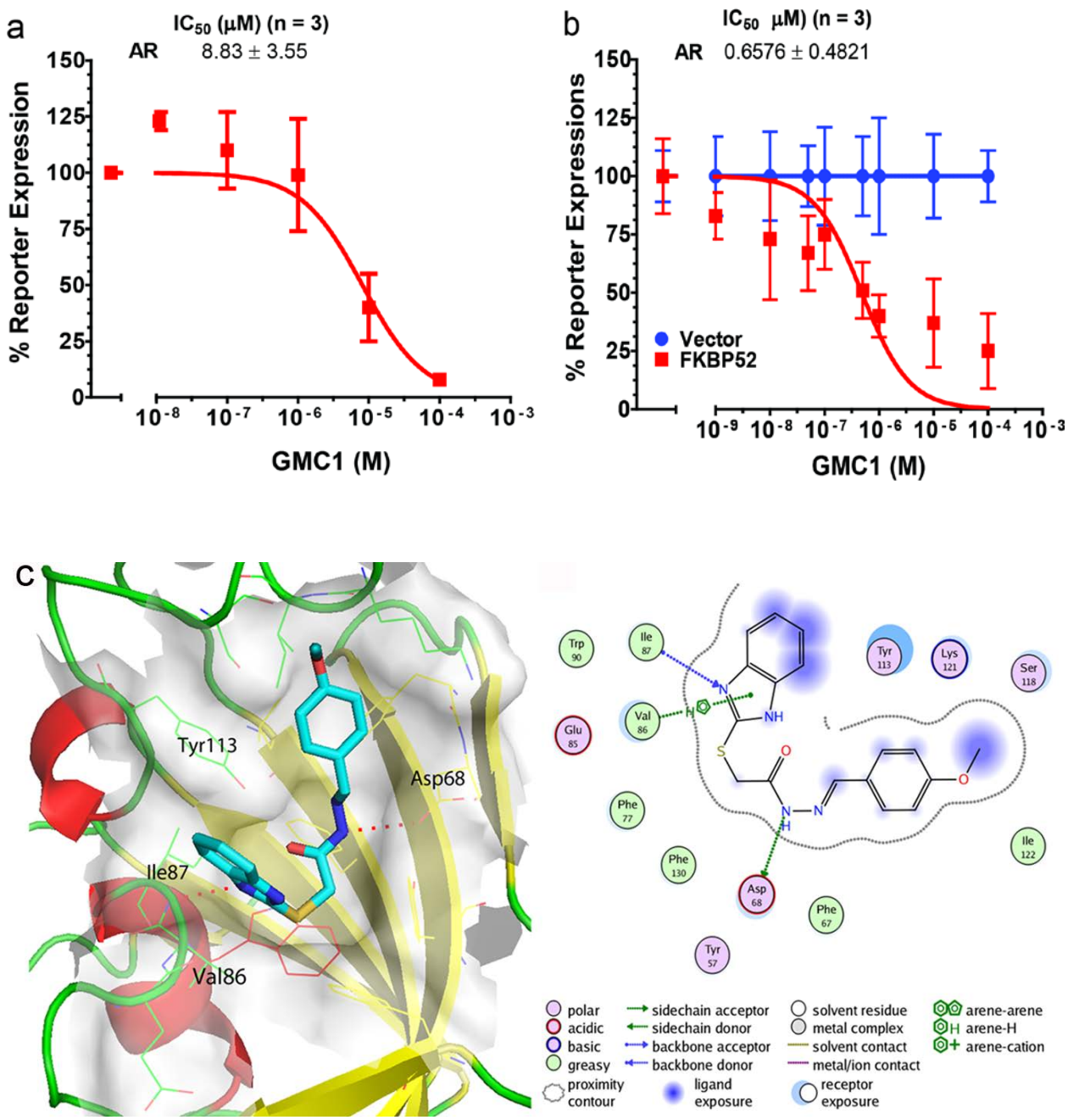

Figure 2.2: GMC1 Inhibits FKBP52-Specific AR-Mediated Activity

Fig. 2.2: GMC1 Inhibits FKBP52-Specific AR-Mediated Activity. (a) MDA-kb2 cells expressing stably transfected AR- and GR-responsive luciferase reporter genes were treated with 200 pM DHT and a range of GMC1 concentrations (0, 0.01, 0.1, 1, 10, and 100 μM) for 16-20 h for testing AR-dependent activity. The graph depicts an average of three independent receptor-mediated luciferase reporter experiments. **(b)** The graphs demonstrated an average of three independent luciferase reporter assays in 52KO MEF cells in the presence and absence of FKBP52 treated with 10 pM DHT and 1 nM DHT, respectively, and a range of GMC1concentrations (0, 0.001, 0.01, 0.05, 0.1, 0.5, 1, 10, 100 μM) for the assessment of FKBP52-specific AR-mediated activity. Each IC_{50} value is represented as means ± s.d. of an average of three independent experiments. **(c)** The ZINC database with 3 million lead-like compounds was processed through the *in silico* screening pipeline and 40 molecules were selected for functional testing. The left panel of **(c)** depicts the docked pose of identified lead molecule GMC1 (cyan) in the FKBP52 PPIase site with key residues labeled. The right panel of **(c)** shows the GMC1-FKBP52 interactions in a 2D diagram.

2.4 DISCUSSION

In this study, we showed that the FKBP52 PPIase catalytic pocket represents a viable drug target for small molecules using structure-based virtual screening methods. We employed FKBP12 in complex with FK506 as a reference, which was later confirmed with the resolved co-crystal structure of FKBP52 FK1-FK506, and identified a predicted target site within the PPIase pocket containing Asp68, Ile87, and Tyr113 as three key residues forming hydrogen bonding with ligands. Using the FKBP52 PPIase as a target site for the *in silico* screen, we obtained 40 structurally diverse hit compounds from 3 million commercially available chemical structures. We evaluated the effect of these selected hit compounds on AR-mediated reporter activity using MDA-kb2 cells. From that screen, we selected compounds that displayed a full inhibitory curve against hormone-induced receptor activity. In order to determine whether the observed inhibition of AR signaling in MDA-kb2 cells was due to FKBP52-specific effects, the molecules were then tested in 52KO MEFs. GMC1 was the resulting lead molecule that demonstrated potent FKBP52-specific AR-regulated signaling with an IC_{50} value at high nanomolar concentrations. Interestingly, GMC1, without optimization by structure-activity relationship (SAR) analysis, inhibited AR activity at a concentration comparable to the AR BF3-binding drug, MJC13, which was developed and optimized previously by our lab. This suggests that disruption of the FKBP52 proline-rich loop interaction with AR is a more potent drug target than targeting the LBD surface. Thus, GMC1 represents a novel and powerful first-in-class drug for directly targeting FKBP52 for the disruption of steroid hormone receptor activity.

CHAPTER 3: *IN VITRO* EVALUTION AND CHARACTERIZATION OF GMC1 IN PROSTATE CANCER CELLULAR MODELS

3.1 RATIONALE

The androgen and AR are central drivers of PCa development and progression as evidenced by the life prolonging effects of ADT using antiandrogens. Antiandrogens are compounds that compete with endogenous androgens for AR, a hormone activated transcription factor, and thereby blocking the biological effects of testosterone and DHT by inducing conformational change of the receptor leading to the inhibition of AR-dependent transcription. Unfortunately, a majority of patients treated with antiandrogens will eventually develop CRPC within 2 years of initial treatment and it is currently incurable [156, 213]. Mounting evidence has suggested that therapeutic failure and castration-resistant progression of the disease are due to resurgence of AR activity [214, 215]. Mechanisms of resistance include AR mutation and amplification, increased intracellular testosterone production, altered co-regulator expression, alternative activation through signaling cross-talk, and elevated expression of constitutively active AR splice variants. [216-221]. In some cases, the AR is bypassed by the activation of alternative signaling pathways such as GR [159, 204-207]. Thus, treatments for CRPC represent a huge unmet clinical need.

It is important to note that AR activity is necessary but not sufficient for the emergence and survival of PCa. Therefore, therapeutic strategies that down-regulate AR activity can be complemented by alternative strategies that target mechanisms promoting cancer metastasis. MJC13 is an excellent example that a first-in-class drug that targets an AR regulatory surface other than LBD is a viable approach to inhibit AR action in early hormone-dependent PCa as well as in CRPC. The compound acts as a surface-directed antagonist inhibiting FKBP52-enhanced AR activity by binding to the AR BF3 surface. BF3 is a novel AR surface that is required for receptor activity; it is often subject to natural mutation in patients with PCa and in AIS. A line of evidence has suggested BF3 constitutes a multifunctional interaction surface for proteins like FKBP52, β-catenin, and Bag-1L [167, 173, 192]. MJC13 has demonstrated effects not only in promoting arrest of the AR-FKBP52-Hsp90 complex in the cytoplasm, reducing rates of AR nuclear translocation, and inhibiting DHT-dependent transcriptional activity; but also in

blocking SRC2 and β-catenin interactions with the receptor [192, 222]. Additionally, MJC13 displays inhibitory effects on androgen responsive genes indistinguishable from classic AR antagonists [222]. Furthermore, it demonstrates impressive inhibitory effects on tumor growth in a prostate cancer xenograft model [223]. Thus, a new class of NRAMs that targets novel regulatory surfaces on AR presents as an attractive therapeutic option.

As aforementioned, targeting AR regulatory proteins including receptor-associated co-chaperones also represents a compelling therapeutic opportunity. FKBP52 is such a candidate that we believe would lead to a more potent and effective drug in treating early hormone-dependent PCa as well as CRPC compared to MJC13 and current FDA-approved antiandrogens. As discussed in Chapter 2, we have demonstrated that the FKBP52 PPIase catalytic pocket is an ideal hydrophobic drug-binding site and targeting it disrupts the architectural integrity of the overhanging proline-rich loop, which is an important interaction surface between the co-chaperone and its specific Hsp90 client proteins including AR, GR, and PR. Given the fact that a combined chemotherapy and GR agonist is a standard treatment in CRPC patients and PR expression is often elevated during the progression of metastatic and recurrent prostatic adenocarcinoma, we believe that a molecule targeting FKBP52 directly would have multiple effects on a variety of targets known to have, or suspected of having, a role in PCa. The resulting initial lead molecule termed GMC1 from Chapter 2 has demonstrated a potent inhibitory effect on FKBP52-specific AR-regulated activity with an IC_{50} value that was comparable to MJC13, which has already been structurally optimized. In this study, we planned to demonstrate that GMC1 inhibits both FKBP52-regulated GR and PR activities and generate proof-of-concept data in various prostate cancer cellular models via detailed *in vitro* evaluations to establish FKBP52 PPIase targeting GMC1 as an effective therapy for PCa.

3.2 MATERIALS AND METHODS

3.2.1 Cell Culture

MDA-kb2 and 52KO MEF were acquired and maintained as described in Chapter 2.2.3. T47D-KBluc (CRL-2865™), 22Rv1 (CRL-2505™), and PC3 (CRL-1435™) were purchased from ATCC. T47D-Bluc cells were generated by stably transfecting T47D human breast cancer cells, which naturally express ERα and ERβ, with pGL2.TATA.Inr.luc.neo that contains three estrogen responsive elements (ERE) upstream of a luciferase reporter gene. They were selected for responsiveness to 17β-estradiol (E2) and were used to screen compounds for estrogenic or anti-estrogenic activity. 22Rv1 is a human prostate carcinoma epithelial cell line derived from a xenograft that was serially propagated in mice after castration-induced regression and relapse of the parental, androgen-dependent CWR22 xenograft [224]. During the progression to androgen independence, an in-frame tandem duplication of exon 3 that encodes the second zinc finger of the AR DNA-binding domain (DBD) occurred, resulting in a constitutively active truncated form of AR lacking the C-terminal LBD [225]. As a result, 22Rv1 cells display both androgen-responsive and androgen-insensitive characteristics. PC3 is an androgen-independent prostate cancer cell line that was derived from a grade IV prostatic adenocarcinoma that metastasized to bone and is negative in AR expression. LNCaP were both purchased from ATCC (CRL-1740™) and generously provided by Dr. Donald Tindall (Mayo Clinic, Rochester, MN). The cell line was derived from a metastatic site of prostate carcinoma and characterized with a T877A mutation in AR LBD [226, 227]. T47D-BLuc and LNCaP were maintained in Hyclone™ RPMI 1640 containing 25mM HEPES and L-glutamine (Thermo Scientific) supplemented with 10% FBS. 22Rv1 were cultured in Hyclone™ RPMI 1640 containing 25mM HEPES and L-glutamine supplemented with Hyclone™ 1% sodium pyruvate (Thermo Scientific), Hyclone™ 1% MEM-nonessential amino acids (MEM-NEAA, Thermo Scientific), and 10% FBS. PC3 were maintained in Gibco® Ham's F12 medium containing L-glutamine supplemented with 5% FBS (Thermo Scientific). T47D-KBluc, LNCaP, 22Rv1, and PC3 were all cultured at 37°C in a humidified environment of 5% CO_2.

3.2.2 Transient Transfections and Luciferase Reporter Assays

The MDA-kb2 and 52KO MEF luciferase reporter assays were performed as previously described in Chapter 2.2.4 with a few modifications. A GR agonist, dexamethasone (DEX; 50 nM), was used to induce GR-mediated luciferase expression in MDA-kb2. The 800 ng per well of mammalian expression vector plasmid (pCI-Neo; Promega) expressing human GR or PR instead of AR were used in the transfection cocktail to determine FKBP52-regulated GR and PR-mediated activities. The deoxycorticosterone (DOC) and progesterone (P4) concentrations used in the experiment corresponded to the pre-determined EC_{50} values at each experimental condition; the 500 nM DOC and 2.5 nM P4 were used in mammalian expression vector control groups and 50 nM DOC and 100 pM P4 were used in mammalian expression vector expressing FKBP52 groups.

LNCaP cells were used to assess GMC1 effects on AR-dependent prostate specific antigen (PSA) luciferase activity. The cells were seeded at 1.5 x 10^5 cells per well in 24-well plates in 500 µL of standard growth media as described in section 3.2.1. The following day, the PSA-Enhancer/Promoter Luciferase (EPLuc) plasmid (0.5 µg per well) was transfected using Lipofectamine® 2000 Reagent with Opti-MEM® reduced serum media containing L-glutamine (Thermo Scientific). The PSA-EPLuc plasmid was constructed as previously described [228]. A 621-bp fragment of PSA minimal promoter (_610 to _11 nt) was amplified by PCR and cloned at the *Sma*I and *Xho*I sites of pGL3-basic luciferase vector (Promega), after which an 823-bp upstream enhancer fragment (_4758 to _3935 bp) containing the _4.1/_3.9 kb PSA core enhancer region was obtained by PCR and inserted upstream of the PSA promoter at *Sac*I and *Sma*I sites resulting in a PSA-EPLuc reporter construct. After 6 h of incubation with transfection mixture, the Opti-MEM® reduced serum media containing L-glutamine was replaced with standard growth media as described previously with the addition of DMSO (inhibitor vehicle control; positive control), Bicalutamide, MDV3100, MJC13, or GMC1 at indicated concentration range, incubated for 24 h at 37°C with supplemental 5% CO_2. The final DMSO concentration in each well did not exceed 0.1%. The cells were harvested and lysed with 100 µL per well of Reporter

Lysis Buffer (Promega). Then the PSA luciferase reporter activity was performed and measured using the Luciferase Assay System (Promega) according to manufacturer's instructions. RLU per well were determined using a Perkin Elmer 420 multi-label counter. Results are represented as relative luciferase activities.

T47D-KBluc cells were used for the Bright-Glo™ luciferase assay system to determine GMC1 effects on ER-regulated activity. The cells were plated at 3 x 10^4 cells per well in 96-well plates in 100 µl of Gibco® RPMI Medium 1640 containing L-glutamine without phenol red (Life Technologies™) supplemented with 10% CS-FBS at 37°C in a humidified environment of 5% CO_2. The medium was replaced the next day with 100 µl of fresh medium without phenol red containing 10% CS-FBS per well dosing with EtOH only (agonist vehicle control), DMSO only (GMC1 vehicle control), DMSO + EtOH (negative control), DMSO plus the agonist (E2, at 10 pM, which is an EC_{50} for the hormone in this cell line; positive control), or the agonist plus GMC1 at a concentration range of 1 nM, 10 nM, 50 nM, 100 nM, 500 nM, 1 µM, 10 µM, and 100 µM, incubated for 16-20 h at 37°C with supplemental 5% CO_2. The final EtOH concentration in each well did not exceed 1% nor did the DMSO. The ER luciferase reporter activity was measured according to the manufacturer's instructions. RLU per well were determined using a Luminoskan Ascent microplate luminometer. GMC1 at each concentration was assayed independently 3 times (3 replicate assays) with duplicate wells per each replicate assay.

3.2.3 Western Immunoblot Analysis

LNCaP and 22Rv1 cells were used to assess GMC1 effects in AR and AR-dependent gene expression. The cells were plated at a density of 5 x 10^5 cells per well in 12-well plates in 1 mL of respective standard growth media as detailed in section 3.2.1 and incubated at 37°C with supplemental 5% CO_2 and allowed to attach for 48 h. The media were removed and cells were then washed three times and replaced with fresh 1 mL of respective growth media modified by replacement of 10% FBS with 10% CS-FBS at 37°C with supplemental 5% CO_2. After 48 h, the

cells were treated with DMSO + EtOH (negative control), DMSO + agonist (DHT, 50 nM for LNCaP and 1 nM for 22Rv1, positive control), or the agonist with a range of GMC1 concentrations (100 nM, 500 nM, 1 µM, 10 µM, 25 µM, 50 µM, 75 µM, and 100 µM) for 24 h. The final EtOH and DMSO concentrations in each well did not exceed 0.1% and 1 %, respectively. The cells were lysed and collected as described in Chapter 2.2.4. The protein concentration was quantitated with Peirce™ Coomassie (Bradford) Protein Assay kit (Thermo Scientific). Proteins (60 µg of lysate) were separated by Criterion™ TGX™ 10-20% Precast Gels (Bio-Rad) and transferred to Immobilon-P polyvinylidene difluoride membranes (PVDF; Millipore). Membranes were blocked for 30 min with 5% nonfat dry milk in Tris-buffered saline containing 0.1% Tween 20 (TBST). The primary mouse monoclonal antibodies used for the experiments were as follows: anti-FKBP51 Hi51C (1:5000; developed in the laboratory of Dr. David Smith and available from our laboratory) and anti-glyceraldehyde-3-phosphate dehydrogenase (GAPDH, 1:3000; loading control; Santa Cruz). The primary rabbit antibodies used for the experiments were as the following: polyclonal anti-AR N-20 (1:1000; Santa Cruz) and monoclonal anti-PSA/KLK3 D11E1 XP® (1:500; Cell Signaling). Primary antibodies were diluted in blocking buffer and incubated with the membranes for 2 h with gently shaking at room temperature with the exception of PSA/KLK3 mAb; it was diluted in 5% w/v bovine serum albumin (BSA; Sigma)/1X TBST and incubated with the membranes at 4°C with gentle shaking, overnight. The membranes were washed 5 times with TBST, 5 min per wash with shaking and subsequently incubated with a 1:5000 dilution of the appropriate alkaline phosphatase (AP)-conjugated goat anti-mouse and goat anti-rabbit antibodies diluted with blocking buffer and incubated with the membranes for 1 h at room temperature with gentle shaking. After washing 5 times with TBST and 2 times with TBS, 5 min per wash, the membranes were developed with Immun-Star™ AP substrate (Bio-Rad) and exposed to CL-XPosure Film (Thermo Scientific).

3.2.4 Prostate-Specific Antigen (PSA) ELISA Assay

LNCaP and 22Rv1 cells were used for the Human PSA ELISA Kit (Alpha Diagnostic International, ADI) to quantify secreted PSA in the media. The cells were plated at a density of 2 x 10^5 cells per well in 12-well plates in 1 mL of respective standard growth media as detailed in section 3.2.1 incubated at 37°C with supplemental 5% CO_2. When cells were attached, they were washed three times and replaced with 1 mL of respective growth media modified by replacement of 10% FBS with 10% CS-FBS at 37°C with supplemental 5% CO_2. After 48 h, the cells were treated with DMSO + EtOH (negative control), DMSO + agonist (DHT, 50 nM for LNCaP and 1 nM for 22Rv1, positive control), or the agonist with a range of GMC1 concentrations (1 µM, 25 µM, 50 µM, 75 µM, and 100 µM) for 24 h. For evaluating basal and hormone-induced PSA secretion in 22Rv1 cells, the aforementioned experimental conditions were used with the exception of GMC1 concentrations; the hormone-induced activity was only tested at a single high dose (100 µM). Supernatant were collected and the assays were performed according to manufacturer's instructions. 25 µL of standards, controls, and supernatant samples were added into appropriate wells containing 100 µL of assay buffer in duplicate, covered, and incubated on a plate shaker (approximately at 200 rpm) for 60 min at room temperature. The wells were washed 3 times with 300 µL of 1X wash buffer followed by the addition of 100 µL of Ab-enzyme conjugate into each well, mixed gently for 10 secs, covered, and incubated the plate on a plate shaker (approximately at 200 rpm) for 30 min at room temperature. The wells were then washed 3 times with 300 µL of 1X wash buffer followed by the addition of 100 µL of TMB substrate per well, mixed gently for 10 secs, cover and incubated the plate on a plate shaker (approximately at 200 rpm) at room temperature until the samples turned dark blue. The reaction was stopped by adding 50 µL of stopping solution to all wells and mixed gently. The absorbance was measured at 450 nm with SpectraMAX 190 (Molecular Devices). GMC1 at each dosing concentration was assayed independently at least 3 times (3 replicate assays) with duplicate wells per each replicate assay.

3.2.5 Cell Proliferation Assay

LNCaP, 22Rv1, and PC3 cells were used to evaluate GMC1 effects on androgen-dependent AR-mediated proliferation using CellTiter96® Non-Radioactive Cell Proliferation Assay (Promega). The experiments were performed according to manufacturer's instructions. The cells were plated at a density of 5 x 10^3 cells per well in 96-well plates in 100 µL of respective standard growth media as detailed above modified by replacement of 5% FBS with 5% CS-FBS incubated 24 h at 37°C in a humidified 5% CO_2 atmosphere. The cells were treated with DMSO + EtOH (negative control), DMSO + synthetic agonist (R1881, 1 nM, positive control), or the synthetic agonist with a range of GMC1 concentrations (1 µM, 25 µM, 50 µM, 75 µM, and 100 µM) for 18-20 h with the exception of PC3; they are androgen-independent prostate cancer cells, therefore, there was no need for the addition of the hormone for the assay. Next day, 15 µL of the Dye Solution were added to each well of GMC1/hormone treated cells and incubated at 37°C in a humidified environment with 5% CO_2 for 4 h. After incubation, 100 µL of the Solubilization/Stop Mix were added to each well and mixed gently to get a uniformly colored solution. The absorbance were then recorded at 570 nm using a 96-well plate reader with the use of a reference wavelength at 660 nm to reduce background contributed by cell debris, fingerprints, and other nonspecific absorbance. GMC1 at each dosing concentration was assayed independently twice (2 replicate assays) with quadruple wells per each replicate assay.

3.2.6 Statistical Analysis

All results for the experiments are presented as means ± standard deviation and displayed as the average of at least duplicate biological samples in a single experiment. Each experiment was repeated at least two independent times. The graphs were presented as an average in a single experiment except for Western immunoblot analysis: representative blots from each experiment were shown. One-way ANOVA followed by a post-test of Bonferroni's Multiple Comparison statistical analysis was performed to analyze the results using GraphPad PRISM. In LNCaP AR-dependent PSA luciferase activity experiments, the mean normalized values from

each dosage concentration for each inhibitor were compared with respective positive control to compare inhibitory effects on promoter activity by using Student's paired *t* test. Differences were considered to be statistically significant at $p \leq 0.05$. Throughout the manuscript, the following convention was used to denote levels of statistical significance: ***, $p \leq 0.001$; **, $p \leq 0.01$; * $p \leq 0.05$.

3.3 RESULTS

3.3.1 GMC1 Demonstrates FKBP52-Specific Inhibition of GR and PR-Mediated Functions

As aforementioned in Chapter 1, FKBP52 functionally potentiates AR, GR, and PR activities, but not ER nor MR despite the significant sequence, structural, and/or functional homology that exists between some SHRs. It has been proven that the co-chaperone's proline-rich loop overhanging the PPIase catalytic pocket in the FK1 domain is responsible for the regulation of receptor activity. Thus, our resulting lead molecule GMC1 that is predicted to bind the FKBP52 pocket resulting in re-orientation of the loop disrupting its interaction with receptors should theoretically also display FKBP52-specific inhibition of both GR and PR as observed with AR (Fig.2.2b), but not ER activity.

GMC1 demonstrated increased potency with maximal inhibition of GR-mediated reporter gene expression in MDA-kb2 cells, which express both AR and GR-responsive luciferase reporter genes, at 100 μM and an IC_{50} value of 2.69 μM (Fig. 3.1a). GMC1 specifically inhibited FKBP52-regulated GR and PR activities in 52KO MEF cells, a true FKBP52 negative background cellular model for testing the co-chaperone-specific effects of the lead molecule, at low micromolar concentrations with IC_{50} values of 1.098 μM and 4.080 μM, respectively (Fig. 3.1b-c).

T47D-KBluc is a breast cancer cell line that endogenously expresses ERα and ERβ that has been stably transfected with a triplet estrogen-responsive-element (ERE)-promoter luciferase reporter gene construct [229]. This cell line does not require transfection and thus provides a sensitive and yet, an inexpensive tool for testing GMC1 effects on ER activity. If GMC1 is an

inhibitor that truly acts via direct targeting of FKBP52, then it should not exhibit inhibitory effects on ER. As evident in Figure 3.1d, the lead molecule displayed no statistically significant inhibition of ER-mediated expression of the luciferase reporter after the cells were treated with a range of concentrations of GMC1 for 16-20 h.

In summary, data here along with the results evident in Figure 2.2a and 2.2b demonstrate that GMC1 is a promising lead molecule that displays inhibition of FKBP52-mediated functional effects on SHRs. GMC1 inhibits AR and GR-mediated signaling in MDA-kb2 cells similarly, but did not functionally affect ER-regulated activity in T47D-KBluc. Importantly, GMC1 demonstrated inhibitory effects on FKBP52-specific AR, GR, and PR functions in 52KO MEF cells with IC_{50} values in high nanomolar to low micromolar concentrations.

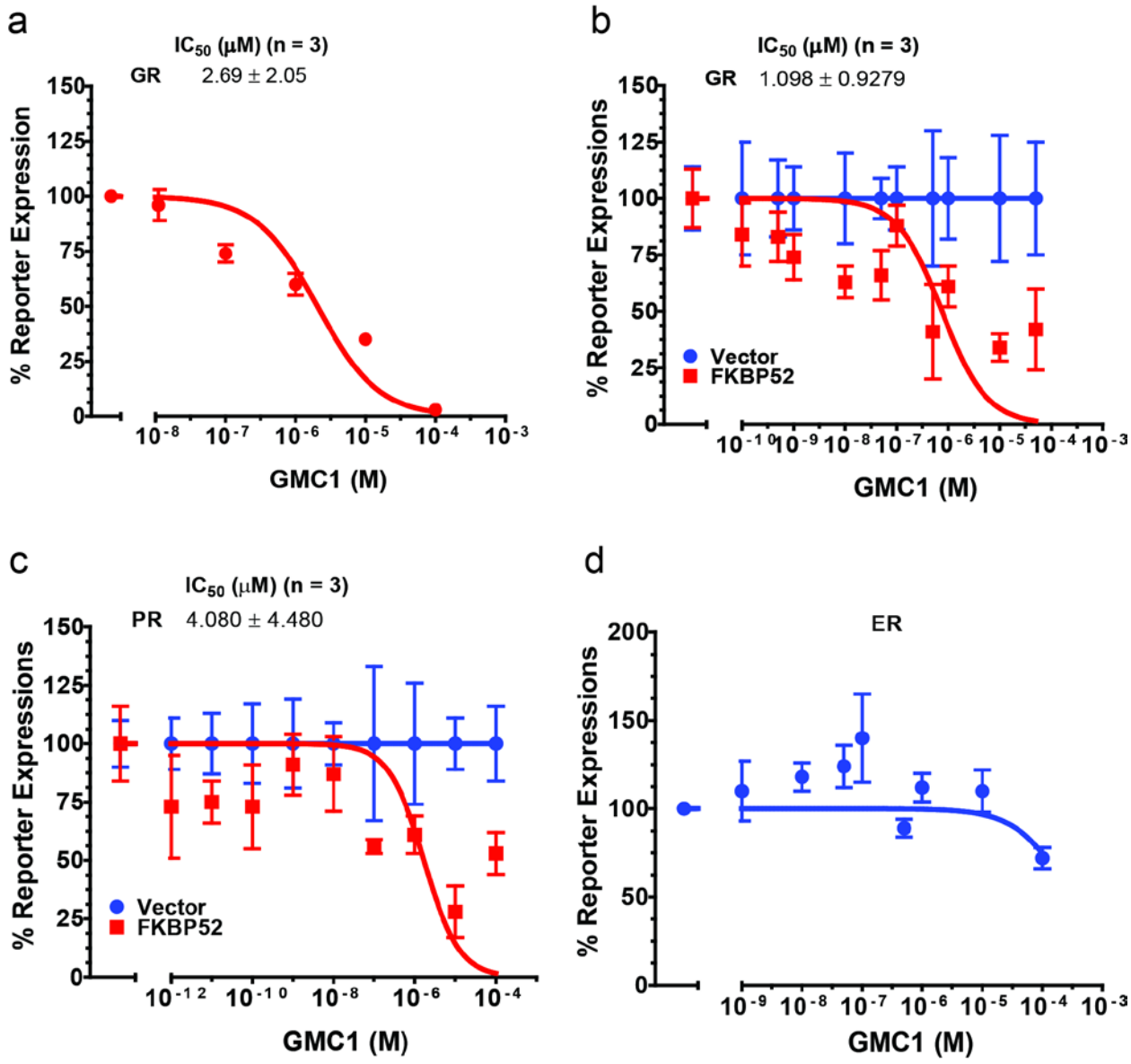

Figure 3.1: GMC1 Inhibits FKBP52-Specific GR and PR-Mediated Activity

Fig. 3.1: GMC1 Inhibits FKBP52-Specific GR and PR-Mediated Activity. (a) MDA-kb2 cells expressing stably transfected AR and GR-responsive luciferase reporter genes were treated with 50 nM DEX and a range of GMC1 concentrations (0, 0.01, 0.1, 1, 10, and 100 μM) for 16-20 h for testing GR-dependent activity. The graph depicts an average of three independent receptor-mediated luciferase reporter experiments. **(b-c)** The graphs show an average of three independent luciferase reporter assays in 52KO MEF cells in the presence and absence of FKBP52 treated with 50 nM DOC and 500 nM DOC, respectively, and a range of GMC1concentrations (0, 0.001, 0.01, 0.05, 0.1, 0.5, 1, 10, 100 μM) for the assessment of FKBP52-specific GR-mediated activity. The same experimental conditions and GMC1 concentrations were used for the examination of FKBP52-specific PR-mediated signaling with the exception of the ligand and its concentrations. P4 serves as an agonist for PR of which 100 pM and 2.5 nM were used to treat the cells in the presence or absence of the co-chaperone, respectively. **(d)** T47D-KBluc cells express ERα and ERβ, hence were used to determine GMC1 effect on ER-regulated activity. They were treated with 10 pM E2 and a range of GMC1 concentrations (0, 0.001, 0.01, 0.05, 0.1, 0.5, 1, 10, 100 μM) for 16-20 h. Each IC_{50} value in the figure is represented as means ± s.d. of an average of three independent experiments.

3.3.2 GMC1 Impairs PSA Expression in Prostate Cancer Cellular Models

We examined the effect of GMC1 on the ligand-dependent PSA secretion by assaying the supernatant of 22Rv1 and LNCaP prostate cancer cells by ELISA. The values were normalized and statistical analyses were performed against no drug treatment. As shown in Figure 3.2a-b, GMC1 effectively inhibited PSA secretion in both cell lines in a dose-dependent manner. 22Rv1 expresses both a full length AR and a constitutively active truncated form of the receptor lacking the C-terminal LBD. As a result, it can both respond to hormone and display hormone-independent growth. Figure 3.2c-d show the relative basal and hormone-induced activities of PSA expression in the presence and absence of ligand, GMC1, and MJC13 [166]. As expected, under androgen-free condition, there was a low level of basal PSA secretion in 22Rv1 and the addition of DHT induced the protein expression at least 2 fold. Interestingly, the treatment of these cells with GMC1 in the absence of hormone reduced basal constitutively active AR-dependent PSA secretion by approximately 50% (Fig. 3.2c) as compare to MJC13 [166], which is an androgen receptor surface-directed antagonist and exhibits no inhibitory effects on PSA expression (Fig. 3.2d). This data demonstrates that the observed dose-dependent inhibition of PSA secretion in the experiment was a true phenomenon and was a drug-dependent effect. The data also suggest that GMC1 has effects on basal activity mediated by the truncated AR protein in 22Rv1 cells.

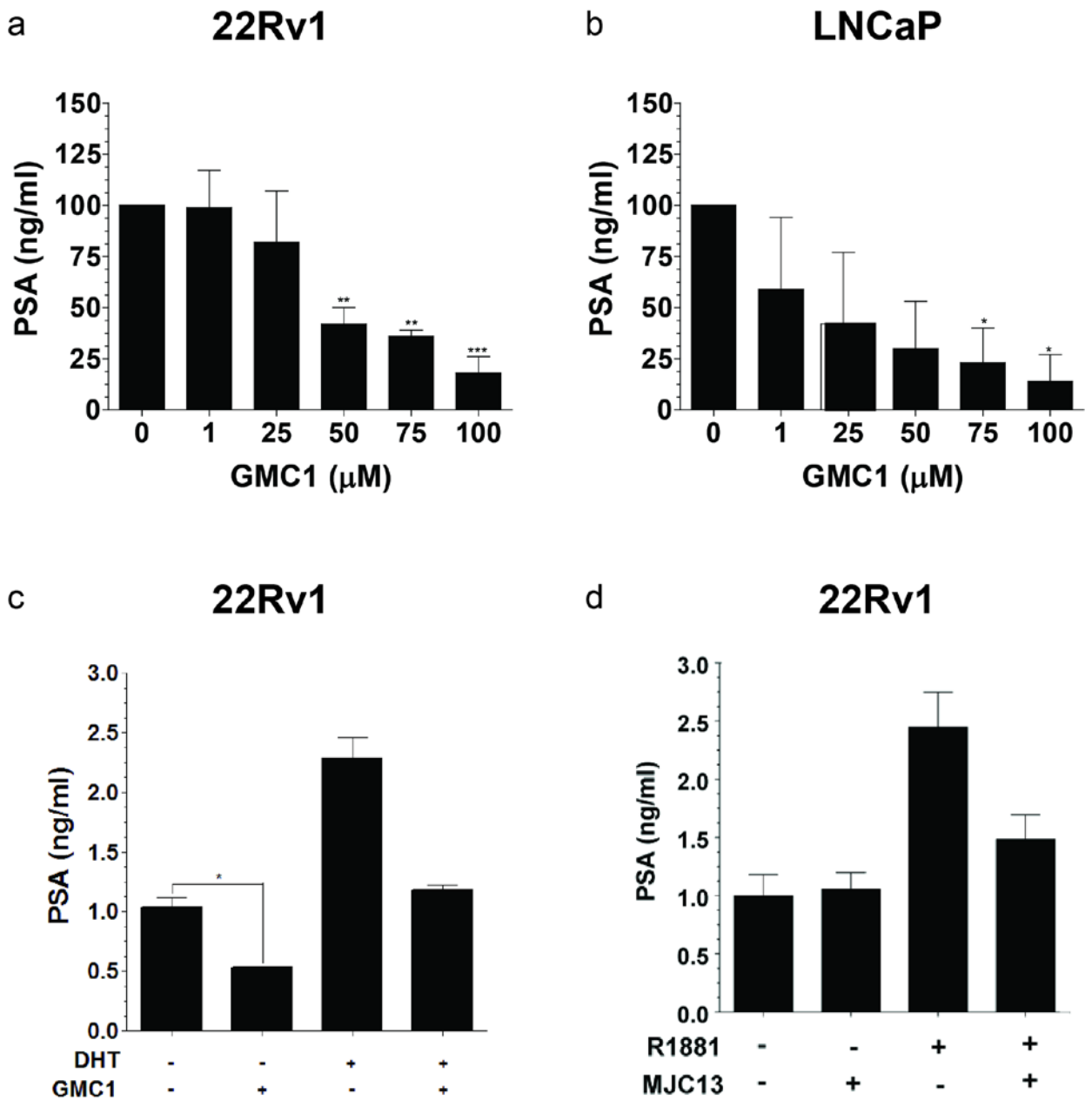

Figure 3.2: GMC1 Reduces AR-Dependent PSA Secretion in Prostate Cancer Cells

Figure 3.2: GMC1 Reduces AR-Dependent PSA Secretion in Prostate Cancer Cells. Results are presented as means ± s.d. with the average of three independent ELISA assays measuring androgen-dependent PSA secretions from 22Rv1 **(a)** and LNCaP **(b)** prostate cancer cells. The cells were treated with DHT (1 nM and 50 nM for 22Rv1 and LNCaP, respectively) and a range of indicated concentrations of GMC1 (0, 1, 25, 50, 75, and 100 μM). Data are expressed as a percentage with the level of PSA in the absence of the compound for each condition set to 100%. The effects of GMC1 and MJC13 on the basal and hormone-induced activities of PSA expressions were assessed by ELISA **(c)** and qPCR **(d)**. **(c)** Cells were treated with presence and absence of hormone (1 nM) and GMC1 (100 μM) for 24 h. **(d)** The data was previously performed and described by our lab [166]. Experiments were performed in duplicate with data shown as relative PSA level in media **(c)** and as PSA expression relative to 18S rRNA **(d)**. The asterisks denote a statistically significant difference as compared to no GMC1 treatment with only the presence of DHT. $*P \leq 0.05$, $**P \leq 0.01$, and *** $P \leq 0.001$ were calculated by One-Way ANOVA followed by Bonferroni's multiple comparison test compared with control.

3.3.3 GMC1 Reduces Transactivation of PSA Promoter in LNCaP Cells

An androgen-responsive luciferase reporter plasmid containing the PSA promoter/enhancer in transiently transfected LNCaP cells was used to examine the effect of GMC1 on the androgen-dependent transcription of endogenous PSA in LNCaP PCa cells. As shown in Fig. 3.3a, the inhibitor reduced the DHT-dependent PSA promoter activity in a concentration-dependent manner. Specifically, GMC1 treatment in the presence of hormone displayed a significant decrease in activity starting at 30 μM, which is comparable with effective concentrations in both the PSA ELISA (Fig. 3.2) and luciferase reporter assays (Fig. 2.2). For comparison, the effects of known and well-characterized AR antagonists, MJC13, MDV3100, and Bicalutamide, were also assessed. Interestingly, our initial lead molecule, GMC1, which has not been optimized structurally to improve its efficacy, reduced transactivation of the PSA promoter activity at a concentration range comparable to MJC13 and classic antiandrogens tested in this study of which the chemical structure has been optimized with well-characterized pharmacological, toxicity profiles, and/or has been used as standard ADT treatments.

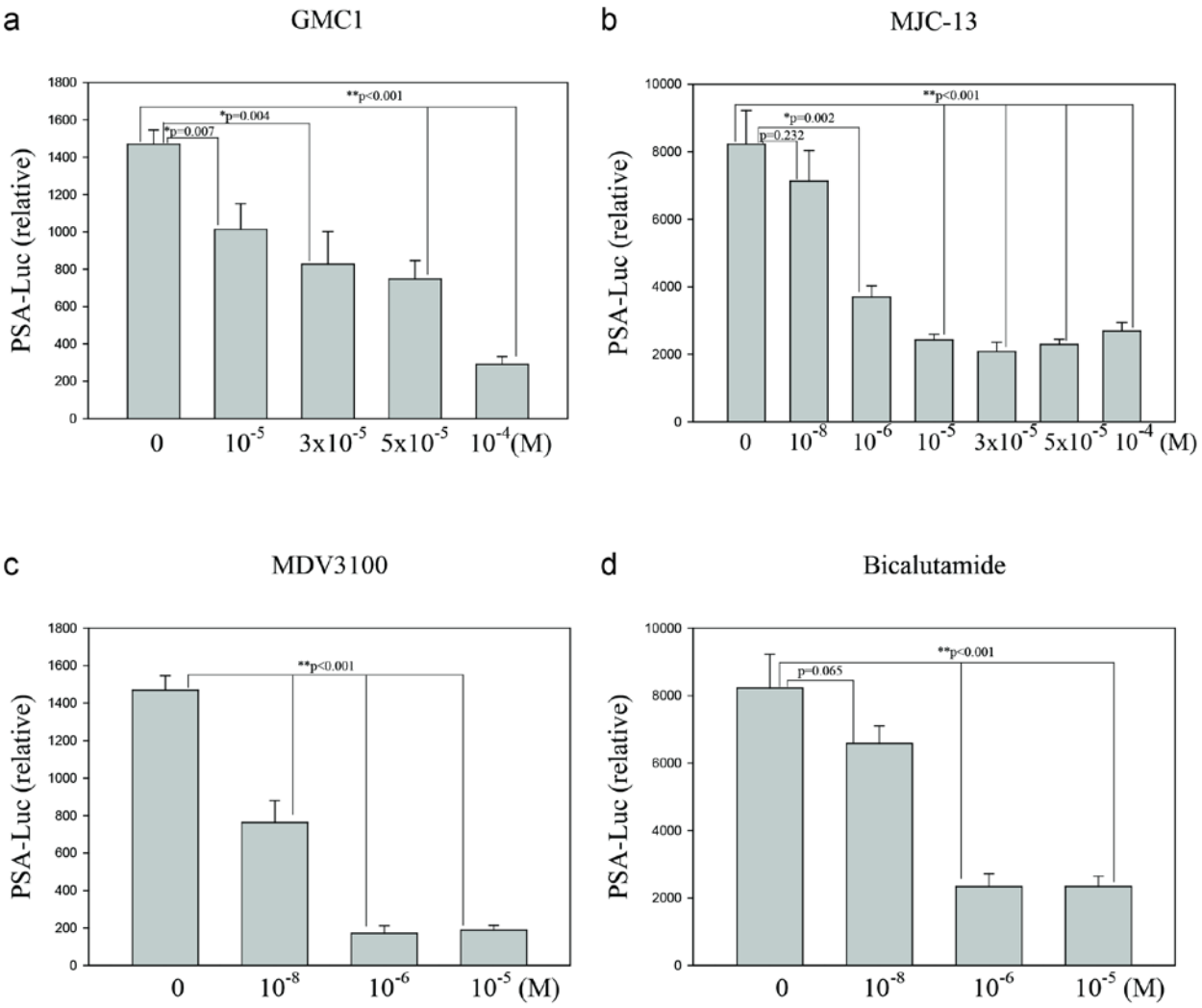

Figure 3.3: GMC1 Suppresses Androgen-Dependent PSA Promoter Activation at Concentrations Comparable to MJC13 and Classic AR Antagonists in LNCaP

LNCaP cells were transiently transfected with androgen-responsive luciferase reporter plasmids containing PSA promoter. They were treated with the indicated concentrations of GMC1 **(a)**, MJC13 **(b)**, MDV3100 **(c)**, and Bicalutimide **(d)** for 24 h. FBS served as the source of the hormone. Each promoter-dependent transcription is shown as relative promoter-dependent luciferase activity. The asterisks denote a statistically significant difference as compared to no drug treatment with only the presence of hormone. $*P \leq 0.05$ and $**P \leq 0.01$ were calculated by Student's *t*-test compared with no treatment control.

3.3.4 GMC1 Decreases Endogenous AR Protein Expression in Prostate Cancer Cells

We examined the effect of GMC1 on the regulation of the AR protein level in both LNCaP and 22Rv1 cells. In 22Rv1 cells the full length AR has a molecular mass of approximately 110 kDa (Fig. 3.4a). Additionally, a prominent smaller AR-specific protein species was detected at approximately 80 kDa, which represents the truncated AR that lacks the C-terminal LBD (Fig 3.4a). In the presence of DHT without GMC1 treatment, the hormone increased the endogenous full length AR level in both cell lines by enhancing the protein's stability (data not shown). However, immunoblot and densitometry analyses of the expressed AR protein after 24 h of treatment with a range of GMC1 concentrations revealed that the molecule significantly suppressed androgen-stimulated receptor protein expression in both PCa cells in a dose-dependent manner (Fig. 3.4). As a control for normalization, GMC1 did not affect GAPDH expression (Fig. 3.4a-b). It is important to note that only the full length AR levels in 22Rv1 and LNCaP cells were significantly inhibited by GMC1, not the truncated receptor product in 22Rv1. Therefore, the molecule only inhibited androgen-dependent endogenous full length AR protein levels. Interestingly, GMC1 began to significantly suppress the androgen-dependent induction of AR activity in 22Rv1 at 0.5 μM compare to LNCaP in which 50 μM of the inhibitor was required to considerably affect the receptor level (lower panels of Fig. 3.4a-b).

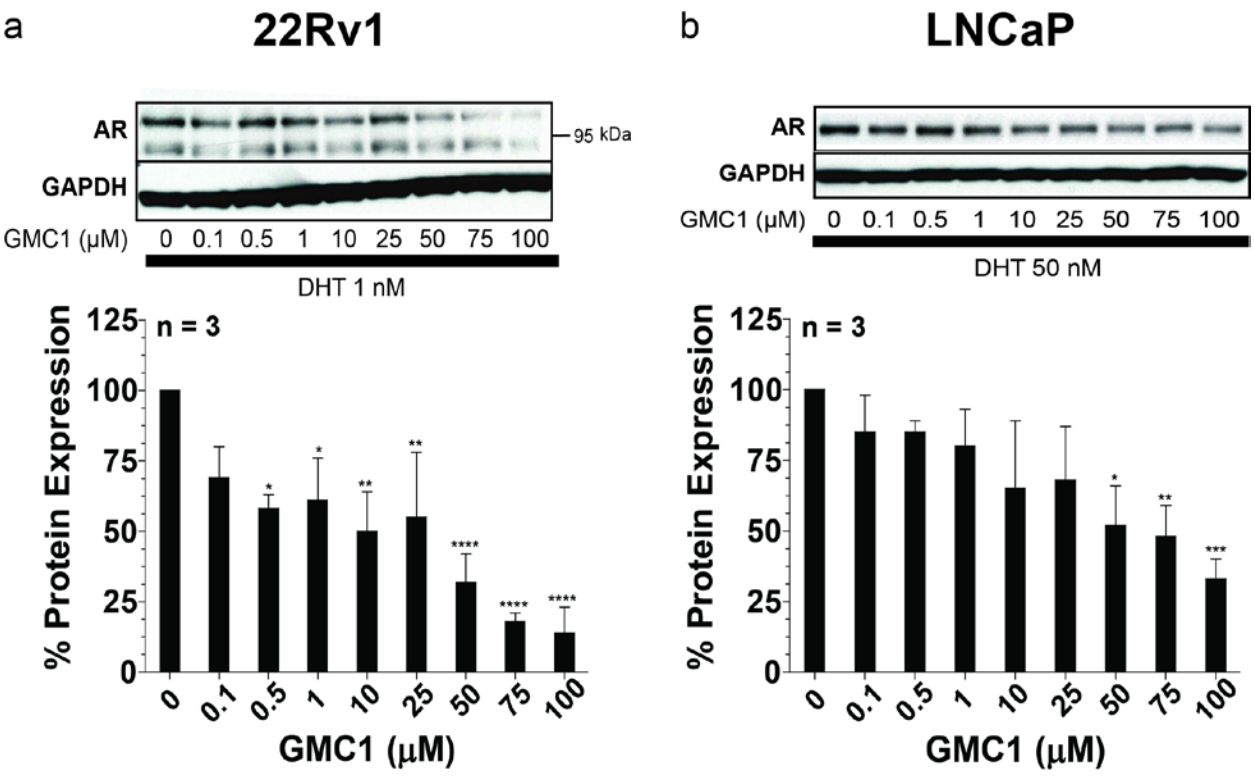

Figure 3.4: GMC1 Decreases Endogenous Androgen-Dependent AR Expression in Prostate Cancer Cellular Models

The effects of GMC1 on hormone-dependent endogenous AR expression were assessed in 22Rv1 **(a)** and LNCaP **(b)** cells by Western immunoblot and densitometry. Lysates from cells grown in the presence and absence of the indicated concentrations of hormone and GMC1 for 24 h were electrophoresed and immunoblotted for AR and GAPDH (loading control) and the protein levels were quantified via densitometry. The upper panels show the representative Western immunoblots. The lower panels represent averaged densitometry data from three independent experiments. Data are displayed as AR level relative to that of loading control, which then calculated as a percentage with the endogenous expression of the receptor in the absence of the compound for the condition set to 100%. The asterisks denote a statistically significant difference as compared to no GMC1 treatment with only the presence of DHT. $*P \leq 0.05$, $**P \leq 0.01$, and $*** P \leq 0.001$ were calculated by One-Way ANOVA followed by Bonferroni's multiple comparison test compared with control.

3.3.5 GMC1 Reduces Endogenous AR-Dependent Gene Expression in Prostate Cancer Cells

PSA is a clinically important biomarker for PCa and it is also a well-known AR-regulated gene in the human prostate gland of which the expression is mainly induced by androgen and regulated by the receptor at the transcriptional level [230]. Besides the canonical AR target PSA, the 51-kDa FK506-Binding Protein (FKBP51), a SHR-associated co-chaperone, is another androgen-regulated gene and has been shown to physically interacted with the AR, promoting receptor signaling, and leading to increased FKBP51 expression in PCa [196, 231]. The hyperexpression of FKBP51 leads to a stimulation of chaperone complex association with AR, which further increases the receptor transcriptional activity by establishing an ultra-short positive feedback loop [196]. This feed-forward mechanism amplifies AR signaling even under a low hormone condition, which often occurs during androgen ablation, allowing FKBP51 to continue to increase the transcriptional activity of the receptor in the absence of hormone [149, 231, 232]. Furthermore, the knockdown of FKPB51 dramatically decreases its hormone-dependent gene transcription and protein expression in PCa cells [149, 232]. Thus, FKBP51 has emerged as a potential novel diagnostic biomarker and/or target for PCa therapy [233, 234]. Taken together, it is important to demonstrate GMC1 can reduce the endogenous level of PSA and FKBP51 in prostate cancer cellular models. We assessed the impact of our lead molecule on the AR-regulated genes by Western immunoblot and densitometry in 22Rv1 and LNCaP cells (Fig. 3.5). Representative blots for FKBP51, PSA, and the loading control GAPDH are shown (Fig. 3.5a-b, upper panels). In the presence of DHT without GMC1 treatment, the hormone increased the endogenous hormone-dependent PSA and FKBP51 levels in 22Rv1 and LNCaP cells as observed in the literature (data not shown). The normalized average densitometry data from three independent experiments demonstrate that GMC1 reduced endogenous androgen-dependent AR-mediated FKBP51 and PSA gene expression in a dose-dependent manner in both prostate cancer cellular models (Fig. 3.5a-b, lower panels). Interestingly, the lead molecule was

observed to suppress the DHT-dependent induction of FKBP51 transcript level more effectively in 22Rv1 as compare to LNCaP, and the reverse was observed for PSA gene expression.

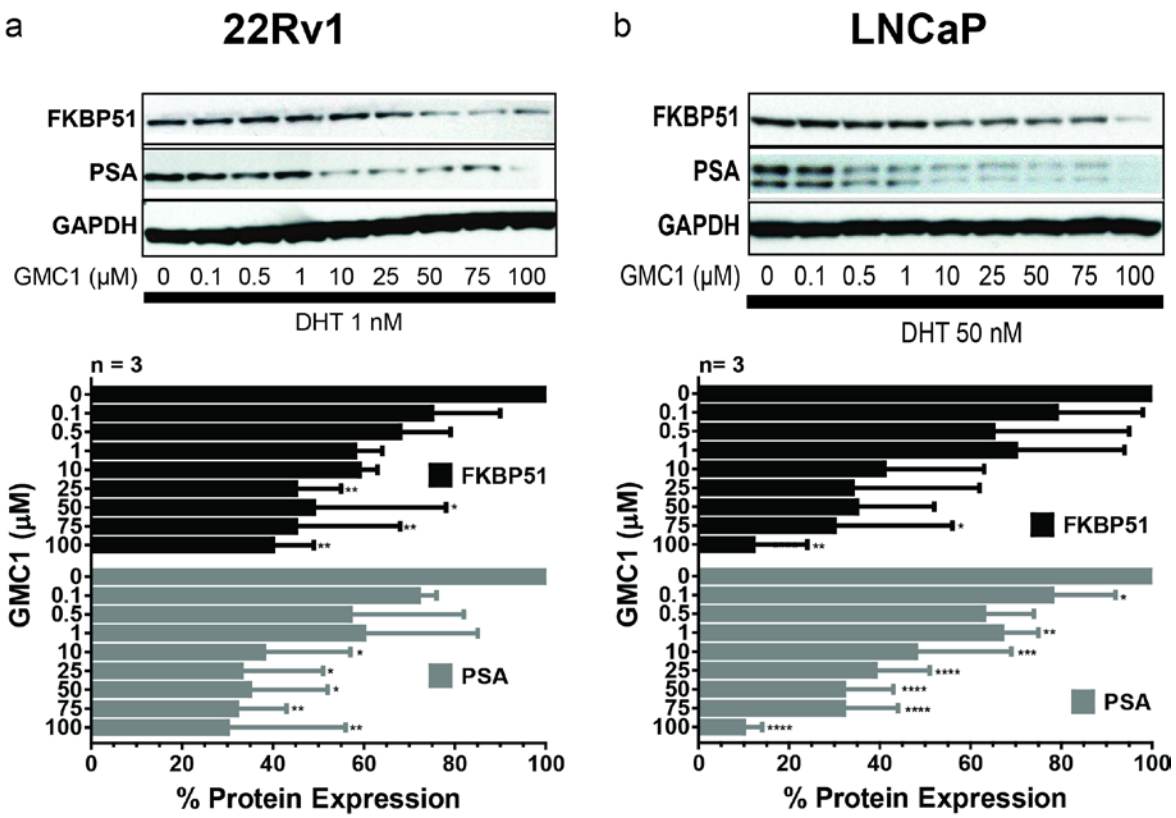

Figure 3.5: GMC1 Reduces Endogenous AR-Dependent Gene Expression in Prostate Cellular Models

The effects of GMC1 on AR-dependent endogenous gene expression were assessed in 22Rv1 **(a)** and LNCaP **(b)** cells by Western immunoblots and quantified via densitometry. Lysates from cells grown in the presence and absence of the indicated concentrations of hormone and GMC1 for 24 h were electrophoresed and immunoblotted for FKBP51, PSA, and GAPDH (loading control) and the protein levels were quantified via densitometry. The upper panels show the representative Western immunoblots. The lower panels represent averaged densitometry data from three independent experiments. Data are displayed as FKBP51 and PSA levels relative to that of loading control, which then calculated as a percentage with the endogenous expression of the proteins in the absence of GMC1 of which the condition is set to 100%. The asterisks denote a statistically significant difference as compared to no GMC1 treatment with only the presence of DHT.*$P \leq 0.05$, **$P \leq 0.01$, *** $P \leq 0.001$ and **** $P \leq 0.0001$ were calculated by One-Way ANOVA followed by Bonferroni's multiple comparison test compared with control.

3.3.6 GMC1 Inhibits AR-Dependent Proliferation in Prostate Cancer Cellular Models

Abnormal cell proliferation rate is one of the characteristics of cancer, which led us to examine the effects of GMC1 on androgen-dependent PCa cell growth using CellTiter96® Non-Radioactive Cell Proliferation Assay in 22Rv1 and LNCaP cells. All treatments were carried out in a steroid-depleted condition containing charcoal-stripped serum. In basal conditions, synthetic androgen R1881 treatment enhanced AR-regulated 22Rv1 and LNCaP proliferation during a 24-hour treatment and the combination of hormone with GMC1 decreased cell growth in a concentration-dependent manner (Fig. 3.6a-b). For comparison, PC3, an AR-negative cell line, was used to demonstrate that the observed inhibitory effects on 22Rv1 and LNCaP were indeed receptor-dependent phenomenon. GMC1 has no effects on the proliferative rate of PC3 cells (Fig. 3.6c), which demonstrates that the molecule down-regulated AR-dependent cell growth. It is noted that the molecule appears to reduce LNCaP proliferation without the presence of hormone at 75 μM and 100 μM. The observed phenomenon might be related to cytotoxicity effect of GMC1 on the cells at those concentrations (Fig. 3.6b). Nevertheless, the trend of GMC1 inhibiting cell growth in an androgen-dependent AR-mediated manner is undeniable. Furthermore, statistical analyses of each data point comparing the cell growth in the absence to the presence of R1881 demonstrated that proliferation was significantly reduced under hormone-dependent conditions at each respective GMC1 concentration.

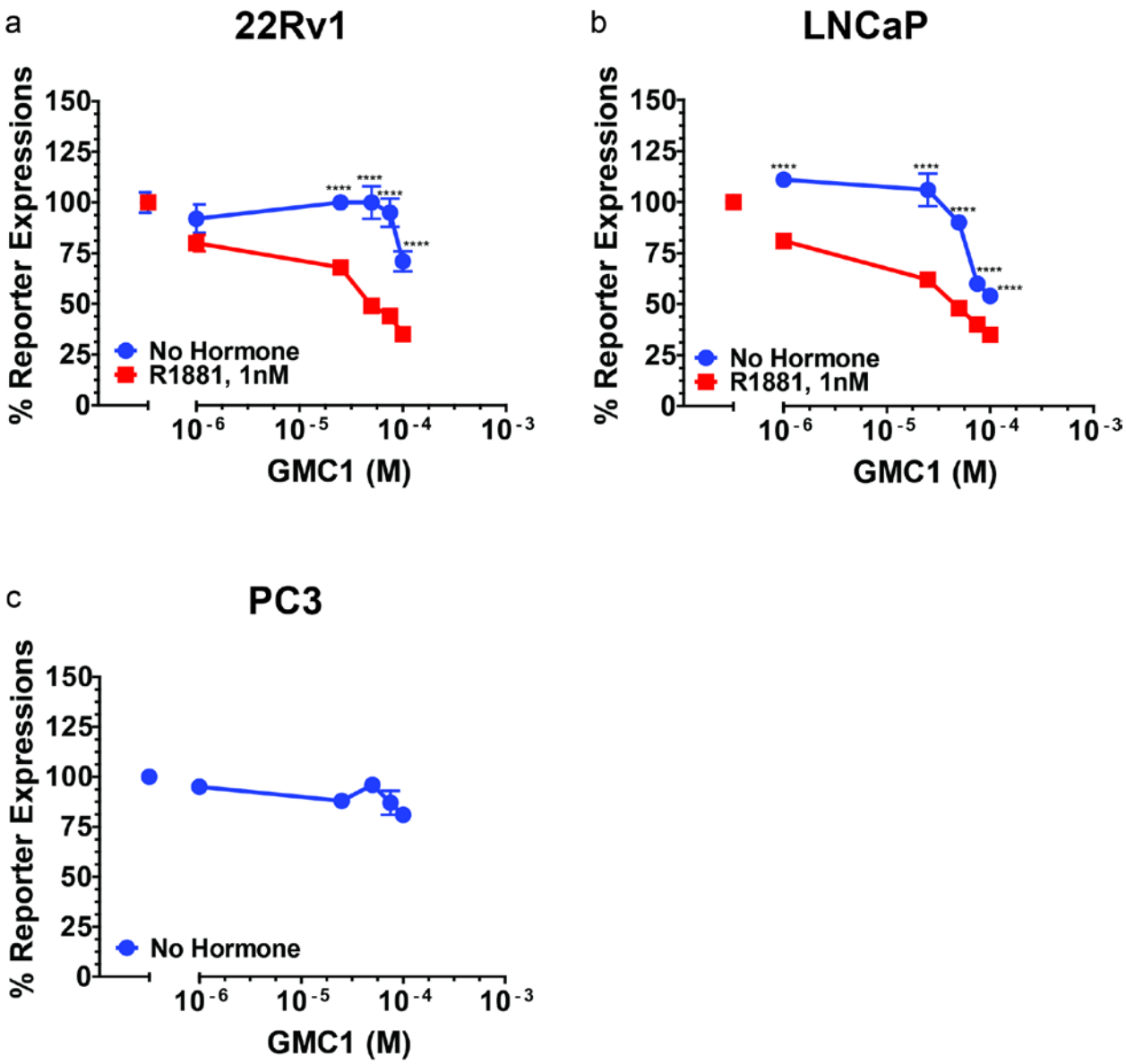

Figure 3.6: GMC1 Down-Regulated Hormone-Dependent AR-Specific Proliferation in Prostate Cancer Cellular Models

Fig. 3.6: GMC1 Down-Regulated Hormone-Dependent AR-Specific Proliferation in Prostate Cancer Cellular Models. GMC1 effectively inhibited androgen-dependent AR-mediated prostate cancer cell growth. Cells were treated in the presence or absence of 1 nM synthetic androgen, R1881, and GMC1 at 0, 1, 25, 50, 75, and 100 μM for 24 h. The absorbance was measured at 570 nM using the appropriate reference wavelength at 660 nM. The graphs are representative of three independent experiments with similar results for 22Rv1 **(a)**, LNCaP **(b)**, and PC3 **(c)**. The AR-negative PC3 cells were used as a control for AR-specificity for the prostate cancer cell growth. GMC1 did not have any effect on the proliferation of the PC3 cells **(c)**. Data at each GMC1 concentration are normalized to the absence of drug treatment in the respective experimental conditions (+/- R1881). The normalized results are calculated as a percentage in the absence of the compound, which is set to 100%. The asterisks denote a statistically significant difference between the presence and absence hormone at each GMC1 concentration. Significant differences at each GMC1 concentrations are indicated (**** $P \leq 0.0001$), which were calculated by One-Way ANOVA followed by Bonferroni's multiple comparison test.

3.4 DISCUSSION

As discussed in Chapter 1, prostate cancer patients, over time, often develop resistance to ADT and invariably progresses switching the antiandrogens from antanonists to agonists of the AR via alternative pathways, such as GR. GR becomes a substitution for the AR to activate similar but distinguishable sets of target genes, which is necessary for maintenance of the resistant phenotype [159]. In addition, studies have shown there is a correlation with PR and prostate tumor progression. PR expression is often elevated during the progression of metastatic and androgen-insensitive prostatic adenocarcinoma [200, 201]. Given FKBP52 is a specific positive regulator of AR, GR and PR signaling, and GMC1 is predicted to be an FKBP52 PPIase-targeting drug, the molecule should inhibit co-chaperone-specific GR and PR functions as demonstrated in AR (Fig. 2.2). In this study, we have shown that our novel lead molecule, GMC1, specifically inhibited FKBP52-enhanced GR and PR activity in a mammalian cell line, which provided a true FKBP52-negative background to test for the co-chaperone-specific effects of the candidate drug. The IC_{50} values for both receptor inhibitory curves were determined at low micromolar concentrations by functional screens consisting of two receptor-mediated luciferase assays assessing drug effects on general receptor activity and FKBP52 specificity (Fig. 3.1a-c). Furthermore, GMC1 did not affect ER function, which is not regulated by FKBP52 thus confirming the molecule's FKBP52-specific effects (Fig. 3.1d).

PSA is a serine protease that is synthesized by both normal and malignant epithelial cells of the human prostate. Under a malignant condition, PSA is expressed at an elevated level which is released into serum and has been proven to be highly correlated with prostate tumor recurrence and progression [230, 235]. We demonstrated that GMC1 effectively reduces PSA secretion. ELISA analysis of PSA levels from 22Rv1 and LNCaP cells showed that GMC1 reduces androgen-dependent AR-mediated PSA secretion from both cell lines in a dose-dependent manner (Fig. 3.2a-b). Interestingly, GMC1 was also able to inhibit constitutive PSA expression but not the AR surface-directed antagonist MJC13 (Fig. 3.2c-d).

Next, we evaluated GMC1 on the transcriptional activity of AR using LNCaP cells using a transiently transfected androgen-responsive luciferase reporter plasmid containing the PSA promoter/enhancer. GMC1 reduced the receptor transactivation activity at a range of concentrations comparable to the structurally optimized MJC13 and clinically used antiandrogens, Bicalutamide and MDV3100, which suppress AR signaling by preventing hormone-induced receptor-chaperone complex dissociation or by direct interaction with the AR LBD (Fig. 3.3). These data suggest that our initial hit molecule, which has not been structurally optimized, could be optimized to a more potent analog that would display significantly increased potency as compared to MJC13, MDV3100, and Bicalutamide.

We have demonstrated that our lead molecule, GMC1, reduced endogenous levels of androgen-dependent AR-regulated PSA and FKBP51 gene expression and effectively inhibited prostate cancer cell proliferation in a concentration-dependent manner (Fig. 3.5 and 3.6). These results correlated with GMC1-mediated downregulation of androgen-responsive full-length AR in a dose-dependent manner (Fig. 3.4). As aforementioned in Chapter 1, FKBP52 association with SHR-chaperone complexes establishes a functionally mature conformation necessary for enhancement of hormone binding to the receptor and leading to its subcellular localization. Thus, GMC1 disruption of the interaction between FKBP52-AR heterocomplex may affect the hormone binding affinity of the receptor. As a result, AR dissociates from the mature chaperone complex, the free receptor re-enters the chaperoning cycle, and eventually is degraded by targeting them to the ubiquitin/proteasome pathway (Fig. 3.4). As a consequence, AR-dependent gene expression and hormone-stimulated proliferation in PCa cells are inhibited (Fig. 3.5 and 3.6).

In summary, *in vitro* studies performed in this chapter demonstrated that the GMC1 is a promising hit molecule that displayed similar inhibition of FKBP52-regulated GR and PR-mediated activities. GMC1 reduced the AR transactivation of hormone-responsive PSA promoter in prostate cancer cells. It also induced AR de-stabilization leading to reduced AR protein levels in 22Rv1 and LNCaP cells. Furthermore, GMC1 inhibited endogenous androgen-

dependent AR-regulated gene expressions and PSA secretions, and down-regulated cell proliferation at concentrations consistent with those observed to be effective in reporter assays. Here, we demonstrated that “indirect AR targeting”, specifically direct targeting of FKBP52, is a promising strategy in combating PCa. Our data suggest that small molecules binding to the PPIase pocket can re-orient the proline-rich loop and affect its interaction with the receptor, thus further highlighting the importance of the architectural integrity of the loop during FKBP52-mediated receptor functions.

CHAPTER 4: VERIFICATION OF GMC1 TARGET SITE AND PRELIMINARY ANIMAL EVALUATIONS

4.1 RATIONALE

In Chapter 2, we used *in silico*-based docking prediction to screen 3 million lead-like small molecules from the ZINC database targeting the FKBP52 PPIase pocket, which resulted in 40 hit molecules. From those 40 compounds we identified GMC1 as the initial hit molecule for further *in vitro* characterization. However, the identification was based on predictive modeling that relies on three key hydrogen bond interactions between residues Asp68, Ile87, and Tyr113 in the catalytic pocket and the selected compounds including GMC1. Thus, it is imperative for us to verify that GMC1 does in fact bind to the PPIase pocket through hydrogen bonding with those residues and/or any other residues within the catalytic cavity. In order to confirm that GMC1 directly bind to the intended target site on the PPIase pocket, we designed and constructed amino acid mutations that may alter the predicted binding site of the compound, disrupting drug inhibition, while not affecting the FKBP52's ability to potentiate AR activity.

Hitherto, we have performed detailed molecular and cellular evaluations of GMC1 and demonstrated its potential as an effective therapeutic treatment of PCa. In this study, we sought to investigate whether the lead molecule's effects on an animal xenograft model of CRPC corroborate with the results from the *in vitro* studies. Unfortunately, due to a lack of hydrophilic functional groups and unavailable basic physicochemical information about our lead compound, the development of a suitable formulation for GMC1 to deliver *in vivo* has been a challenging task. Therefore, our collaborator, Dr. Xie from Texas Southern University has led preformulation studies of GMC1 to determine its physicochemical properties and developed an optimal formulation for the lead molecule that was suitable for administration into mouse prostate cancer model. The formulated GMC1 was then administered and evaluated in a CRPC xenograft mouse model by our collaborator, Dr. Chaudhary's group from Clark Atlanta University.

4.2 MATERIALS AND METHODS

4.2.1 Cell Culture

52KO MEFs were acquired and maintained as described in Chapter 2.2.3.

4.2.2 Transient Transfection and Luciferase Reporter Assay

52KO MEF luciferase reporter assays were performed as described in Chapter 2.2.4. The plasmids used here were the same as previously described except for the addition of FKBP52-D68A (800 ng per well), FKBP52-V86A (800 ng per well), FKBP52-I87A (800 ng per well), and FKBP52-Y113A (800 ng per well) to the experiments. These mutants were directly generated in the pCI-Neo mammalian expression vector expressing FKBP52 using the Quick Change II Site-Directed Mutagenesis Kit (Agilent Technologies) according to the manufacturer's instructions. Each functional mutagenesis experiment contains the following plasmids: a constitutive β-galactosidase expression plasmid (50 ng per well; transfection control), a hormone-responsive firefly luciferase reporter (400 ng per well), a pCI-Neo mammalian expression vector (800 ng per well; Promega) expressing AR (800 ng per well), an empty pCI-Neo mammalian expression vector (800 ng per well; negative control), a pCI-Neo mammalian expression vector expressing FKBP52 (800 ng per well; positive control), and a pCI-Neo mammalian expression vector expressing either FKBP52-D68A (800 ng per well), FKBP52-V86A (800 ng per well), FKBP52-I87A (800 ng per well), or FKBP52-Y113A (800 ng per well).

4.2.3 GMC1 Formulation

4.2.3.1 Solubility

A liquid chromatography-mass spectrometry and liquid chromatography-tandem mass spectrometry (LC-MS/MS) method was developed and validated for GMC1, which was custom synthesized (purify ≥ 99%) by ChemBridge Corporation (San Diego, CA), to determine the concentration of GMC1 in various solvents. The provisional solubility (n = 1) of GMC1 in water, soybean oil, oleic acid, Tween 80, capyrol (propylene glycol type 1), EtOH, cremophor,

labrasol, polyethylene glycol 400 (PEG 400), polyethylene glycol 300 (PEG 300), DMSO, N, N-dimethylacetamide (DMA) was determined by shake-flask method.

4.2.3.2 Lipophilicity

The lipophilicity of GMC1 was examined as the logarithm of partition coefficient (logP) of the solute between water and 1-octanol using the shaker method. The logP was calculated according to Equation 1:

$$\text{LogP} = \log \frac{C_o}{C_w} \qquad (1)$$

where C_o and C_w represents the concentrations of GMC1 in 1-octanol and aqueous phase, respectively.

4.2.3.3 Plasma Protein Binding

In vitro healthy human plasma samples of GMC1 were prepared by diluting the stock solution with acetonitrile and spiking in the plasma at five different concentrations: 100, 500, 1000, 2000, and 5000 ng/mL to evaluate GMC1 plasma protein binding. The fraction unbound GMC1 (f_u) was determined as Equation 2:

$$f_u = \frac{c_u}{c_t} \qquad (2)$$

where C_u is the unbound concentration and C_t is the total concentration. The plasma protein was then determined by $1 - f_u$.

4.2.3.4 Co-Solvency

Co-solvent systems with various compositions and ratios of labrasol, PEG 300, and DMA were prepared with GMC1 concentration at 5 mg/mL and 10 mg/mL. Each system was diluted with normal saline at the ratios of 1:1, 1:4, 1:9, 1:19 (v/v), then the optimal formulation for GMC1 was selected based on its solubility, precipitation upon dilution, and solvent toxicity. The optimal co-solvent formulation of GMC1 was stored at 4°C and analyzed via LC-MS/MS to determine the amount of GMC1 present.

4.2.4 Xenograft Mouse Model

4.2.4.1 Preparation of Tumor Cells

LNCaP-Inhibitor of differentiation 4 (Id4) cells were grown in a complete medium (10% volume/volume (v/v) FBS in RPMI 1640 medium). LNCaP-Id4$^{-/-}$ cells were generated as previously described [236, 237]. Id4 was stably silenced in LNCaP cells using a gene specific small hairpin RNA (shRNA) retroviral vector (Open Biosystems #RHS1764-97196818). Successful Id4 gene silencing was confirmed by qRT-PCR and Western immunoblot analyses. When cells were 70-80% confluent, 3-4 h before harvesting, medium was replaced with fresh medium to remove dead and detached cells. Then the fresh medium was removed, and cells were washed with PBS. After adding a minimum amount of trypsin-EDTA, cells were dispersed by adding complete medium (5:1), and then centrifuged immediately at 1500 rpm for 5 min. After re-suspending the cell pellet with complete medium (1:1), cells were counted using a hemocytometer.

4.2.4.2 Tumor inoculation

The work area was prepared by disinfecting all hood surfaces with 70% ethanol. The inoculation area of each mouse was cleaned and sterilized with an alcohol pad. A freshly prepared cell suspension was agitated to prevent the cells from settling, and then mixed with matrigel. One µL of the mixture (containing 2×10^6 cells) was injected subcutaneously into the lower flank of each of the 14 (4-week old) castrated NCRNU-Male Athymic Nude mice (Taconic Biosciences) using a 27-gauge syringe. Tumor diameters were measured with digital calipers, and the tumor volume was calculated each week using the Equation 3:

$$V = \frac{W^2 \times L}{2} \qquad (3)$$

where V is the tumor volume, W is the tumor width, and L is the tumor length. At the end of the experiments, the mice were laid to rest by asphyxiation, the tumors were surgically removed, weighed, and the volume was measured.

4.2.5 Preclinical Efficacy

GMC1 drug therapy was started 4 weeks after inoculation, when the tumors reached an average volume of about 100 mm^3. Mice were randomized into two groups with 7 mice in each group. The work area was prepared by disinfecting all hood surfaces with 70% ethanol. The tumor site of each mouse was cleaned and sterilized with an alcohol pad. The test group was administered 5mg/kg GMC1 by intratumoral administration in the optimal co-solvent formulation twice weekly for four consecutive weeks. The control group was administered the equivalent amount of co-solvent vehicle without GMC1 following the same schedule. Tumor volumes were recorded prior to each treatment.

4.2.6 Statistical Analysis

Data analyses were performed and figures were generated as described in Chapter 3.2.6. Experiments in section 4.2.3 were conducted in triplicate. Tumor volumes were analyzed using One-Way ANOVA followed by Bonferroni's multiple comparison test to determine the significance between test and control groups at each time point. Statistical significance was reported if P value was ≤ 0.05.

4.3 RESULTS

4.3.1 Characterization of GMC1 Binding to PPIase Catalytic Pocket with Competitive Fluorescence Polarization Assay

Fluorescence polarization (FP) is a powerful tool that is often used to study molecular interactions including SHR-ligand binding by measuring the polarization value of a weighted average of the bound versus unbound states of the fluorescent molecules [238, 239]. Our collaborator, Dr. Felix Hausch and his laboratory from Max Planck Institute for Psychiatry, developed and performed FP assays for the competition of fluorescently-labelled tracers with FK506 (Tacrolimus), which is a known FKBP52 binder, and GMC1 for binding to the FKBP52 PPIase pocket to verify the GMC1 target site. Given the observed effects on the FKBP52-specific receptor-mediated luciferase functions and *in vitro* studies in prostate cancer cellular

models, we were surprised that the competitive binding of GMC1 to FKBP52 was not detected in FP experiments (data not shown). However, GMC1 is a much smaller molecule that is predicted to have only half of the binding affinity to the catalytic pocket compared to FK506 (data not shown). As a result, it is likely that GMC1 simply failed to displace FK506 from the PPIase pocket. Therefore, we have generated functional FKBP52 PPIase mutants, which should maintain potentiation of the receptor activity but influence GMC1 inhibition if the drug does target the predicted binding sites from the docking simulations.

4.3.2 Identification of GMC1 Target Site on PPIase Catalytic Pocket Using Functional Mutagenesis Studies

We have identified D68, I87 and Y113 as three key residues within the FKBP52 PPIase pocket that form important hydrogen bond interactions with ligands in Chapter 2. GMC1 was predicted to bind through these specific residues within the catalytic pocket and induce re-orientation of the proline-rich loop disrupting the co-chaperone's interaction with SHRs. Interestingly, based on the molecular docking model depicted in Figure 6, we have observed that Val86 within the PPIase pocket is also predicted to form a close interaction with GMC1 although it does not create a hydrogen bond with the molecule. Thus, we generated FKBP52-D68A, V86A, I87A, and Y113A mutants via site-directed mutagenesis and performed functional luciferase studies to assess the effects that the mutations have on GMC1's ability to inhibit receptor activity.

The FKBP52-D68A, V86A, I87A, and Y113A mutants were first evaluated to confirm these mutations within the PPIase pocket did not impair FKBP52-mediated potentiation of the AR activity in 52KO MEFs. Any mutants that did not obstruct the potentiation ability of FKBP52 were subsequently tested for the co-chaperone-enhanced receptor-mediated luciferase expression in the presence of GMC1. As shown in Figure 4.1, mutations at positions D68, V86, and I87 did not impair FKBP52 potentiation of the receptor function, but the Y113A mutant did. Therefore, only the FKBP52-D68A, V86A, and I87A mutants were further assessed for their effects on GMC1 inhibition. In comparison to FKBP52-WT, the mutation at position D68 in

PPIase pocket caused GMC1 to have a two-fold decrease in the inhibition of FKBP52-regulated AR activity (Fig. 4.2).

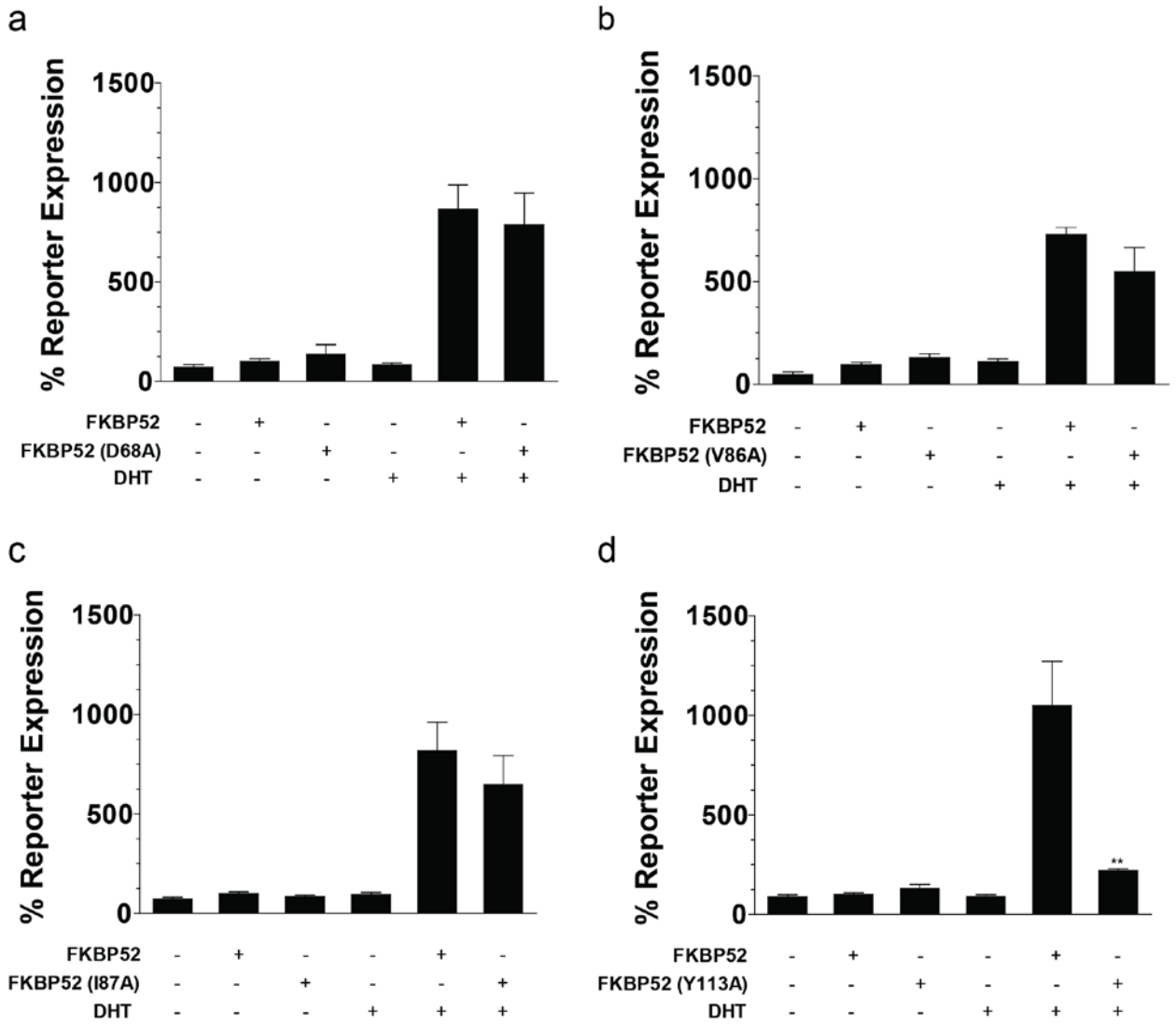

Fig. 4.1: FKBP52 PPIase Domain Mutants and Receptor Function

Fig. 4.1: FKBP52 PPIase Domain Mutants and Receptor Function. (a-c) Site-directed mutagenesis mutants at residues D68, V86, and I87 within the FKBP52 PPIase pocket maintain the FKBP52 potentiation of AR function. However, this co-chaperone-enhanced receptor activity is significantly decreased for FKBP52-Y113A mutant **(d)**. AR, the receptor-inducible reporter plasmid, and the constitutively active β-galactosidase reporter plasmids were co-transfected simultaneously with each of the plasmids indicated for the different treatment groups in 52KO MEFs. Cells were induced at 10 pM DHT or EtOH for 16-18 h. Following cell lysis, AR expression was assessed by luciferase assay. The data represents the averaged reporter expression (luciferase activity/β-galactosidase activity ± s.d.) of at least two replicates. The asterisks denote a statistically significant difference by comparing the FKBP52-mutants to WT with only the presence of DHT. $^{**}P \leq 0.01$ was calculated by One-Way ANOVA followed by Bonferroni's multiple comparison tests.

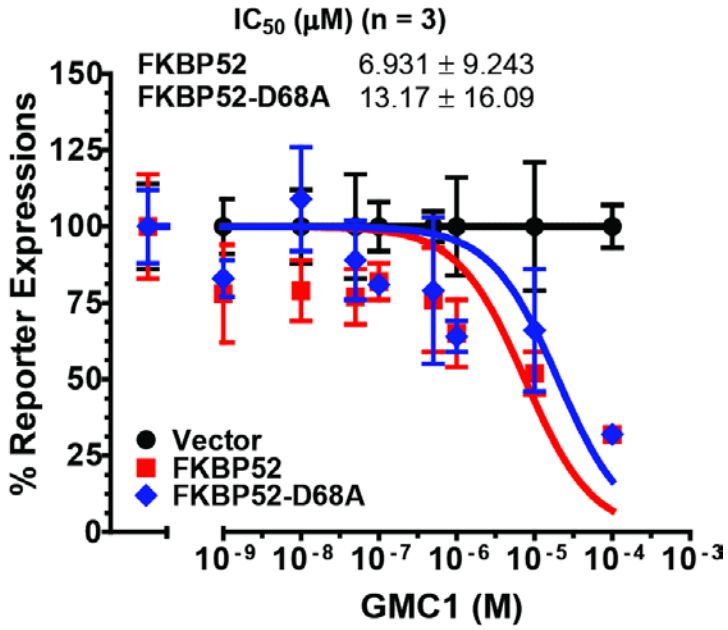

Figure 4.2: FKBP52-D68A PPIase Domain Mutants Disrupted GMC1 Binding and Affected Its Inhibitory Effect on Receptor Function

D68 is the GMC1 binding sites within the FKBP52 PPIase Pocket within the FK1 domain. FKBP52-D68A mutant affects GMC1 inhibitory effect on the AR-mediated activity by two-fold. The graph represents an average of three independent luciferase reporter assays in 52KO MEF cells in the presence of empty pCI-Neo mammalian expression vector (negative control), FKBP52-WT (positive control), and FKBP52-mutants treated with 1 nM DHT (negative control) and 10 pM (positive control and mutants), and a range of GMC1concentrations (0, 0.001, 0.01, 0.05, 0.1, 0.5, 1, 10, 100 µM) for the assessment of FKBP52-specific AR-mediated activity. Each IC_{50} value is represented as means ± s.d. of an average of three independent experiments.

4.3.3 Optimal Formulation of GMC1

As aforementioned, GMC1 was predicted to have low aqueous solubility due to its lack of hydrophilic functional groups, thus, it is important to perform preformulation studies to establish the lead molecule's basic physicochemical properties in order to develop a solution formulation suitable for *in vivo* administration.

The provisional solubility of GMC1 in water, soybean oil, oleic acid, Tween 80, capyrol, EtOH cremophor, labrasol, PEG 400, PEG 300, DMSO, and DMA was determined. The results were summarized in Table 4.1. As evident in the table, GMC1 was not hydrophilic and poorly soluble in water, but moderate to highly miscible with labrasol, PEG 400, PEG300, DMSO and DMA. Thus, these water-miscible solvents could be used as solubility enhancers to increase GMC1 aqueous solubility during formulation studies to improve the dissolution rate and bioavailability of the drug.

Lipophilicity is another common physicochemical parameter for drug discovery compounds. It is needed for the molecules to permeate through the various biological membranes. The lipophilicity (logP) of GMC1 between water and 1-octanol tested by the shake-flask method was 1.39 ± 0.05, which was within the Lipsinski rule-of-five value (logP < 5) [240].

The plasma protein binding of GMC1 in healthy human plasma at concentrations of 100, 500, 1000, 2000, and 5000 ng/mL were found to be 71.9 ± 5.4 %, 89.4 ± 1.9 %, 96.0 ± 1.1 %, 97.3 ± 0.7 %, 98.6 ± 0.2 %, respectively. These data indicate that GMC1 is highly plasma protein bound and the binding is concentration-independent.

Cyclodextrins (CD) are nonreducing, crystalline, water soluble, and cyclic oligosaccharides consisting of glucose monomers arranged in a donut shaped ring having hydrophobic cavity and hydrophilic outer surface [241]. Given the architectural characteristics and amphiphilic properties of the cyclodextrin molecules, they are often used to create complexes with hydrophobic compounds and improving the aqueous solubility, dissolution rate, and bioavailability of poor water soluble drugs [241, 242]. Our collaborator, Dr. Xie's group has

developed an intravenous formulation of GMC1 using 2-hydroxypropyl-β-cyclodextrin (HP-β-CD). The solubility of GMC1 in 50% weight/volume (w/v) HP-β-CD solution is 0.75 ± 0.07 mg/mL, which was a 250-fold increase in aqueous solubility. However, a co-solvent system using the water-miscible solvents from Table 4.1 in various compositions and ratios has proven to be a better strategic formulation for GMC1 than using cyclodextrin. The optimal co-solvent formulation for GMC1 is LP4 (Table 4.2), which increased the aqueous solubility of the molecule by 3333-fold at 10 mg/mL concentration. This formulation system was selected based on the solubility and precipitation of GMC1 and solvent toxicity, which allowed the drug to be safely administered to animal subjects orally, subcutaneously, and intravenously. Given the co-solvent formulation improved the GMC1 aqueous solubility by 13-fold in comparison to the CD formulation and was stable for, at least, 1 month at 4°C. The co-solvent system based on LP4 composition and ratio was the selected optimal solution formulation for GMC1 for *in vivo* administration.

Table 4.1 Solubility of GMC1 in Various Solvents

Solvent	Solubility (mg/mL)
Water	0.003
Soybean oil	0.06
Oleic Acid	0.30
Tween 80	1.73
Capyrol	2.53
Ethanol	5.10
Cremophor	12.52
Labrasol	21.83
PEG 400	28.13
PEG 300	28.25
DMSO	>100
N, N-dimethyl acetamide	>100

Table 4.2 GMC1 Co-Solvent Systems

Label	GMC1 Concentration (mg/mL)	Precipitation upon dilution with normal saline (v/v)			
		1:1	1:4	1:9	1:19
LP1	5	N	N	N	N
LP2	5	Y	Y	Y	Y
LP3	5	N	N	N	N
LP4	**10**	**N**	**N**	**N**	**N**
LP5	10	N	N	N	N
DLT1	5	N	N	N	N
DLT2	5	N	N	N	N

4.3.4 Preclinial GMC1 Efficacy

Our collaborator, Dr. Chaudhary's group investigated the therapeutic effects of GMC1 on the regression of tumor size, volume, and weight in the four week-old castrated male athymic nude mice. The CRPC xenograft mouse models were generated by injecting LNCaP-Id4$^{-/-}$ cells subcutaneously into the lower flank of mice resulting in aggressive forms of prostate tumors. 5 mg/kg GMC1 treatment began at 4 weeks post-inoculation with tumor volume at approximately 100 mm^3 via intratumoral injection twice weekly for a month. As evident in Figure 4.3, GMC1 significantly reduced tumor size, volume, and weight in test (GMC1-treated) group compare to control (vehicle-treated). The drug treatment began to display inhibitory effects on the tumor growth at 2-week GMC1-post-injection and reached a significant inhibition of tumor growth at week 3 and 4 while the tumor volume in the control group continually increased (Fig. 4.3a). Furthermore, statistical analyses of tumor volumes within the test group revealed a progressive increase in tumor regression by demonstrating a significant decrease in tumor volume comparing week 4 post-GMC1-administration with week1 and 2 (**$P \leq 0.01$, asterisks not shown in Fig. 4.3a).

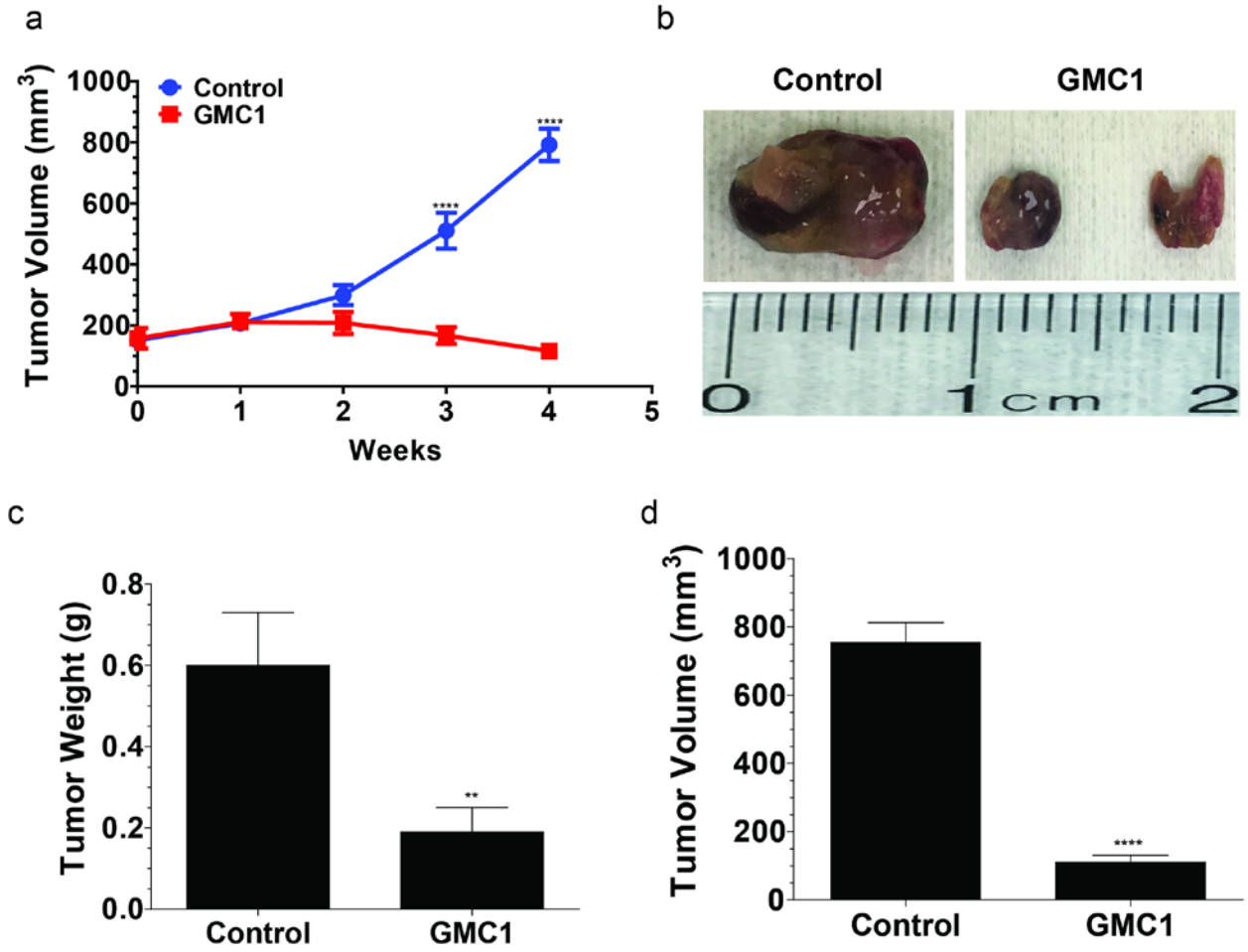

Figure 4.3: Treatment of LNCaP-Id4$^{-/-}$ Generated Prostate Tumor with GMC1 Significantly Decreased Tumor Size and Induced Tumor Regression

Fig. 4.3: Treatment of LNCaP-Id4$^{-/-}$ Generated Prostate Tumor with GMC1 Significantly Decreased Tumor Size, Volume, Weight, and Induced Tumor Regression. GMC1 treatment started 2 weeks post-inoculation of tumor cells by administering 5 mg/kg of the drug twice weekly for 4 consecutive weeks via intratumoral injection. **(a)** Tumor diameters were measured with a digital vernier caliper, then the volumes were calculated using Equation 3 described in section 4.2.4.2. Data displays the weekly measurements of 4 control tumors vs. 4 GMC1-treated tumors. The asterisks denote a statistically significant difference between the control and GMC1 treatment groups at each time point. Significant differences are indicated (**** $P \leq 0.0001$), which were calculated by One-Way ANOVA followed by Bonferroni's multiple comparison test. **(b-d)** At the end of the experiment, mice were sacrificed and tumors were extracted along with the respective measurements of the tumor volume and weight. The data represents an average of 4 tumor measurements per experimental group. Representative tumor images for each experimental condition are displayed in **(b)**. The asterisks denote a statistically significant difference as compared to no drug treatment. **$P \leq 0.01$ and ****$P \leq 0.0001$ were calculated by Student's *t*-test compared with no treatment control.

4.4 DISCUSSION

We have generated mutations at D68, V86, I87, and Y113 positions in the FKBP52 PPIase pocket based on the evidence that it forms important hydrogen bonds with GMC1 and/or establishes pertinent interactions between the residues and our lead molecule. Our collaborator, Dr. Cherkasov's group have performed molecular dynamic simulation and alanine-scanning on the predicted FKBP52-GMC1 complex in which Y113 showed the most reasonable energy difference between FKBP52-WT and the mutants (data not shown). Interestingly, functional mutagenesis studies demonstrated that the FKBP52-Y113A mutant abrogated the co-chaperone's receptor potentiation function (Fig. 4.1d). This phenomenon could be due to the fact that by changing tyrosine to alanine at position 113 induced too much structure instability within the PPIase domain resulting in an abolishment of the co-chaperone's function. We have observed that mutation at D68 affected the inhibitory effects of GMC1 on FKBP52-regulated AR-mediated activity (Fig. 4.2). The mutant did not impair the molecule's inhibition of receptor function completely, but it did demonstrate a reduction trend of the IC_{50} value by two-fold, which suggests that GMC1 interacts weakly with D68.

Assessing the physicochemimal properties of drug compounds are typical early steps in drug discovery. A good compound has high enough water solubility to be able to dissolve to blood/plasma and other aqueous bodily fluids, whilst also having certain amount of lipophilicity to permeate across biological membranes (*i.e.* intestine wall). In this study, our collaborator, Dr. Xie's group found that GMC1 was highly plasma protein bound, and the binding is concentration-independent. Based on the free drug hypothesis, only the free unbound fraction of a drug at the therapeutic target site exerts pharmacological activity [243]. Thus, it was necessary and important to develop an appropriate formulation for GMC1 to be delivered to the therapeutic target biophase for preclinical efficacy studies. The optimal formulation was identified to be LP4 (Table 4.2), which was selected based on consideration of three factors: GMC1 solubility, GMC1 precipitation upon aqueous dilution, and solvent toxicity. The LP4 formulation increased GMC1 aqueous solubility by a 3333 fold at 10 mg/mL, which can be safely administered to

animal subjects orally, subcutaneously, and intravenously. This optimal formulation was also found to be stable at 4°C for a minimum of one month.

Given there was no established pharmacokinetic profile on therapeutic window and toxicity of GMC1, our collaborator, Dr. Chaudhary's group decided to deliver the drug via intratumoral injection, thus bypassing the major obstacles associated with systemic delivery while taking advantage of solid tumor barriers to prevent rapid drug clearance and promote local drug retention, and lower concentration in healthy tissues [244-246]. The data showed that 5 mg/kg GMC1 twice weekly intratumoral administration with LP4 co-solvent formulation significantly inhibited the tumor growth and induced tumor regression (Fig. 4.3). Given the aggressive nature and androgen independence of the LNCaP-Id4$^{-/-}$ tumor model [236, 237], these findings are encouraging and warrant further preclinical development of GMC1.

CHAPTER 5: CONCLUSIONS

PCa is one of the most common cancers and the second leading cause of cancer deaths in men in industrialized nations and remains a major challenge to treat effectively [247-249]. AR is an androgen-activated transcription factor that belongs to the nuclear receptor family and plays an important role in promoting the development of PCa [250]. In addition, studies have shown that the AR signaling axis remains active as the disease evolves from androgen-sensitive cancer to castration-resistant [251, 252]. In fact, aberrant AR signaling is a hallmark of CRPC. Therefore, AR has been the most common therapeutic target for the treatment of PCa and the mainstay for it is hormone-ablation therapy using antiandrogens and/or ADT [216, 253-256].

Current clinically approved antiandrogens, such as Flutamide (Eulexin) [257], Bicalutamide (Casodex) [258], and Enzalutamide (MDV3100) [259] prevent androgens from carrying out their biological function by directly binding and blocking the AR LBD, hence inducing repressive activity [260, 261]. The efficacy of antiandrogen treatment is temporary, and typically after a median of 18-24 months, the disease progresses to CRPC, which becomes nonresponsive to ADT and fatal with no curative therapy available. The antiandrogen resistance mechanisms are mainly thought to be due to spontaneously acquired mutations in the AR LBD including T877A, W741L/C, H874Y, and F876L, which convert the drugs from receptor antagonists to agonists [163, 224, 262-265]. In addition, most of the antiandrogens share the same structural motif responsible for effective AR LBD binding. As a result, there is an unmet clinical need in developing treatments for CRPC. Researchers including our lab have focused their efforts on the development of drugs targeting alternative sites on AR and its regulatory proteins, and AR inhibitors for which the binding sites are currently unknown [165].

Our lab has developed an AR BF3 surface-directed AR antagonist termed MJC13, which inhibits FKBP52 regulation of AR by blocking the dissociation of AR-FKBP52-Hsp90 complex and retaining the hetercomplex in the cytoplasm resulting in a loss of AR nuclear translocation and inhibition of androgen-dependent gene expression and proliferation in prostate cancer cells [166]. Additionally, we have shown that MJC13 effectively prevents β-catenin interaction with the AR LBD and the synergistic up-regulation of the receptor by FKBP52 and β-catenin [192],

which suggests that the drug might be able to block AR reactivation that occurs in response to Wnt/β-catenin signaling stimulation in CRPC.

While the targeting of the alternative FKBP52 regulatory surface on AR is a promising therapeutic strategy as demonstrated by MJC13, a novel drug directly targeting FKBP52 by interrupting the proline-rich loop interaction with AR would likely be a more potent and effective strategy in treating PCa. The reasons are illustrated in Figure 1.4. First, the FKBP52 PPIase pocket is an ideal hydrophobic drug binding site and is also a known "druggable" target as FK506 (Tacrolimus) is already FDA-approved for use in the clinic. Second, given the conservation of the PPIase pocket across FKBP family members, drugs targeting the FKBP52 PPIase pocket would likely target the closely related FKBP51 protein, which is also a positive regulator of AR in PCa [196]. Third, FKBP52 is a known positive regulator of GR and PR in addition to AR. Thus, direct targeting of the co-chaperone would target the activity of all three receptors simultaneously, which have been shown to be expressed to higher levels in PCa and/or to confer resistant to current antiandrogen treatments [159, 197-201]. Lastly, FKBP52 directly regulates NFκB and inhibition of its signaling has recently been demonstrated to restore CRPC responsiveness to ADT [202, 203]. These FKBP52-regulated AR functions are all through the co-chaperone's proline-rich loop interaction with the receptor; therefore, the loop has emerged as a potential molecular target for pharmacological intervention. Unfortunately, the proline-rich loop does not represent an ideal hydrophobic drug binding pocket, however, the PPIase catalytic pocket underneath the loop does. The available co-crystal structure of FKBP12 bound to FK506 suggests that small molecules docked within the PPIase pocket could re-orient the proline-rich loop conformation leading to the disruption of interaction with the receptor LBD at this surface. Thus, the overall goal of this dissertation study was to develop and characterize a novel small molecule targeting the FKBP52 PPIase pocket that leads to disruption of proline-rich loop interactions between the co-chaperone and AR for the treatment of advanced PCa. Furthermore, we aimed to develop a solution formulation of GMC1 and use the formulation to determine the efficacy of GMC1 in a human prostate cancer xenograft mouse model.

5.1 Structure-Based *In Silico* Screen is a Viable Methodology for Identification of GMC1 Targeting FKBP52 PPIase Pocket

As aforementioned, the FKBP52 proline-rich loop surface does not represent an ideal hydrophobic drug binding site, but the PPIase pocket underneath the loop does. This catalytic region is a well-characterized hydrophobic cavity that forms strong hydrophobic interactions with ligands except a few polar residues, which are Asp68, Ile87 and Tyr113 in FKBP52, for creating hydrogen bonds with binding molecules (Fig. 2.1). We employed a FKBP52 PPIase pocket-targeted *in silico* screen on a ZINC database with 3 million commercially available lead-like compounds and identified 40 structurally diverse hit compounds. We performed functional AR-mediated luciferase assays on the compounds for their effect on FKBP52-regulated AR-dependent activity. GMC1 was the resulting lead molecule that demonstrated a potent FKBP52-specific inhibition of AR function with an IC_{50} value 0.6576 μM (Fig. 2.2b).

Interestingly, following the completion of the screen, we have observed that GMC1 is structurally similar to a recently identified novel compound, D44, that targets the PPIase of an FKBP protein from *Plasmodium*, which has been studied as a potential anti-malaria drug [266]. Similar to our efforts in finding a lead molecule, Harikishore *et al.* employed a structure-based *in silico* library screening of commercially available compounds and identified D44. The inhibitor's mode of action is through binding of the PPIase pocket of FKBP35 of malaria parasites *Plasmodium falciparum* and *Plasmodium vivax* (*Pf*FKBP35 and *Pv*FKBP35) [266]. In addition, D44 is a small molecule that antagonizes *Plasmodium* FKBP35 without interacting with and activating the calcineurin pathway upon binding to FKBP as FK506 does. Therefore, it would be interesting to assess whether GMC1 can elicit similar growth inhibition of the malaria parasites as D44 by modulating *Pf*FKBP35 and *Pv*FKBP35 functions via binding to the PPIase domain as they share sequence and structural similarities within canonical FKBP family members including FKBP52.

5.2 SMALL MOLECULE FKBP52 INHIBITOR GMC1 AS A POTENTIAL TREATMENT FOR ADVANCED PCA

FKBP52 is a relevant factor in AR, GR, and PR-related physiology and diseases, which have been firmly established in both *in vivo* and *in vitro* studies. The 52KO mouse models demonstrated that in the absence of the co-chaperone, the animal displayed phenotypes that are consistent with the insensitivity syndromes that result in defective AR, GR, and PR signaling. Our data demonstrated that GMC1 is effective in inhibiting FKBP52-specific AR, GR and PR-mediated activity (Fig. 2.2 and Fig. 3.1) suggesting its therapeutic potential to serve as a potent drug candidate in treating diseases and/or averting side effects associated with current ADT resulting from androgen, glucocorticoid, and progesterone insensitivity. Also, the data suggests that GMC1 has the ability to deter the disease resistance that arises from cross-talk between the receptors, which often occur in CRPC and confer resistance to antiandrogen treatments. It is noteworthy that GMC1, a small molecule that has not been structurally optimized by SAR, exhibited FKBP52-specific inhibitory effect on AR-regulated function at high nanomolar concentration (Fig. 2.2b), which is comparable to what we observed in structurally optimized MJC13. It suggests that disrupting the FKBP52 proline-rich loop interaction surface with AR is a more powerful drug target than targeting the alternative binding site on the LBD. Given that GMC1 does not share similar structural properties to the current antiandrogens (Flutamide, Bicalutamide, and MDV3100), and does not bind to the AR LBD, we predict that it will not produce the partial agonistic effects that are seen with the antiandrogens.

PSA, also known as kallikerin-related peptidase 3 (KLK3), is a chymotrypsin-like kallikrein that is produced at very high levels by prostate cancer cells in comparison to normal prostate secretory-luminal epithelial cells [267-269]. This protein has been used extensively as a biomarker to screen for PCa, to detect recurrence following local therapies, and to monitor response to systemic therapies for metastatic disease. Despite the current controversies over the effectiveness of PSA as a PCa screening test, the fact that PSA levels do have a correlation with prognosis of the disease is irrefutable. We employed ELISA analysis to assess GMC1 effects on

PSA secretion in 22Rv1 and LNCaP prostate cancer cells. GMC1 exhibited a concentration-dependent reduction in hormone-stimulated PSA secretion (Fig. 3.2a-b). Interestingly, the data showed an inhibition of basal PSA activity in 22Rv1 cells, which might suggest that GMC1 could have effects on AR splice variants (Fig. 3.2c). Moreover, the impairment of androgen-stimulated PSA secretion from 22Rv1 cells was more potent as compared to LNCaP, which only responds to hormone and displays DHT-dependent PSA production (Fig 3.2). Taken together, these data suggest that GMC1 may be effective in inhibiting hormone-independent PSA secretion as often occurs in CRPC.

GMC1 inhibitory effect on AR signaling was examined using PSA promoter as it is the best characterized androgen-responsive model. As shown in Fig. 3.3a, the hormone-induced PSA promoter activity was reduced in a concentration-dependent manner by our lead molecule. GMC1 significantly suppressed the hormone-mediated AR transactivation activity at 30 μM and higher concentrations of which is comparable to SAR optimized MJC13 and clinically used Bicalutamide and MDV3100 (Fig. 3.3). Our lead molecule GMC1 effectively reduced transactivation of PSA promoter in LNCaP, which express the AR-T877A mutation, suggesting that our molecule could be effective against Flutamide-resistant AR. In recent years, the AR T877A mutant along with a series of acquired spontaneous mutations in AR LBD have contributed to a phenomenon termed antiandrogen withdrawal syndrome (AWS), which is characterized by a decline in serum PSA levels and a regression of tumors after discontinuation of antiandrogen administration in patients with recurrent PCa [270, 271]. These acquired mutations often broaden ligand specificity and confer an antagonist-to-agonist switch that drives phenotypic resistance in CRPC. It would be interesting to perform transactivation assays to assess GMC1 effects on antiandrogen agonist-switch AR mutants which include W741L/C (Bicalutamide) [272], F876L (MDV3100) [163], H874Y (Flutamide) [273], etc. We expect our lead molecule to maintain its antagonistic effect on the mutated AR and circumvent the AWS occurrence given the molecular mechanism of GMC1 is targeting FKBP52 PPIase pocket to

disrupt the proline-rich loop interaction surface with AR instead of binding to AR LBD as current antiandrogens do.

Androgen signaling is through ligand-dependent AR activation leading to the modulation androgen-regulated genes including AR, PSA, and FKBP51, which are essential for the development of the prostate and also responsible for the pathogenesis of PCa. Therefore, they have recently emerged as promising prognostic biomarkers for PCa and candidates for cancer therapy. We examined the effects of GMC1 on the endogenous levels of androgen-responsive AR, FKBP51 and PSA expressions using Western immunoblots and densitometry analyses in prostate cancer cells (Fig. 3.4 and Fig. 3.5). Our data showed GMC1 promotes degradation of AR in the presence of DHT (Fig. 3.4) and suppressed androgen-dependent AR-mediated PSA and FKBP51 expressions in concentration-dependent manners (Fig. 3.5). These results demonstrate that GMC1 induced AR protein instability resulting in a reduced number of the receptor molecules capable of binding hormone leading to decreased androgen-dependent AR, PSA, and FKBP51 gene expression. This disrupts the FKBP51 positive feed forward mechanism with AR and abolishes the amplification of AR signaling which often occurs in the low-hormone conditions that happen during androgen ablation. Therefore, the data suggest GMC1 could be effective in treating CRPC. It is interesting to note that GMC1 appears to have a greater influence on 22Rv1 compared to LNCaP; it consistently requires lower concentrations to achieve significant inhibition of ligand-dependent AR-regulated activities (Fig. 3.4 and Fig. 3.5). Additionally, the lead molecule at high dose, 100 μM, was observed to reduce the expression of the constitutively active truncated AR at approximately 80 kDa (Fig. 3.4a) and as aforementioned, the decreasing basal PSA secretion level in 22Rv1 (Fig. 3.2a, inset). These observations suggest that GMC1 could affect functions of constitutively active AR splice variants, which are frequently expressed at high level in CRPC.

One of the hallmarks of cancer is uncontrollable cell proliferation, thus we carried out cell proliferation assays with three prostate cancer cell lines: AR-positive LNCaP and 22Rv1 cells and AR-negative PC3 prostate cancer cells, to determine whether GMC1 affects tumor cell

proliferation. Our lead molecule antagonized the proliferative effect of the synthetic androgen R1881 without any significant effect on the growth of AR-negative PC3 cells at the same concentrations (Fig. 3.6), which demonstrates that the inhibition of proliferation observed in AR-positive LNCaP and 22Rv1 cells was mediated through antagonism of AR. It was observed that GMC1 appeared to affect the growth of LNCaP in the absence of R1881 at 75 µM and 100 µM, which suggests that our molecule could be slightly cytotoxic at those concentrations. However, the trend of GMC1 inhibiting cell growth in an androgen-dependent AR-mediated manner is indisputable. Additionally, the statistical analyses comparing the data points at higher concentrations in the absence and presence of R118A demonstrated that GMC1 significantly antagonized the hormone-dependent proliferative effect (Fig. 3.6b) and the observed phenomenon was not due to cytotoxicity.

5.3 Confirmation of GMC1 Binding to the Proposed Site on the FKBP52 PPIase Catalytic Pocket

We attempted to prove that the FKBP52 PPIase pocket inhibitor GMC1 does directly bind to the predicted target site in the hydrophobic cavity by performing a competitive FP assay with a known FKBP inhibitor FK506 targeting the catalytic groove. Unfortunately, we did not detect any competitive binding of GMC1 to the PPIase pocket due to the nature of its small size and low binding affinity for the catalytic cavity compared to the control binder. Thus, in order to verify that GMC1 directly binds to the predicted target site on the catalytic pocket, we designed and constructed amino acid mutations that may alter the predicted binding site of the compound while not affecting the FKBP52 potentiation of AR function. We generated alanine point mutations at D68, V86, I87, and Y113 in the full-length human FKBP52. Among these, three mutants, FKBP52-D68A, V87A, and I87A maintained FKBP52-mediated AR function, while the mutation at Y113 destroyed the co-chaperone-regulated receptor activity and was not considered further (Fig. 4.1). GMC1 was tested on the three mutants and compared to the luciferase activities obtained with AR and wild type FKBP52. There was a trend for GMC1 inhibition of FKBP52-mediated AR function with the D68A mutation, suggesting that our lead molecule

interacts weakly with the residue in the proposed FKBP52 PPIase pocket target site (Fig. 4.2a). Unfortunately, I was not able to complete receptor-mediated luciferase assays of FKBP52-V86A and I87A mutants at the time of dissertation completion to determine the effects of those mutations have on AR function in the presence of GMC1. It would be interesting to see which residue in the PPIase pocket significantly influenced GMC1 inhibitory function. Even if none of the mutants strongly affect the inhibition, this does not mean that GMC1 has no interaction with the predicted binding site. It simply could suggest that all three residues, D68, V86, and I87, are required and equally important for GMC1 binding and displaying the potent inhibitory effects we observed *in vitro*.

5.4 Solution Formulation Development and Efficacy of GMC1 in Preclinical CRPC Animal Model

We successfully developed and optimized a co-solvent formulation allowing for *in vivo* administration of GMC1 that is based on the compound's physicochemical properties. The optimal co-solvent system for GMC1 is with LP4 formulation (Table 4.3). It is stable and suitable for further preclinical and clinical evaluations of safety and efficacy. The formulation was successfully applied in a preliminary preclinical efficacy study in an androgen-independent prostate cancer xenograft mouse model and showed significant regression of tumor size and volume (Fig. 4.3). This proof-of-principle data demonstrates that inhibition of FKBP52-specific activity via disrupting its proline-rich loop interaction with AR is an effective and promising strategy in treating CRPC.

5.5 Proposed Mechanism

Based on the *in vitro* evidence, it is hypothesized that binding of FKBP52 to the extreme C-terminus of Hsp90 brings the proline-rich loop overhanging the FKBP52 FK1 domain in close proximity to the receptor LBD leading to regulation of hormone binding and subcellular localization. GMC1 interrupts this interaction by disrupting the architectural integrity of the

loop, subsequently inducing dissociation of the mature chaperone complex and degradation of AR via the ubiquitin/proteasome pathway (Fig. 5.1).

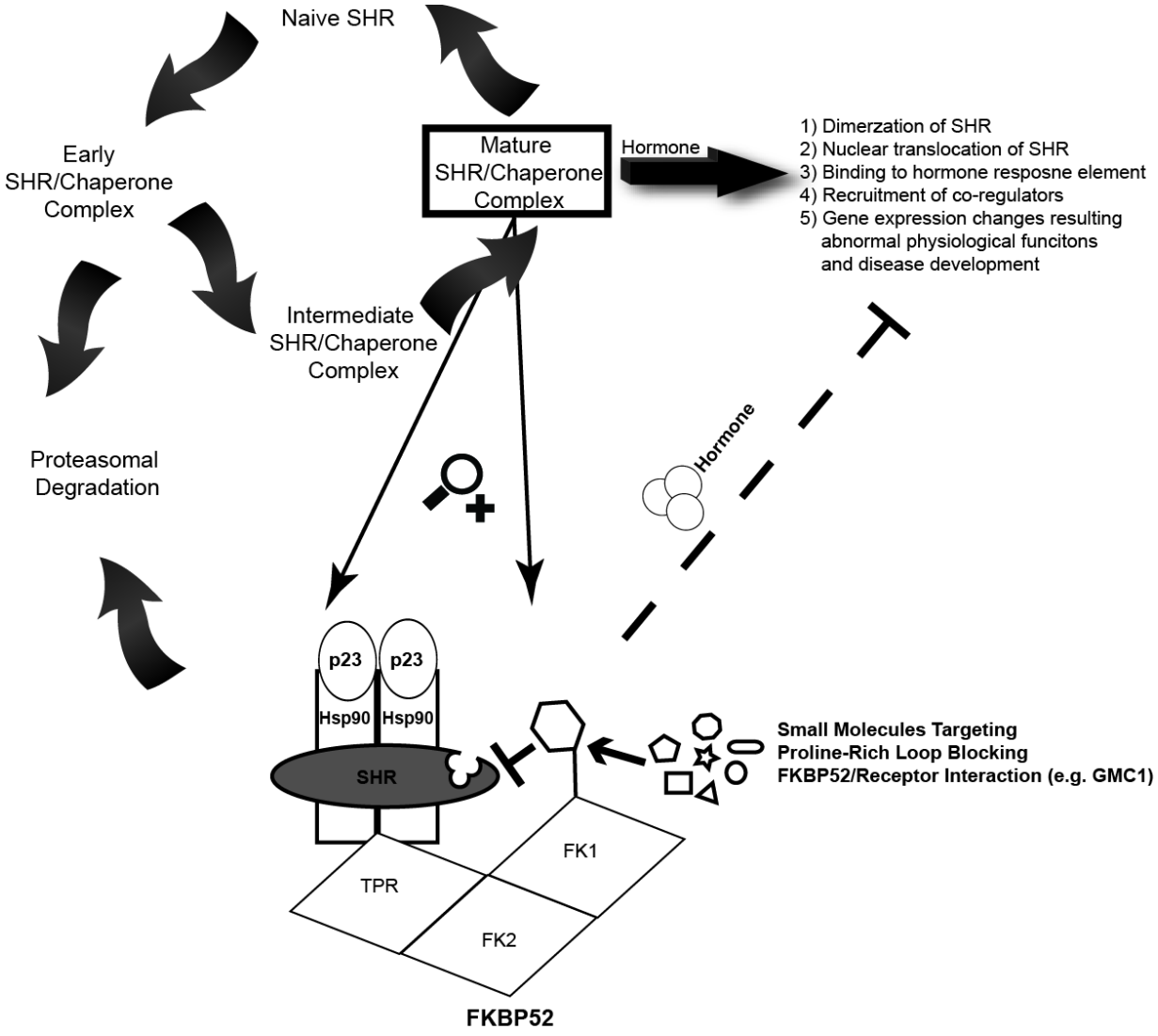

Figure 5.1: Proposed Mechanism of Action of FKBP52-Specific Small Molecule Inhibitors

Fig. 5.1: Proposed Mechanism of Action of FKBP52-Specific Small Molecule Inhibitors. FKBP52 is a TPR-containing co-chaperone that plays a critical role in the chaperone-dependent folding of SHRs to their functionally mature conformations that are competent for hormone binding. It acts as a specific positive regulator of AR, GR, and PR functions through the interaction of the proline-rich loop with the LBD of the SHRs. Upon ligand binding, the receptor dimerizes and translocates to the nucleus, which then binds to the HRE and recruits other co-regulators resulting in regulation of various physiological functions. Direct targeting the FKBP52 proline-rich loop interaction surface with the receptor LBD with small molecules (*e.g.* GMC1) prevent ligand binding and leading to disruptions of SHR/Hsp90/FKBP52 heterocomplex such that client proteins are directed to the proteasome for degradation.

5.6 CONCLUDING REMARKS

In this study, we have identified GMC1 as a first-in-class inhibitor directly targeting the FKBP52 co-chaperone for the treatment of PCa. Give that GMC1 affects AR, GR and PR, but has no effect on ER, the data support the predicted targeting of FKBP52 directly. We propose that GMC1 interferes with the receptor-chaperone hetercomplex formation via binding to the FKBP52 PPIase catalytic pocket in the FK1 domain, which induces re-orientation of the proline-rich loop overhang the cavity and disrupting the interaction surface with AR and/or causing a spatial re-orientation within the asymmetrical intermediate chaperone complex preventing its progression into mature stage of chaperone cycle. Further studies will be required to validate this mechanism of action. Regardless, the consequences of inhibition of AR transactivation activity, receptor-dependent gene expression, and androgen-stimulated proliferation and PSA secretion in prostate cancer cell lines are indisputable. Due to its unique mechanism of action, we believe GMC1 will be able to prevent aberrant AR signaling that is caused by cross-talk between the signaling pathways (*e.g.* Wnt/β-catenin, NFκB), circumventing AR LBD mutation-based resistance arising from antiandrogen treatments (*e.g.* Flutamide, Bicalutamide, MDV3100), and eluding the bypass of AR blockade via alternative SHR pathways (*e.g.* GR, PR). We also believe GMC1 is a more potent and effective drug for the treatment of CRPC than MJC13, Flutamide, Bicalutamide, and MDV3100, thereby filling a major unmet need in prostate cancer therapy. Additionally, GMC1 could serve as a second line therapy for CRPC previously treated with ADT and/or could be administered concurrently with antiandrogens to mitigate undesirable side effects and resistance. Furthermore, given the functional roles of FKBP52 in AR, GR, and PR-specific phenotypes and its elevated expression in ER-negative breast tumors, GMC1 also represents an attractive treatment option and/or target for other endocrine-associated diseases, such as male contraception, obesity/metabolic syndrome, stress and depression, and ER-negative breast cancer.

5.7 FUTURE DIRECTIONS

There is incontrovertible evidence that the onset of CRPC coincides with the renewed AR signaling even without androgen stimulation, and the expression of constitutively active AR splice variants are commonly increased in recurrent PCa following castration and continue to drive tumor progression in the face of potent AR LBD inhibitory agents. Thus, we would like to further investigate and characterize the inhibitory effects of GMC1 on androgen-independent prostate cancer cell lines (*e.g.* VCaP), the constitutively active AR splice variants (*e.g.* AR-V7), and the receptor-transcription activation functions that arise from spontaneous mutations in the AR LBD (*e.g.* W741L/C, F876L, and H874Y) that often confer antiandrogens the antagonist-to-agonist switch that drives AWS in CRPC. Studies have shown that β-catenin and NFκB signaling pathways often cross-talk with AR contributing to CRPC development and progression. β-catenin and NFκB have also been found to interact directly with FKBP52. Thus, it would be interesting to assess GMC1 effects on the stability and interactions between SHR-FKBP52 heterocomplex with β-catenin and/or NFκB. In addition, we would like to determine the X-ray crystallographic structure of the FKBP52 PPIase pocket in the FK1 domain in complex with GMC1 and perform an SAR analysis of our lead molecule, from which we will gain structural insights into the mode of action of our compound and improve its efficacy, potency, and solubility.

REFERENCES

1. Chen, S. and D.F. Smith, *Hop as an adaptor in the heat shock protein 70 (Hsp70) and hsp90 chaperone machinery.* J Biol Chem, 1998. **273**(52): p. 35194-200.
2. Dittmar, K.D., et al., *Reconstitution of the steroid receptor.hsp90 heterocomplex assembly system of rabbit reticulocyte lysate.* J Biol Chem, 1996. **271**(22): p. 12833-9.
3. Freeman, B.C., et al., *The p23 molecular chaperones act at a late step in intracellular receptor action to differentially affect ligand efficacies.* Genes Dev, 2000. **14**(4): p. 422-34.
4. Hernandez, M.P., A. Chadli, and D.O. Toft, *HSP40 binding is the first step in the HSP90 chaperoning pathway for the progesterone receptor.* J Biol Chem, 2002. **277**(14): p. 11873-81.
5. Hutchison, K.A., et al., *The 23-kDa acidic protein in reticulocyte lysate is the weakly bound component of the hsp foldosome that is required for assembly of the glucocorticoid receptor into a functional heterocomplex with hsp90.* J Biol Chem, 1995. **270**(32): p. 18841-7.
6. Johnson, B.D., et al., *Hop modulates Hsp70/Hsp90 interactions in protein folding.* J Biol Chem, 1998. **273**(6): p. 3679-86.
7. Johnson, J., et al., *Characterization of a novel 23-kilodalton protein of unactive progesterone receptor complexes.* Mol. Cell. Biol., 1994. **14**: p. 1956-1963.
8. Johnson, J. and D. Toft, *A novel chaperone complex for steroid receptors involving heat shock proteins, immunophilins, and p23.* J. Biol. Chem., 1994. **269**: p. 24989-24993.
9. Kosano, H., et al., *The assembly of progesterone receptor-hsp90 complexes using purified proteins.* J Biol Chem, 1998. **273**(49): p. 32973-9.
10. McLaughlin, S.H., et al., *The co-chaperone p23 arrests the Hsp90 ATPase cycle to trap client proteins.* J Mol Biol, 2006. **356**(3): p. 746-58.
11. Smith, D.F., *Dynamics of heat shock protein 90-progesterone receptor binding and the disactivation loop model for steroid receptor complexes.* Mol Endocrinol, 1993. **7**(11): p. 1418-29.
12. Smith, D.F., et al., *Identification of a 60-kilodalton stress-related protein, p60, which interacts with hsp90 and hsp70.* Mol Cell Biol, 1993. **13**(2): p. 869-76.
13. Murphy, P.J., et al., *Visualization and mechanism of assembly of a glucocorticoid receptor.Hsp70 complex that is primed for subsequent Hsp90-dependent opening of the steroid binding cleft.* J Biol Chem, 2003. **278**(37): p. 34764-73.
14. Fan, C.Y., S. Lee, and D.M. Cyr, *Mechanisms for regulation of Hsp70 function by Hsp40.* Cell Stress Chaperones, 2003. **8**(4): p. 309-16.
15. Hernandez, M.P., W.P. Sullivan, and D.O. Toft, *The assembly and intermolecular properties of the hsp70-Hop-hsp90 molecular chaperone complex.* J Biol Chem, 2002. **277**(41): p. 38294-304.
16. Connell, P., et al., *The co-chaperone CHIP regulates protein triage decisions mediated by heat-shock proteins.* Nat Cell Biol, 2001. **3**(1): p. 93-6.
17. Jiang, J., et al., *CHIP is a U-box-dependent E3 ubiquitin ligase: identification of Hsc70 as a target for ubiquitylation.* J Biol Chem, 2001. **276**(46): p. 42938-44.
18. Ballinger, C.A., et al., *Identification of CHIP, a novel tetratricopeptide repeat-containing protein that interacts with heat shock proteins and negatively regulates chaperone functions.* Mol Cell Biol, 1999. **19**(6): p. 4535-45.

19. Meacham, G.C., et al., *The Hsc70 co-chaperone CHIP targets immature CFTR for proteasomal degradation.* Nat Cell Biol, 2001. **3**(1): p. 100-5.
20. Stankiewicz, M., et al., *CHIP participates in protein triage decisions by preferentially ubiquitinating Hsp70-bound substrates.* FEBS J, 2010. **277**(16): p. 3353-67.
21. Takayama, S., et al., *BAG-1 modulates the chaperone activity of Hsp70/Hsc70.* EMBO J, 1997. **16**(16): p. 4887-96.
22. Luders, J., J. Demand, and J. Hohfeld, *The ubiquitin-related BAG-1 provides a link between the molecular chaperones Hsc70/Hsp70 and the proteasome.* J Biol Chem, 2000. **275**(7): p. 4613-7.
23. Luders, J., et al., *Distinct isoforms of the cofactor BAG-1 differentially affect Hsc70 chaperone function.* J Biol Chem, 2000. **275**(20): p. 14817-23.
24. Luders, J., et al., *Cofactor-induced modulation of the functional specificity of the molecular chaperone Hsc70.* Biol Chem, 1998. **379**(10): p. 1217-26.
25. Sondermann, H., et al., *Structure of a Bag/Hsc70 complex: convergent functional evolution of Hsp70 nucleotide exchange factors.* Science, 2001. **291**(5508): p. 1553-7.
26. Demand, J., et al., *Cooperation of a ubiquitin domain protein and an E3 ubiquitin ligase during chaperone/proteasome coupling.* Curr Biol, 2001. **11**(20): p. 1569-77.
27. Shimamoto, S., et al., *Ca2+/S100 proteins act as upstream regulators of the chaperone-associated ubiquitin ligase CHIP (C terminus of Hsc70-interacting protein).* J Biol Chem, 2013. **288**(10): p. 7158-68.
28. Frydman, J. and J. Hohfeld, *Chaperones get in touch: the Hip-Hop connection.* Trends Biochem. Sci., 1997. **22**: p. 87-92.
29. Hohfeld, J., Y. Minami, and F.U. Hartl, *Hip, a novel cochaperone involved in the eukaryotic Hsc70/Hsp40 reaction cycle.* Cell, 1995. **83**(4): p. 589-98.
30. Irmer, H. and J. Hohfeld, *Characterization of functional domains of the eukaryotic co-chaperone Hip.* J Biol Chem, 1997. **272**(4): p. 2230-5.
31. Prapapanich, V., et al., *Molecular cloning of human p48, a transient component of progesterone receptor complexes and an Hsp70-binding protein.* Mol Endocrinol, 1996. **10**(4): p. 420-31.
32. Prapapanich, V., et al., *Mutational analysis of the hsp70-interacting protein Hip.* Mol Cell Biol, 1996. **16**(11): p. 6200-7.
33. Gaiser, A.M., F. Brandt, and K. Richter, *The non-canonical Hop protein from Caenorhabditis elegans exerts essential functions and forms binary complexes with either Hsc70 or Hsp90.* J Mol Biol, 2009. **391**(3): p. 621-34.
34. Schmid, A.B., et al., *The architecture of functional modules in the Hsp90 co-chaperone Sti1/Hop.* EMBO J, 2012. **31**(6): p. 1506-17.
35. Chadli, A., et al., *GCUNC-45 is a novel regulator for the progesterone receptor/hsp90 chaperoning pathway.* Mol Cell Biol, 2006. **26**(5): p. 1722-30.
36. Ebong, I.O., et al., *Heterogeneity and dynamics in the assembly of the heat shock protein 90 chaperone complexes.* Proc Natl Acad Sci U S A, 2011. **108**(44): p. 17939-44.
37. Li, J., K. Richter, and J. Buchner, *Mixed Hsp90-cochaperone complexes are important for the progression of the reaction cycle.* Nat Struct Mol Biol, 2011. **18**(1): p. 61-6.
38. Southworth, D.R. and D.A. Agard, *Client-loading conformation of the Hsp90 molecular chaperone revealed in the cryo-EM structure of the human Hsp90:Hop complex.* Mol Cell, 2011. **42**(6): p. 771-81.

39. Meyer, P., et al., *Structural basis for recruitment of the ATPase activator Aha1 to the Hsp90 chaperone machinery.* EMBO J, 2004. **23**(3): p. 511-9.
40. Prodromou, C., et al., *The ATPase cycle of Hsp90 drives a molecular 'clamp' via transient dimerization of the N-terminal domains.* EMBO J, 2000. **19**(16): p. 4383-92.
41. Chadli, A., et al., *Analysis of Hsp90 cochaperone interactions reveals a novel mechanism for TPR protein recognition.* Biochemistry, 2008. **47**(9): p. 2850-7.
42. Shimamoto, S., et al., *S100 proteins regulate the interaction of Hsp90 with Cyclophilin 40 and FKBP52 through their tetratricopeptide repeats.* FEBS Lett, 2010. **584**(6): p. 1119-25.
43. Shimamoto, S., et al., *Interactions of S100A2 and S100A6 with the tetratricopeptide repeat proteins, Hsp90/Hsp70-organizing protein and kinesin light chain.* J Biol Chem, 2008. **283**(42): p. 28246-58.
44. Angeletti, P.C., D. Walker, and A.T. Panganiban, *Small glutamine-rich protein/viral protein U-binding protein is a novel cochaperone that affects heat shock protein 70 activity.* Cell Stress Chaperones, 2002. **7**(3): p. 258-68.
45. Paul, A., et al., *The cochaperone SGTA (small glutamine-rich tetratricopeptide repeat-containing protein alpha) demonstrates regulatory specificity for the androgen, glucocorticoid, and progesterone receptors.* J Biol Chem, 2014. **289**(22): p. 15297-308.
46. Tobaben, S., et al., *A trimeric protein complex functions as a synaptic chaperone machine.* Neuron, 2001. **31**(6): p. 987-99.
47. Scheufler, C., et al., *Structure of TPR domain-peptide complexes: critical elements in the assembly of the Hsp70-Hsp90 multichaperone machine.* Cell, 2000. **101**(2): p. 199-210.
48. Buchanan, G., et al., *Collocation of androgen receptor gene mutations in prostate cancer.* Clin Cancer Res, 2001. **7**(5): p. 1273-81.
49. Buchanan, G., et al., *Control of androgen receptor signaling in prostate cancer by the cochaperone small glutamine rich tetratricopeptide repeat containing protein alpha.* Cancer Res, 2007. **67**(20): p. 10087-96.
50. Hessling, M., K. Richter, and J. Buchner, *Dissection of the ATP-induced conformational cycle of the molecular chaperone Hsp90.* Nat Struct Mol Biol, 2009. **16**(3): p. 287-93.
51. Mickler, M., et al., *The large conformational changes of Hsp90 are only weakly coupled to ATP hydrolysis.* Nat Struct Mol Biol, 2009. **16**(3): p. 281-6.
52. Harst, A., H. Lin, and W.M. Obermann, *Aha1 competes with Hop, p50 and p23 for binding to the molecular chaperone Hsp90 and contributes to kinase and hormone receptor activation.* Biochem J, 2005. **387**(Pt 3): p. 789-96.
53. Weaver, A.J., et al., *Crystal structure and activity of human p23, a heat shock protein 90 co- chaperone*. J Biol Chem, 2000. **275**(30): p. 23045-52.
54. Weikl, T., K. Abelmann, and J. Buchner, *An unstructured C-terminal region of the Hsp90 co-chaperone p23 is important for its chaperone function.* J Mol Biol, 1999. **293**(3): p. 685-91.
55. Chadli, A., et al., *Dimerization and N-terminal domain proximity underlie the function of the molecular chaperone heat shock protein 90.* Proc Natl Acad Sci U S A, 2000. **97**(23): p. 12524-9.
56. Grenert, J.P., B.D. Johnson, and D.O. Toft, *The importance of ATP binding and hydrolysis by hsp90 in formation and function of protein heterocomplexes.* J Biol Chem, 1999. **274**(25): p. 17525-33.

57. Ma, L., et al., *Abdominal B (AbdB) Hoxa genes: regulation in adult uterus by estrogen and progesterone and repression in mullerian duct by the synthetic estrogen diethylstilbestrol (DES).* Dev Biol, 1998. **197**(2): p. 141-54.
58. Obermann, W.M., et al., *In vivo function of Hsp90 is dependent on ATP binding and ATP hydrolysis.* J Cell Biol, 1998. **143**(4): p. 901-10.
59. Panaretou, B., et al., *ATP binding and hydrolysis are essential to the function of the Hsp90 molecular chaperone in vivo.* Embo J, 1998. **17**(16): p. 4829-36.
60. Richter, K., S. Walter, and J. Buchner, *The Co-chaperone Sba1 connects the ATPase reaction of Hsp90 to the progression of the chaperone cycle.* J Mol Biol, 2004. **342**(5): p. 1403-13.
61. Siligardi, G., et al., *Co-chaperone regulation of conformational switching in the Hsp90 ATPase cycle.* J Biol Chem, 2004. **279**(50): p. 51989-98.
62. Pratt, W.B., et al., *Role of hsp90 and the hsp90-binding immunophilins in signalling protein movement.* Cell Signal, 2004. **16**(8): p. 857-72.
63. Echeverria, P.C., et al., *Nuclear import of the glucocorticoid receptor-hsp90 complex through the nuclear pore complex is mediated by its interaction with Nup62 and importin beta.* Mol Cell Biol, 2009. **29**(17): p. 4788-97.
64. Pratt, W.B., Y. Morishima, and Y. Osawa, *The Hsp90 chaperone machinery regulates signaling by modulating ligand binding clefts.* J Biol Chem, 2008. **283**(34): p. 22885-9.
65. Cheung, J. and D.F. Smith, *Molecular chaperone interactions with steroid receptors: an update.* Mol Endocrinol, 2000. **14**(7): p. 939-46.
66. Dittmar, K.D., et al., *Folding of the glucocorticoid receptor by the heat shock protein (hsp) 90-based chaperone machinery. The role of p23 is to stabilize receptor.hsp90 heterocomplexes formed by hsp90.p60.hsp70.* J Biol Chem, 1997. **272**(34): p. 21213-20.
67. Czar, M.J., et al., *Evidence that the FK506-binding immunophilin heat shock protein 56 is required for trafficking of the glucocorticoid receptor from the cytoplasm to the nucleus.* Mol Endocrinol, 1995. **9**(11): p. 1549-60.
68. Galigniana, M.D., et al., *Evidence that the peptidylprolyl isomerase domain of the hsp90-binding immunophilin FKBP52 is involved in both dynein interaction and glucocorticoid receptor movement to the nucleus.* J Biol Chem, 2001. **276**(18): p. 14884-9.
69. Galat, A., *Peptidylprolyl cis/trans isomerases (immunophilins): biological diversity--targets--functions.* Curr Top Med Chem, 2003. **3**(12): p. 1315-47.
70. Lebeau, M.C., et al., *P59, an hsp 90-binding protein. Cloning and sequencing of its cDNA and preparation of a peptide-directed polyclonal antibody.* J Biol Chem, 1992. **267**(7): p. 4281-4.
71. Massol, N., et al., *Rabbit FKBP59-heat shock protein binding immunophillin (HBI) is a calmodulin binding protein.* Biochem Biophys Res Commun, 1992. **187**(3): p. 1330-5.
72. Pirkl, F., et al., *Localization of the chaperone domain of FKBP52.* J Biol Chem, 2001. **276**(40): p. 37034-41.
73. Wu, B., et al., *3D structure of human FK506-binding protein 52: Implications for the assembly of the glucocorticoid receptor/Hsp90/immunophilin heterocomplex.* Proc Natl Acad Sci U S A, 2004. **101**(22): p. 8348-53.
74. Chambraud, B., et al., *Overexpression of p59-HBI (FKBP59), full length and domains, and characterization of PPlase activity.* Biochem Biophys Res Commun, 1993. **196**(1): p. 160-6.

75. Barent, R.L., et al., *Analysis of FKBP51/FKBP52 chimeras and mutants for Hsp90 binding and association with progesterone receptor complexes.* Mol Endocrinol, 1998. **12**(3): p. 342-54.
76. Cheung-Flynn, J., et al., *C-terminal Sequences outside the Tetratricopeptide Repeat Domain of FKBP51 and FKBP52 Cause Differential Binding to Hsp90.* J Biol Chem, 2003. **278**(19): p. 17388-94.
77. Barnes, J.A. and A.V. Gomes, *PEST sequences in calmodulin-binding proteins.* Mol Cell Biochem, 1995. **149-150**: p. 17-27.
78. Blatch, G.L. and M. Lassle, *The tetratricopeptide repeat: a structural motif mediating protein-protein interactions.* Bioessays, 1999. **21**(11): p. 932-9.
79. Goebl, M. and M. Yanagida, *The TPR snap helix: a novel protein repeat motif from mitosis to transcription.* Trends Biochem Sci, 1991. **16**(5): p. 173-7.
80. Radanyi, C., B. Chambraud, and E. Baulieu, *The ability of the immunophilin FKBP59-HBI to interact with the 90-kDa heat shock protein is encoded by its tetratricopeptide repeat domain.* Proc. Natl. Acad. Sci. U.S.A., 1994. **91**: p. 11197-11201.
81. Russell, L.C., et al., *Identification of conserved residues required for the binding of a tetratricopeptide repeat domain to heat shock protein 90.* J Biol Chem, 1999. **274**(29): p. 20060-3.
82. Riggs, D.L., et al., *The Hsp90-binding peptidylprolyl isomerase FKBP52 potentiates glucocorticoid signaling in vivo.* EMBO J, 2003. **22**(5): p. 1158-67.
83. Pirkl, F. and J. Buchner, *Functional analysis of the Hsp90-associated human peptidyl prolyl cis/trans isomerases FKBP51, FKBP52 and Cyp40.* J Mol Biol, 2001. **308**(4): p. 795-806.
84. Sinars, C.R., et al., *Structure of the large FK506-binding protein FKBP51, an Hsp90-binding protein and a component of steroid receptor complexes.* Proc Natl Acad Sci U S A, 2003. **100**(3): p. 868-73.
85. Riggs, D.L., et al., *Noncatalytic role of the FKBP52 peptidyl-prolyl isomerase domain in the regulation of steroid hormone signaling.* Mol Cell Biol, 2007. **27**(24): p. 8658-69.
86. Callebaut, I., et al., *An immunophilin that binds M(r) 90,000 heat shock protein: main structural features of a mammalian p59 protein.* Proc Natl Acad Sci U S A, 1992. **89**(14): p. 6270-4.
87. Le Bihan, S., et al., *The mammalian heat shock protein binding immunophilin (p59/HBI) is an ATP and GTP binding protein.* Biochem Biophys Res Commun, 1993. **195**(2): p. 600-7.
88. Blackburn, E.A. and M.D. Walkinshaw, *Targeting FKBP isoforms with small-molecule ligands.* Curr Opin Pharmacol, 2011. **11**(4): p. 365-71.
89. Edlich, F., et al., *A novel calmodulin-Ca2+ target recognition activates the Bcl-2 regulator FKBP38.* J Biol Chem, 2007. **282**(50): p. 36496-504.
90. Edlich, F., et al., *Bcl-2 regulator FKBP38 is activated by Ca2+/calmodulin.* EMBO J, 2005. **24**(14): p. 2688-99.
91. Maestre-Martinez, M., et al., *New structural aspects of FKBP38 activation.* Biol Chem, 2010. **391**(10): p. 1157-67.
92. Bracher, A., et al., *Crystal structures of the free and ligand-bound FK1-FK2 domain segment of FKBP52 reveal a flexible inter-domain hinge.* J Mol Biol, 2013. **425**(22): p. 4134-44.

93. Miyata, Y., et al., *Phosphorylation of the immunosuppressant FK506-binding protein FKBP52 by casein kinase II: regulation of HSP90-binding activity of FKBP52.* Proc Natl Acad Sci U S A, 1997. **94**(26): p. 14500-5.
94. Cox, M.B., et al., *FK506-binding protein 52 phosphorylation: a potential mechanism for regulating steroid hormone receptor activity.* Mol Endocrinol, 2007. **21**(12): p. 2956-67.
95. Qing, K., et al., *Adeno-associated virus type 2-mediated gene transfer: role of cellular FKBP52 protein in transgene expression.* J Virol, 2001. **75**(19): p. 8968-76.
96. Qing, K., et al., *Adeno-associated virus type 2-mediated gene transfer: role of cellular T-cell protein tyrosine phosphatase in transgene expression in established cell lines in vitro and transgenic mice in vivo.* J Virol, 2003. **77**(4): p. 2741-6.
97. Cheung-Flynn, J., et al., *Physiological role for the cochaperone FKBP52 in androgen receptor signaling.* Mol Endocrinol, 2005. **19**(6): p. 1654-66.
98. Tranguch, S., et al., *Cochaperone immunophilin FKBP52 is critical to uterine receptivity for embryo implantation.* Proc Natl Acad Sci U S A, 2005. **102**(40): p. 14326-31.
99. Mustafi, S.M., D.M. LeMaster, and G. Hernandez, *Differential conformational dynamics in the closely homologous FK506-binding domains of FKBP51 and FKBP52.* Biochem J, 2014. **461**(1): p. 115-23.
100. Yong, W., et al., *Essential role for Co-chaperone Fkbp52 but not Fkbp51 in androgen receptor-mediated signaling and physiology.* J Biol Chem, 2007. **282**(7): p. 5026-36.
101. Hong, J., et al., *Deficiency of co-chaperone immunophilin FKBP52 compromises sperm fertilizing capacity.* Reproduction, 2007. **133**(2): p. 395-403.
102. Yang, Z., et al., *FK506-binding protein 52 is essential to uterine reproductive physiology controlled by the progesterone receptor A isoform.* Mol Endocrinol, 2006. **20**(11): p. 2682-94.
103. Tranguch, S., D.F. Smith, and S.K. Dey, *Progesterone receptor requires a co-chaperone for signalling in uterine biology and implantation.* Reprod Biomed Online, 2006. **13**(5): p. 651-60.
104. Tranguch, S., et al., *FKBP52 deficiency-conferred uterine progesterone resistance is genetic background and pregnancy stage specific.* J Clin Invest, 2007. **117**(7): p. 1824-34.
105. Hirota, Y., et al., *Uterine FK506-binding protein 52 (FKBP52)-peroxiredoxin-6 (PRDX6) signaling protects pregnancy from overt oxidative stress.* Proc Natl Acad Sci U S A, 2010. **107**(35): p. 15577-82.
106. Hirota, Y., et al., *Deficiency of immunophilin FKBP52 promotes endometriosis.* Am J Pathol, 2008. **173**(6): p. 1747-57.
107. Sanchez, E.R., *Chaperoning steroidal physiology: lessons from mouse genetic models of Hsp90 and its cochaperones.* Biochim Biophys Acta, 2012. **1823**(3): p. 722-9.
108. Wadekar, S.A., D. Li, and E.R. Sanchez, *Agonist-activated glucocorticoid receptor inhibits binding of heat shock factor 1 to the heat shock protein 70 promoter in vivo.* Mol Endocrinol, 2004. **18**(3): p. 500-8.
109. Warrier, M., et al., *Susceptibility to diet-induced hepatic steatosis and glucocorticoid resistance in FK506-binding protein 52-deficient mice.* Endocrinology, 2010. **151**(7): p. 3225-36.
110. Ward, B.K., et al., *Expression of the estrogen receptor-associated immunophilins, cyclophilin 40 and FKBP52, in breast cancer.* Breast Cancer Res Treat, 1999. **58**(3): p. 267-80.

111. Kumar, P., et al., *Estradiol-regulated expression of the immunophilins cyclophilin 40 and FKBP52 in MCF-7 breast cancer cells.* Biochem Biophys Res Commun, 2001. **284**(1): p. 219-25.
112. Ostrow, K.L., et al., *Pharmacologic unmasking of epigenetically silenced genes in breast cancer.* Clin Cancer Res, 2009. **15**(4): p. 1184-91.
113. Cochrane, D.R., et al., *Role of the androgen receptor in breast cancer and preclinical analysis of enzalutamide.* Breast Cancer Res, 2014. **16**(1): p. R7.
114. Barik, S., *Immunophilins: for the love of proteins.* Cell Mol Life Sci, 2006. **63**(24): p. 2889-900.
115. Kang, C.B., et al., *FKBP family proteins: immunophilins with versatile biological functions.* Neurosignals, 2008. **16**(4): p. 318-25.
116. Haelens, A., et al., *The hinge region regulates DNA binding, nuclear translocation, and transactivation of the androgen receptor.* Cancer Res, 2007. **67**(9): p. 4514-23.
117. Hernandez, F. and J. Avila, *Tauopathies.* Cell Mol Life Sci, 2007. **64**(17): p. 2219-33.
118. Cao, W. and M. Konsolaki, *FKBP immunophilins and Alzheimer's disease: a chaperoned affair.* J Biosci, 2011. **36**(3): p. 493-8.
119. Chambraud, B., et al., *The immunophilin FKBP52 specifically binds to tubulin and prevents microtubule formation.* FASEB J, 2007. **21**(11): p. 2787-97.
120. Chambraud, B., et al., *A role for FKBP52 in Tau protein function.* Proc Natl Acad Sci U S A, 2010. **107**(6): p. 2658-63.
121. Gerard, M., et al., *Inhibition of FK506 binding proteins reduces alpha-synuclein aggregation and Parkinson's disease-like pathology.* J Neurosci, 2010. **30**(7): p. 2454-63.
122. Brecht, S., et al., *Changes in peptidyl-prolyl cis/trans isomerase activity and FK506 binding protein expression following neuroprotection by FK506 in the ischemic rat brain.* Neuroscience, 2003. **120**(4): p. 1037-48.
123. Quinta, H.R., et al., *Subcellular rearrangement of hsp90-binding immunophilins accompanies neuronal differentiation and neurite outgrowth.* J Neurochem, 2010. **115**(3): p. 716-34.
124. Bush, A.I., *Metals and neuroscience.* Curr Opin Chem Biol, 2000. **4**(2): p. 184-91.
125. Tapiero, H., D.M. Townsend, and K.D. Tew, *Trace elements in human physiology and pathology. Copper.* Biomed Pharmacother, 2003. **57**(9): p. 386-98.
126. Barnham, K.J. and A.I. Bush, *Metals in Alzheimer's and Parkinson's diseases.* Curr Opin Chem Biol, 2008. **12**(2): p. 222-8.
127. Drago, D., S. Bolognin, and P. Zatta, *Role of metal ions in the abeta oligomerization in Alzheimer's disease and in other neurological disorders.* Curr Alzheimer Res, 2008. **5**(6): p. 500-7.
128. Kong, G.K., et al., *Structure of Alzheimer's disease amyloid precursor protein copper-binding domain at atomic resolution.* Acta Crystallogr Sect F Struct Biol Cryst Commun, 2007. **63**(Pt 10): p. 819-24.
129. Veldhuis, N.A., et al., *Phosphorylation regulates copper-responsive trafficking of the Menkes copper transporting P-type ATPase.* Int J Biochem Cell Biol, 2009. **41**(12): p. 2403-12.
130. Sanokawa-Akakura, R., et al., *Control of Alzheimer's amyloid beta toxicity by the high molecular weight immunophilin FKBP52 and copper homeostasis in Drosophila.* PLoS One, 2010. **5**(1): p. e8626.

131. Sanokawa-Akakura, R., et al., *A novel role for the immunophilin FKBP52 in copper transport.* J Biol Chem, 2004. **279**(27): p. 27845-8.
132. Santamaria-Kisiel, L., A.C. Rintala-Dempsey, and G.S. Shaw, *Calcium-dependent and -independent interactions of the S100 protein family.* Biochem J, 2006. **396**(2): p. 201-14.
133. Wright, N.T., et al., *S100A1: Structure, Function, and Therapeutic Potential.* Curr Chem Biol, 2009. **3**(2): p. 138-145.
134. Zimmer, D.B., et al., *S100-mediated signal transduction in the nervous system and neurological diseases.* Cell Mol Biol (Noisy-le-grand), 2005. **51**(2): p. 201-14.
135. Goel, M., et al., *Regulation of drosophila trpl channels by immunophilin fkbp59.* J Biol Chem, 2001. **276**(42): p. 38762-73.
136. Sinkins, W.G., et al., *Association of immunophilins with mammalian TRPC channels.* J Biol Chem, 2004. **279**(33): p. 34521-9.
137. Silverstein, A.M., et al., *Different regions of the immunophilin FKBP52 determine its association with the glucocorticoid receptor, hsp90, and cytoplasmic dynein.* J Biol Chem, 1999. **274**(52): p. 36980-6.
138. Mamane, Y., et al., *Posttranslational regulation of IRF-4 activity by the immunophilin FKBP52.* Immunity, 2000. **12**(2): p. 129-40.
139. Fusco, D., et al., *The RET51/FKBP52 complex and its involvement in Parkinson disease.* Hum Mol Genet, 2010. **19**(14): p. 2804-16.
140. Chambraud, B., et al., *FAP48, a new protein that forms specific complexes with both immunophilins FKBP59 and FKBP12. Prevention by the immunosuppressant drugs FK506 and rapamycin.* J Biol Chem, 1996. **271**(51): p. 32923-9.
141. Krummrei, U., E.E. Baulieu, and B. Chambraud, *The FKBP-associated protein FAP48 is an antiproliferative molecule and a player in T cell activation that increases IL2 synthesis.* Proc Natl Acad Sci U S A, 2003. **100**(5): p. 2444-9.
142. Zhong, L., et al., *Improved transduction of primary murine hepatocytes by recombinant adeno-associated virus 2 vectors in vivo.* Gene Ther, 2004. **11**(14): p. 1165-9.
143. Desmetz, C., et al., *Identification of a new panel of serum autoantibodies associated with the presence of in situ carcinoma of the breast in younger women.* Clin Cancer Res, 2009. **15**(14): p. 4733-41.
144. Gougelet, A., et al., *Estrogen receptor alpha and beta subtype expression and transactivation capacity are differentially affected by receptor-, hsp90- and immunophilin-ligands in human breast cancer cells.* J Steroid Biochem Mol Biol, 2005. **94**(1-3): p. 71-81.
145. Liu, Y., et al., *Proteomic mining in the dysplastic liver of WHV/c-myc mice--insights and indicators for early hepatocarcinogenesis.* FEBS J, 2010. **277**(19): p. 4039-53.
146. Shipp, C., K. Watson, and G.L. Jones, *Associations of HSP90 client proteins in human breast cancer.* Anticancer Res, 2011. **31**(6): p. 2095-101.
147. Yang, W.S., et al., *Proteomic approach reveals FKBP4 and S100A9 as potential prediction markers of therapeutic response to neoadjuvant chemotherapy in patients with breast cancer.* J Proteome Res, 2012. **11**(2): p. 1078-88.
148. Lin, J.F., et al., *Identification of candidate prostate cancer biomarkers in prostate needle biopsy specimens using proteomic analysis.* Int J Cancer, 2007. **121**(12): p. 2596-605.
149. Periyasamy, S., et al., *FKBP51 and Cyp40 are positive regulators of androgen-dependent prostate cancer cell growth and the targets of FK506 and cyclosporin A.* Oncogene, 2010. **29**(11): p. 1691-701.

150. Gelmann, E.P., *Molecular biology of the androgen receptor.* J Clin Oncol, 2002. **20**(13): p. 3001-15.
151. Weatherman, R.V., R.J. Fletterick, and T.S. Scanlan, *Nuclear-receptor ligands and ligand-binding domains.* Annu Rev Biochem, 1999. **68**: p. 559-81.
152. Heemers, H.V. and D.J. Tindall, *Androgen receptor (AR) coregulators: a diversity of functions converging on and regulating the AR transcriptional complex.* Endocr Rev, 2007. **28**(7): p. 778-808.
153. Pereira de Jesus-Tran, K., et al., *Comparison of crystal structures of human androgen receptor ligand-binding domain complexed with various agonists reveals molecular determinants responsible for binding affinity.* Protein Sci, 2006. **15**(5): p. 987-99.
154. Leibowitz-Amit, R. and A.M. Joshua, *Targeting the androgen receptor in the management of castration-resistant prostate cancer: rationale, progress, and future directions.* Curr Oncol, 2012. **19**(Suppl 3): p. S22-31.
155. Matias, P.M., et al., *Structural evidence for ligand specificity in the binding domain of the human androgen receptor. Implications for pathogenic gene mutations.* J Biol Chem, 2000. **275**(34): p. 26164-71.
156. Agoulnik, I.U. and N.L. Weigel, *Androgen receptor action in hormone-dependent and recurrent prostate cancer.* J Cell Biochem, 2006. **99**(2): p. 362-72.
157. Mohler, J.L., et al., *The androgen axis in recurrent prostate cancer.* Clin Cancer Res, 2004. **10**(2): p. 440-8.
158. Seruga, B., A. Ocana, and I.F. Tannock, *Drug resistance in metastatic castration-resistant prostate cancer.* Nat Rev Clin Oncol, 2011. **8**(1): p. 12-23.
159. Arora, V.K., et al., *Glucocorticoid receptor confers resistance to antiandrogens by bypassing androgen receptor blockade.* Cell, 2013. **155**(6): p. 1309-22.
160. Balbas, M.D., et al., *Overcoming mutation-based resistance to antiandrogens with rational drug design.* Elife, 2013. **2**: p. e00499.
161. Chen, C.D., et al., *Molecular determinants of resistance to antiandrogen therapy.* Nat Med, 2004. **10**(1): p. 33-9.
162. Joseph, J.D., et al., *A clinically relevant androgen receptor mutation confers resistance to second-generation antiandrogens enzalutamide and ARN-509.* Cancer Discov, 2013. **3**(9): p. 1020-9.
163. Korpal, M., et al., *An F876L mutation in androgen receptor confers genetic and phenotypic resistance to MDV3100 (enzalutamide).* Cancer Discov, 2013. **3**(9): p. 1030-43.
164. Yokoyama, N.N., et al., *Wnt signaling in castration-resistant prostate cancer: implications for therapy.* Am J Clin Exp Urol, 2014. **2**(1): p. 27-44.
165. Moore, T.W., C.G. Mayne, and J.A. Katzenellenbogen, *Minireview: Not picking pockets: nuclear receptor alternate-site modulators (NRAMs).* Mol Endocrinol, 2009. **24**(4): p. 683-95.
166. De Leon, J.T., et al., *Targeting the regulation of androgen receptor signaling by the heat shock protein 90 cochaperone FKBP52 in prostate cancer cells.* Proc Natl Acad Sci U S A, 2011. **108**(29): p. 11878-83.
167. Estebanez-Perpina, E., et al., *A surface on the androgen receptor that allosterically regulates coactivator binding.* Proc Natl Acad Sci U S A., 2007. **104**(41): p. 16074-9. Epub 2007 Oct 2.

168. Christiaens, V., et al., *Characterization of the two coactivator-interacting surfaces of the androgen receptor and their relative role in transcriptional control.* J Biol Chem, 2002. **277**(51): p. 49230-7.
169. Estebanez-Perpina, E., et al., *The molecular mechanisms of coactivator utilization in ligand-dependent transactivation by the androgen receptor.* J Biol Chem, 2005. **280**(9): p. 8060-8.
170. He, B., J.A. Kemppainen, and E.M. Wilson, *FXXLF and WXXLF sequences mediate the NH2-terminal interaction with the ligand binding domain of the androgen receptor.* J Biol Chem, 2000. **275**(30): p. 22986-94.
171. Heery, D.M., et al., *A signature motif in transcriptional co-activators mediates binding to nuclear receptors.* Nature, 1997. **387**(6634): p. 733-6.
172. Hur, E., et al., *Recognition and accommodation at the androgen receptor coactivator binding interface.* PLoS Biol, 2004. **2**(9): p. E274.
173. Grosdidier, S., et al., *Allosteric conversation in the androgen receptor ligand-binding domain surfaces.* Mol Endocrinol, 2012. **26**(7): p. 1078-90.
174. Jehle, K., et al., *Coregulator control of androgen receptor action by a novel nuclear receptor-binding motif.* J Biol Chem, 2014. **289**(13): p. 8839-51.
175. Chesire, D.R., et al., *In vitro evidence for complex modes of nuclear beta-catenin signaling during prostate growth and tumorigenesis.* Oncogene, 2002. **21**(17): p. 2679-94.
176. Huber, A.H., W.J. Nelson, and W.I. Weis, *Three-dimensional structure of the armadillo repeat region of beta-catenin.* Cell, 1997. **90**(5): p. 871-82.
177. Xing, Y., et al., *Crystal structure of a full-length beta-catenin.* Structure, 2008. **16**(3): p. 478-87.
178. Xu, W. and D. Kimelman, *Mechanistic insights from structural studies of beta-catenin and its binding partners.* J Cell Sci, 2007. **120**(Pt 19): p. 3337-44.
179. Yang, F., et al., *Linking beta-catenin to androgen-signaling pathway.* J Biol Chem, 2002. **277**(13): p. 11336-44.
180. Song, L.N., et al., *Beta-catenin binds to the activation function 2 region of the androgen receptor and modulates the effects of the N-terminal domain and TIF2 on ligand-dependent transcription.* Mol Cell Biol, 2003. **23**(5): p. 1674-87.
181. Li, H., et al., *Synergistic effects of coactivators GRIP1 and beta-catenin on gene activation: cross-talk between androgen receptor and Wnt signaling pathways.* J Biol Chem, 2004. **279**(6): p. 4212-20.
182. Yumoto, F., et al., *Structural basis of coactivation of liver receptor homolog-1 by beta-catenin.* Proc Natl Acad Sci U S A, 2012. **109**(1): p. 143-8.
183. Masiello, D., et al., *Recruitment of beta-catenin by wild-type or mutant androgen receptors correlates with ligand-stimulated growth of prostate cancer cells.* Mol Endocrinol, 2004. **18**(10): p. 2388-401.
184. Pawlowski, J.E., et al., *Liganded androgen receptor interaction with beta-catenin: nuclear co-localization and modulation of transcriptional activity in neuronal cells.* J Biol Chem, 2002. **277**(23): p. 20702-10.
185. Truica, C.I., S. Byers, and E.P. Gelmann, *Beta-catenin affects androgen receptor transcriptional activity and ligand specificity.* Cancer Res, 2000. **60**(17): p. 4709-13.

186. Schweizer, L., et al., *The androgen receptor can signal through Wnt/beta-Catenin in prostate cancer cells as an adaptation mechanism to castration levels of androgens.* BMC Cell Biol, 2008. **9**: p. 4.
187. Yardy, G.W. and S.F. Brewster, *Wnt signalling and prostate cancer.* Prostate Cancer Prostatic Dis, 2005. **8**(2): p. 119-26.
188. Chesire, D.R. and W.B. Isaacs, *Ligand-dependent inhibition of beta-catenin/TCF signaling by androgen receptor.* Oncogene, 2002. **21**(55): p. 8453-69.
189. Wang, G., J. Wang, and M.D. Sadar, *Crosstalk between the androgen receptor and beta-catenin in castrate-resistant prostate cancer.* Cancer Res, 2008. **68**(23): p. 9918-27.
190. Lawson, D.A. and O.N. Witte, *Stem cells in prostate cancer initiation and progression.* J Clin Invest, 2007. **117**(8): p. 2044-50.
191. Marimuthu, A., et al., *TR surfaces and conformations required to bind nuclear receptor corepressor.* Mol Endocrinol, 2002. **16**(2): p. 271-86.
192. Storer Samaniego, C., et al., *The FKBP52 Cochaperone Acts in Synergy with beta-Catenin to Potentiate Androgen Receptor Signaling.* PLoS One, 2015. **10**(7): p. e0134015.
193. Liang, S., et al., *Quantification of a New Anti-Cancer Molecule MJC13 Using a Rapid, Sensitive, and Reliable Liquid Chromatography-Tandem Mass Spectrometry Method.* American Journal of Modern Chromatography, 2014. **1**(1): p. 1-11.
194. Liang, S., et al., *Solution Formulation Development and Efficacy of MJC13 in a Preclinical Model of Castrate-Resistant Prostate Cancer.* Pharmaceutical Development and Technology, in press.
195. Shafi, A.A., M.B. Cox, and N.L. Weigel, *Androgen receptor splice variants are resistant to inhibitors of Hsp90 and FKBP52, which alter androgen receptor activity and expression.* Steroids, 2013. **78**(6): p. 548-54.
196. Ni, L., et al., *FKBP51 promotes assembly of the Hsp90 chaperone complex and regulates androgen receptor signaling in prostate cancer cells.* Mol Cell Biol, 2010. **30**(5): p. 1243-53.
197. Kassi, E. and P. Moutsatsou, *Glucocorticoid receptor signaling and prostate cancer.* Cancer Lett, 2011. **302**(1): p. 1-10.
198. Reynolds, A.R. and N. Kyprianou, *Growth factor signalling in prostatic growth: significance in tumour development and therapeutic targeting.* Br J Pharmacol, 2006. **147 Suppl 2**: p. S144-52.
199. Cluning, C., et al., *The helix 1-3 loop in the glucocorticoid receptor LBD is a regulatory element for FKBP cochaperones.* Mol Endocrinol, 2013. **27**(7): p. 1020-35.
200. Bonkhoff, H., et al., *Progesterone receptor expression in human prostate cancer: correlation with tumor progression.* Prostate, 2001. **48**(4): p. 285-91.
201. Check, J.H., et al., *Progesterone receptor antagonist therapy has therapeutic potential even in cancer restricted to males as evidenced from murine testicular and prostate cancer studies.* Anticancer Res, 2010. **30**(12): p. 4921-3.
202. Erlejman, A.G., et al., *NF-kappaB transcriptional activity is modulated by FK506-binding proteins FKBP51 and FKBP52: a role for peptidyl-prolyl isomerase activity.* J Biol Chem, 2014. **289**(38): p. 26263-76.
203. Jin, R., et al., *Inhibition of NF-kappa B signaling restores responsiveness of castrate-resistant prostate cancer cells to anti-androgen treatment by decreasing androgen receptor-variant expression.* Oncogene, 2014. **15**(10): p. 302.

204. Isikbay, M., et al., *Glucocorticoid receptor activity contributes to resistance to androgen-targeted therapy in prostate cancer.* Horm Cancer, 2014. **5**(2): p. 72-89.
205. Sahu, B., et al., *FoxA1 specifies unique androgen and glucocorticoid receptor binding events in prostate cancer cells.* Cancer Res, 2013. **73**(5): p. 1570-80.
206. Sharifi, N., *Steroid sidestep: evading androgen ablation by abiraterone.* Clin Cancer Res, 2015. **21**(6): p. 1240-2.
207. Yemelyanov, A., et al., *Differential targeting of androgen and glucocorticoid receptors induces ER stress and apoptosis in prostate cancer cells: a novel therapeutic modality.* Cell Cycle, 2012. **11**(2): p. 395-406.
208. Sastry, G.M., et al., *Protein and ligand preparation: parameters, protocols, and influence on virtual screening enrichments.* J Comput Aided Mol Des, 2013. **27**(3): p. 221-34.
209. Irwin, J.J. and B.K. Shoichet, *ZINC--a free database of commercially available compounds for virtual screening.* J Chem Inf Model, 2005. **45**(1): p. 177-82.
210. Friesner, R.A., et al., *Glide: a new approach for rapid, accurate docking and scoring. 1. Method and assessment of docking accuracy.* J Med Chem, 2004. **47**(7): p. 1739-49.
211. Zsoldos, Z., et al., *eHiTS: a new fast, exhaustive flexible ligand docking system.* J Mol Graph Model, 2007. **26**(1): p. 198-212.
212. Wilson, V.S., et al., *A novel cell line, MDA-kb2, that stably expresses an androgen- and glucocorticoid-responsive reporter for the detection of hormone receptor agonists and antagonists.* Toxicol Sci., 2002. **66**(1): p. 69-81.
213. Pagliarulo, V., et al., *Contemporary role of androgen deprivation therapy for prostate cancer.* Eur Urol, 2012. **61**(1): p. 11-25.
214. Egan, A., et al., *Castration-resistant prostate cancer: adaptive responses in the androgen axis.* Cancer Treat Rev, 2014. **40**(3): p. 426-33.
215. Knudsen, K.E. and H.I. Scher, *Starving the addiction: new opportunities for durable suppression of AR signaling in prostate cancer.* Clin Cancer Res, 2009. **15**(15): p. 4792-8.
216. Chen, Y., C.L. Sawyers, and H.I. Scher, *Targeting the androgen receptor pathway in prostate cancer.* Curr Opin Pharmacol, 2008. **8**(4): p. 440-8.
217. Guo, Z., et al., *A novel androgen receptor splice variant is up-regulated during prostate cancer progression and promotes androgen depletion-resistant growth.* Cancer Res, 2009. **69**(6): p. 2305-13.
218. Hu, R., et al., *Ligand-independent androgen receptor variants derived from splicing of cryptic exons signify hormone-refractory prostate cancer.* Cancer Res, 2009. **69**(1): p. 16-22.
219. Knudsen, K.E. and T.M. Penning, *Partners in crime: deregulation of AR activity and androgen synthesis in prostate cancer.* Trends Endocrinol Metab, 2010. **21**(5): p. 315-24.
220. Li, Y., et al., *Intragenic rearrangement and altered RNA splicing of the androgen receptor in a cell-based model of prostate cancer progression.* Cancer Res, 2011. **71**(6): p. 2108-17.
221. Sun, S., et al., *Castration resistance in human prostate cancer is conferred by a frequently occurring androgen receptor splice variant.* J Clin Invest, 2010. **120**(8): p. 2715-30.
222. Suh, J.H., et al., *Similarities and Distinctions in Actions of Surface-Directed and Classic Androgen Receptor Antagonists.* PLoS One, 2015. **10**(9): p. e0137103.

223. Liang, S., et al., *Solution formulation development and efficacy of MJC13 in a preclinical model of castration-resistant prostate cancer.* Pharm Dev Technol, 2016. **21**(1): p. 121-6.
224. Sramkoski, R.M., et al., *A new human prostate carcinoma cell line, 22Rv1.* In Vitro Cell Dev Biol Anim, 1999. **35**(7): p. 403-9.
225. Tepper, C.G., et al., *Characterization of a novel androgen receptor mutation in a relapsed CWR22 prostate cancer xenograft and cell line.* Cancer Res, 2002. **62**(22): p. 6606-14.
226. Horoszewicz, J.S., et al., *LNCaP model of human prostatic carcinoma.* Cancer Res, 1983. **43**(4): p. 1809-18.
227. Maggiolini, M., et al., *The mutant androgen receptor T877A mediates the proliferative but not the cytotoxic dose-dependent effects of genistein and quercetin on human LNCaP prostate cancer cells.* Mol Pharmacol, 2002. **62**(5): p. 1027-35.
228. Gao, N., et al., *The role of hepatocyte nuclear factor-3 alpha (Forkhead Box A1) and androgen receptor in transcriptional regulation of prostatic genes.* Mol Endocrinol, 2003. **17**(8): p. 1484-507.
229. Wilson, V.S., K. Bobseine, and L.E. Gray, Jr., *Development and characterization of a cell line that stably expresses an estrogen-responsive luciferase reporter for the detection of estrogen receptor agonist and antagonists.* Toxicol Sci, 2004. **81**(1): p. 69-77.
230. Kim, J. and G.A. Coetzee, *Prostate specific antigen gene regulation by androgen receptor.* J Cell Biochem, 2004. **93**(2): p. 233-41.
231. Febbo, P.G., et al., *Androgen mediated regulation and functional implications of fkbp51 expression in prostate cancer.* J Urol, 2005. **173**(5): p. 1772-7.
232. Makkonen, H., et al., *Long-range activation of FKBP51 transcription by the androgen receptor via distal intronic enhancers.* Nucleic Acids Res., 2009. **37**(12): p. 4135-48. Epub 2009 May 11.
233. Mostaghel, E.A., et al., *Intraprostatic androgens and androgen-regulated gene expression persist after testosterone suppression: therapeutic implications for castration-resistant prostate cancer.* Cancer Res., 2007. **67**(10): p. 5033-41.
234. Velasco, A.M., et al., *Identification and validation of novel androgen-regulated genes in prostate cancer.* Endocrinology, 2004. **145**(8): p. 3913-24.
235. Balk, S.P., Y.J. Ko, and G.J. Bubley, *Biology of prostate-specific antigen.* J Clin Oncol, 2003. **21**(2): p. 383-91.
236. Sharma, P., et al., *Id4 deficiency attenuates prostate development and promotes PIN-like lesions by regulating androgen receptor activity and expression of NKX3.1 and PTEN.* Mol Cancer, 2013. **12**: p. 67.
237. Patel, D., et al., *Inhibitor of differentiation 4 (ID4) inactivation promotes de novo steroidogenesis and castration-resistant prostate cancer.* Mol Endocrinol, 2014. **28**(8): p. 1239-53.
238. Lea, W.A. and A. Simeonov, *Fluorescence polarization assays in small molecule screening.* Expert Opin Drug Discov, 2011. **6**(1): p. 17-32.
239. Kozany, C., et al., *Fluorescent probes to characterise FK506-binding proteins.* Chembiochem, 2009. **10**(8): p. 1402-10.
240. Lipinski, C.A., *Lead- and drug-like compounds: the rule-of-five revolution.* Drug Discov Today Technol, 2004. **1**(4): p. 337-41.
241. Uekama, K., F. Hirayama, and T. Irie, *Cyclodextrin Drug Carrier Systems.* Chem Rev, 1998. **98**(5): p. 2045-2076.

242. Savjani, K.T., A.K. Gajjar, and J.K. Savjani, *Drug solubility: importance and enhancement techniques.* ISRN Pharm, 2012. **2012**: p. 195727.
243. Smith, D.A., L. Di, and E.H. Kerns, *The effect of plasma protein binding on in vivo efficacy: misconceptions in drug discovery.* Nat Rev Drug Discov, 2010. **9**(12): p. 929-39.
244. French, J.T., et al., *Interventional therapy of head and neck cancer with lipid nanoparticle-carried rhenium 186 radionuclide.* J Vasc Interv Radiol, 2010. **21**(8): p. 1271-9.
245. Holback, H. and Y. Yeo, *Intratumoral drug delivery with nanoparticulate carriers.* Pharm Res, 2011. **28**(8): p. 1819-30.
246. Xie, H., et al., *Effect of intratumoral administration on biodistribution of 64Cu-labeled nanoshells.* Int J Nanomedicine, 2012. **7**: p. 2227-38.
247. Jemal, A., et al., *Global cancer statistics.* CA Cancer J Clin, 2011. **61**(2): p. 69-90.
248. Sridhar, S.S., et al., *Castration-resistant prostate cancer: from new pathophysiology to new treatment.* Eur Urol, 2014. **65**(2): p. 289-99.
249. Yuan, X., et al., *Androgen receptor functions in castration-resistant prostate cancer and mechanisms of resistance to new agents targeting the androgen axis.* Oncogene, 2014. **33**(22): p. 2815-25.
250. Roy, A.K., et al., *Regulation of androgen action.* Vitam Horm, 1999. **55**: p. 309-52.
251. Jenster, G., *The role of the androgen receptor in the development and progression of prostate cancer.* Semin Oncol, 1999. **26**(4): p. 407-21.
252. Taplin, M.E., *Drug insight: role of the androgen receptor in the development and progression of prostate cancer.* Nat Clin Pract Oncol, 2007. **4**(4): p. 236-44.
253. Aragon-Ching, J.B., *The evolution of prostate cancer therapy: targeting the androgen receptor.* Front Oncol, 2014. **4**: p. 295.
254. Carver, B.S., *Strategies for targeting the androgen receptor axis in prostate cancer.* Drug Discov Today, 2014. **19**(9): p. 1493-7.
255. Culig, Z., *Targeting the androgen receptor in prostate cancer.* Expert Opin Pharmacother, 2014. **15**(10): p. 1427-37.
256. Karantanos, T., et al., *Understanding the mechanisms of androgen deprivation resistance in prostate cancer at the molecular level.* Eur Urol, 2015. **67**(3): p. 470-9.
257. Goldspiel, B.R. and D.R. Kohler, *Flutamide: an antiandrogen for advanced prostate cancer.* DICP, 1990. **24**(6): p. 616-23.
258. Blackledge, G.R., I.D. Cockshott, and B.J. Furr, *Casodex (bicalutamide): overview of a new antiandrogen developed for the treatment of prostate cancer.* Eur Urol, 1997. **31 Suppl 2**: p. 30-9.
259. Semenas, J., N. Dizeyi, and J.L. Persson, *Enzalutamide as a second generation antiandrogen for treatment of advanced prostate cancer.* Drug Des Devel Ther, 2013. **7**: p. 875-81.
260. Gillatt, D., *Antiandrogen treatments in locally advanced prostate cancer: are they all the same?* J Cancer Res Clin Oncol, 2006. **132 Suppl 1**: p. S17-26.
261. Maeda, O. and M. Usami, *[Antiandrogen in prostate cancer].* Nihon Rinsho, 2002. **60 Suppl 11**: p. 188-92.
262. Attardi, B.J., et al., *Steroid hormonal regulation of growth, prostate specific antigen secretion, and transcription mediated by the mutated androgen receptor in CWR22Rv1 human prostate carcinoma cells.* Mol Cell Endocrinol, 2004. **222**(1-2): p. 121-32.

263. Bohl, C.E., et al., *Structural basis for antagonism and resistance of bicalutamide in prostate cancer.* Proc Natl Acad Sci U S A, 2005. **102**(17): p. 6201-6.
264. Bohl, C.E., et al., *Structural basis for accommodation of nonsteroidal ligands in the androgen receptor.* J Biol Chem, 2005. **280**(45): p. 37747-54.
265. O'Neill, D., et al., *Development and exploitation of a novel mutant androgen receptor modelling strategy to identify new targets for advanced prostate cancer therapy.* Oncotarget, 2015. **6**(28): p. 26029-40.
266. Harikishore, A., et al., *Small molecule Plasmodium FKBP35 inhibitor as a potential antimalaria agent.* Sci Rep, 2013. **3**: p. 2501.
267. Denmeade, S.R. and J.T. Isaacs, *The role of prostate-specific antigen in the clinical evaluation of prostatic disease.* BJU Int, 2004. **93 Suppl 1**: p. 10-5.
268. Lilja, H., *A kallikrein-like serine protease in prostatic fluid cleaves the predominant seminal vesicle protein.* J Clin Invest, 1985. **76**(5): p. 1899-903.
269. Watt, K.W., et al., *Human prostate-specific antigen: structural and functional similarity with serine proteases.* Proc Natl Acad Sci U S A, 1986. **83**(10): p. 3166-70.
270. Schellhammer, P.F., et al., *Prostate specific antigen decreases after withdrawal of antiandrogen therapy with bicalutamide or flutamide in patients receiving combined androgen blockade.* J Urol, 1997. **157**(5): p. 1731-5.
271. Scher, H.I. and G.J. Kolvenbag, *The antiandrogen withdrawal syndrome in relapsed prostate cancer.* Eur Urol, 1997. **31 Suppl 2**: p. 3-7; discussion 24-7.
272. Hara, T., et al., *Novel mutations of androgen receptor: a possible mechanism of bicalutamide withdrawal syndrome.* Cancer Res, 2003. **63**(1): p. 149-53.
273. Tan, J., et al., *Dehydroepiandrosterone activates mutant androgen receptors expressed in the androgen-dependent human prostate cancer xenograft CWR22 and LNCaP cells.* Mol Endocrinol, 1997. **11**(4): p. 450-9.

GLOSSARY

AAV – Adeno-associated virus

Ab – Antibody

AD – Alzheimer's disease

ADP – Adenosine diphosphate

ADT – Androgen deprivation therapy

AF2 – Activation function 2

Aha1 – ATPase homologue 1

AIS – Androgen insensitivity syndrome

ANOVA – Analysis of variance

AP – Alkaline phosphatase

APP – Amyloid precursor protein

AR – Androgen receptor

ARE – Androgen response element

ATCC – American type culture collection

ATP – Adenosine triphosphate

AWS – Antiandrogen withdraw syndrome

Aβ – Beta-amyloid

BAG-1 – Bcl-2-associated athanogene

BF3 – Binding function 3

BSA – Bovine serum albumin

Ca^{2+} - Calcium

CaM – Calmodulin

CD - Cyclodextrin

CHIP – Carboxyl terminus of Hsp70-interacting protein

CKII – Casein kinase II

CO_2 – Carbon dioxide

CRPC – Castration-resistant prostate cancer

CS – Charcoal-stripped

CSC – Cancer stem cell

Cu – Copper

CuBD – Copper binding domain

Cyp40 – Cyclophilin 40

DBD – DNA binding domain

DEX - Dexamethasone

DHT – Dihydrotestosterone

DMA – N, N-dimethylacetamide

DMSO – Dimethyl sulfoxide

DOC – Deoxycorticosterone

E2 - 17β-estradiol

EC_{50} – Half maximal effective concentration

EDTA – Ethylenediaminetetraacetic acid

ELISA – Enzyme-linked immunosorbent assay

EPLuc – Enhancer/promoter luciferase

ER – Estrogen receptor

ERE – Estrogen response element

EtOH – Ethanol

FBS – Fetal bovine serum

FK1 – FKBP12-like domain1

FK2 – FKBP12-like domain 2

FKBP12 – 12-kDA FK506-binding protein

FKBP35 – 35-kDa FK506-binding protein

FKBP38 – 38-kDa FK506-binding protein

FKBP51 – 51-kDa FK506-binding protein

FKBP52 – 52-kDa FK506-binding protein

*Pf*FKBP35 – *Plasmodium falciparum* FKBP35

*Pv*FKBP35 – *Plasmodium vivax* FKBP35

FP – Fluorescence polarization

FRET – Fluorescence resonance energy transfer

FTDP – Fronto-temporal dementia and parkinsonism linked to chromosome 17

GAPDH – Glyceraldehyde-3-phosphate dehydrogenase

GR – Glucocorticoid receptor

GRIP1 – Glutamate receptor-interacting protein 1

GSK3β – Glycogen synthetase kinase 3β

GTP – Guanosine triphosphate

HEPE - 12S-hydroxy-5Z,8Z,10E,14Z,17Z-eicosapentaenoic acid

HIP – Hsp70-interacting protein

HOP – Hsp70/Hsp90 organization protein

HP-β-CD – 2-hydroxypropyl-β-cyclodextrin

HRE – Hormone response element

Hsp – Heat shock protein

IC_{50} – Half maximal inhibitory concentration

ID4 – Inhibitor of differentiation 4

IRF-4 – Interferon regulatory factor 4

KLK3 – Kallikrein-related peptidase 3

LBD – Ligand binding domain

LC-MS/MS – Liquid chromatography-mass spectrometry and liquid chromatography-tandem mass spectrometry

logP – Logarithm of partition coefficient

LRH-1 – Liver receptor homolog-1

MAP – Microtubule-associated protein

MD – Middle domain

MEF – Mouse embryonic fibroblast

52KO MEF - Mouse embryonic fibroblast cells from homozygous FKBP52 knockout embryos

MEM/EBSS – Minimal essential media/Earle's balanced salt solution

MMFF – Merck molecular force field

MMTV – Mouse mammary tumor virus

MOE – Molecular operating environment

M-PER – Mammalian protein extraction reagent

MR – Mineralocorticoid receptor

NEAA – Nonessential amino acid

NFT – Neurofibrillary tangle

NLS – Nuclear localization signal

NRAM – Nuclear receptor alternative-site modulator

NTD – N-terminal domain

OPLS – Optimized potential for liquid simulations

P4 – Progesterone

PBS – Phosphate buffered saline

PCa – Prostate cancer

PCR – Polymerase chain reaction

PDB – Protein data bank

PHF – Paired helical filament

PEG 300 – Polyethylene glycol 300

PEG 400 – Polyethylene glycol 400

PPIase – Peptidyl-prolyl cis/trans isomerase

PR – Progesterone receptor

PRDX6 – Peroxiredoxin-6

PSA – Prostate specific antigen

PVDF – Polyvinylidene difluoride

RLU – Relative light unit

RMSD – Root-mean-square deviation

RPM – Revolution per min

RPMI – Roswell Park Memorial Institute

S.D. – Standard deviation

SAR – Structure-activity relationship

SGTA – Small glutamine-rich tetracopeptide repeat-containing protein alpha

SHR – Steroid hormone receptor

shRNA – Shor hairpin RNA

SP – Sum-of-pairs

SRC-2 – Steroid receptor co-activator 2

α-Syn – α-Synuclein

TBST – Tris-buffered saline containing tween

TCF – T-cell factor

TIF2 – Transcriptional mediators/intermediatry factor 2

TMB – 3,3’,5,5’-Tetramethylbenzidine

TPR – Tetratricopeptide repeat

TRPC – Transient receptor potential channel

TRPL – Transient receptor potential-like

CURRICULUM VITA

Naihsuan C. Guy was born and raised in Tainan, Taiwan until the age of 14. She has lived and attended American schools in Okinawa, Japan for a few years then moved to Alamagordo, NM to finish her last two years of high school. Naihsuan attended and graduated from New Mexico State University and University of Arizona with her bachelor's and master's degree in microbiology and immunobiology, respectively. In 2009, she was accepted into the doctoral program in Biological Sciences- Pathobiology at the University of Texas at El Paso and joined Dr. Marc B. Cox's research laboratory.

Naihsuan was the recipient of numerous honors and awards including the prestigious Dr. Keelung Hong Graduate Research Fellowship, a three-time recipient of Dodson Research Grant from University of Texas at El Paso, and various regional and national travel awards for attending scientific conferences. She was also a recipient of a Graduate Student Instructor Teaching Portfolio Award at the Sun Conference of Teaching and Learning from University of Texas at El Paso. Furthermore, she participated in Paso Del Norte Venture Competition and Expo and her team was awarded with a second place under student track and received a $2,000 cash price.

While pursuing her degree, Naihsuan worked as a research associate and an assistant instructor for Human Anatomy and Physiology II for the Department of Biological Sciences at University of Texas at El Paso. She was also employed as a part-time lecturer for the Department of Biological Sciences in El Paso Community College-Mission del Paso Campus.

Naihsuan presented her research at regional and national conferences. She co-authored two original research articles and published as first author for one book chapter and one review article. She is in the preparation of publishing at least three more original research articles as first author and coauthor.

Naihsuan's Dissertation entitled, "Identification and Characterization of Small Molecules Targeting FKBP52 as a Novel Treatment for Prostate Cancer," was supervised by Dr. Marc B.

Cox. Under his guidance, she focused her research in developing and characterizing novel therapeutic molecules for hormone-associated diseases including prostate cancer. Her findings have an important positive impact within the field as her molecule averted the dependence of steroid hormone receptors for hormone activation and expected to stay effective while the hormone-associated diseases advance to the hormone-refractory late stage. She has accepted a position with Vaccine and Infectious Disease Organization-International Vaccine Centre in Saskatoon, Canada.

Permanent address: 5890 Bandolero Dr. Apt 1048
El Paso, TX 79912

This thesis/dissertation was typed by Naihsuan C. Guy.